Universitat Autònoma de Barcelona

Understanding the mechanisms of drought-induced mortality in trees

Núria Garcia Forner

Understanding the mechanisms of drought-induced mortality in trees

- TESI DOCTORAL -

Memòria presentada per:

Núria Garcia Forner

Per optar al grau de doctor per la UAB del Programa de doctorat en Ecologia Terrestre coordinat pel Centre de Recerca Ecològica i Aplicacions Forestals

Amb el vist i plau del director de tesi:

Jordi Martínez Vilalta
Professor Agregat
Universitat Autònoma de Barcelona

Bellaterra, desembre del 2015

A la meva família

Abstract

Plants are exposed to several environmental stressors including drought and extreme temperatures that can limit their growth and survival. Water availability is considered the main limiting factor for plant productivity. Plants display a plethora of strategies to cope with drought and maintain an adequate water balance, including modifications of the leaf area, stomatal control, changes in biomass allocation, modifications of source/sink carbon balance, and resistance to xylem embolism. Despite this, drought-induced forest mortality is a widespread phenomenon with potentially large ecosystem-level implications and is expected to increase due to increasing drought events as a result of ongoing climate change. Understanding how the complex network of traits involved in drought resistance determine species' or individuals' to survive drought is critical to assess the vulnerability of current vegetation to changes in climate and the potential impacts on ecosystem functioning and services.

In 2008, McDowell *et al.* summarized drought-induced mortality mechanisms in a coherent and simple hydraulic framework. They hypothesized two main, non-exclusive physiological mechanisms leading to plant death under drought: hydraulic failure and carbon starvation. Hydraulic failure is the point at which whole-plant water transport becomes blocked due to excessive cavitation resulting from critical tensions in the xylem. Carbon starvation is the situation in which carbon supply from photosynthesis, carbon stocks or autophagy fails to meet the minimum metabolic needs. According to this framework, the preponderance of one or the other mechanism depends on the drought intensity and duration and plants' ability to regulate their water potential (Ψ_w). Isohydric species might be more vulnerable to carbon starvation due to earlier stomatal closure to maintain relatively constant Ψ_w (and avoid embolism), while anisohydric species would be more susceptible to hydraulic failure as soil dries as they operate with narrow hydraulic safety margins due to their lower Ψ_w.

The previous framework is centered on stomatal behavior, regardless of the plethora of traits involved in plant drought responses. In addition, stomata respond to several factors besides Ψ_w, hence assuming that iso/anisohydric

regulation of Ψ_w is able to fully explain stomatal behavior may be misleading. For these reasons, the main objectives in this thesis were to: (1) determine if differences in stomatal regulation between species relate to iso/anisohydric behaviors and how these are associated to different mortality mechanisms under drought, warming or both; (2) test the assumptions that relate anisohydric behaviors with higher stomatal conductances and longer periods of carbon uptake under drought, and isohydric behaviors with stronger stomatal control and wider hydraulic safety margins; and (3) understand how morphological and physiological traits and their plasticity in response to drought explain, and to what extent, time until death within species.

To address targets (1) and (2) we studied two reference models with contrasted drought-vulnerability between species: piñon-juniper and holm oak systems. In both cases, we compared drought responses between isohydric (*Pinus edulis* and *Quercus ilex*) and anisohydric species (*Juniperus monosperma* and *Phillyrea latifolia*), emphasizing stomatal regulation and carbon and water economies. In these species, we provided evidence that more anisohydric behavior is not necessarily related with looser stomatal responses to Ψ_w and, thus, with higher levels of xylem embolism. Likewise, stronger regulation of Ψ_w (isohydric behavior) was neither associated with earlier stomatal closure under drought nor with higher carbon constrains. Both studies challenge widespread notions and warn against linking iso/anisohydry with contrasted stomatal behaviors and mortality mechanisms. At the tree level in *Pinus sylvestris* (3), sustaining carbon uptake and carbon stocks above some critical level was the key factor prolonging survival under extreme drought, even at expenses of higher water losses. Fully integrating carbon and water economies is the key challenge to advance our understanding of drought responses and mortality mechanisms in plants.

Contents

Chapter 1

General introduction

Why study drought?

Plants are exposed to several environmental stresses that can limit their growth and survival, including sudden changes in light, extreme temperatures (and VPD), nutrient and water scarcity, among others. Plant responses to these stressors have been extensively studied due to their potential impact on crop productivity (Grace, 1988; Jones, 1990; Bugbee, 1995; Jones and Tardieu, 1998). Among these environmental factors, water availability is considered the main limiting factor for plant productivity (Boyer, 1982). During drought, plants may respond to keep an adequate water balance (water uptake vs. water losses), including adjustments at different organizational levels and time-scales (Chaves *et al.*, 2003; Maseda and Fernández, 2006; Regier *et al.*, 2009; Mencuccini, 2014). The strategies to cope with drought involve a plethora of traits including leaf area reductions, stomatal control, resistance to xylem embolism, modifications of the source-sink carbon balance or changes in below to aboveground biomass allocation (Mencuccini, 2014). The impact of drought (and/or high temperatures) on vegetation depends on drought frequency and severity (Schneider *et al.*, 2007; Sperlich *et al.*, 2015) but also to the success of these adjustments of the carbon and water economies at the individual level (Parolari *et al.*, 2014).

Despite the ability of many plants to maintain an adequate hydration under water stress, episodes of drought-induced mortality have been identified worldwide during the last decades and are expected to increase under ongoing climate change (Allen *et al.*, 2010; Carnicer *et al.*, 2011; Peng *et al.*, 2011; IPCC, 2013). The potential impact of these forest die-off events is still uncertain (Lloret *et al.*, 2012; Anderegg *et al.*, 2013*a*; Allen *et al.*, 2015; Hartmann *et al.*, 2015; Meir *et al.*, 2015). However, determining why some species or individuals are more resistant to increasing drought than others is critical to understand forests vulnerability to the new expected conditions under climate change, predict where future die-off spots might occur, identify potential shifts in vegetation composition and establish the impact these changes may have on ecosystem function and services.

The physiology of plants under drought

From the plethora of traits involved in the short time responses of plants to water stress, stomatal behavior plays a central role and has been studied since the 19th century (Kramer and Boyer, 1995). Stomata ability to regulate water use in relation to carbon gain in higher plants was formalized by Cowan (1982) and Farquhar and Sharkey (1982). Under water stress stomatal closure is the main mechanism by which plants may avoid or delay tissue dehydration by transpiration but, at the same time, carbon uptake and thus assimilation are constrained. Plants reduce their stomatal conductance as water demand increases relative to water supply, to maintain transpiration below critical values above which the tension reached in the xylem causes generalized loss of hydraulic conductivity due to embolism (Sperry *et al.*, 2002). However, stomatal opening and closure is a complex response, dependent on a number of environmental factors including light intensity and quality, temperature, relative humidity and VPD (Wilson, 1948; Zhang *et al.*, 2011; Guyot *et al.*, 2012; Rogiers *et al.*, 2012*b*) through their effect on internal factors such as tissue water status (Farquhar and Sharkey, 1982), hormone regulators e.g. ABA concentrations (Tardieu and Simonneau, 1998; Mcadam and Brodribb, 2014) or the internal circadian rhythm (Raschke, 1975; Mencuccini *et al.*, 2000; Dios *et al.*, 2015). Interrelations between all of these factors make it difficult to establish their relative importance in determining stomatal behavior (Kramer and Boyer, 1995). Farquhar and Sharkey (1982) concluded that stomatal conductance normally limits transpiration but it slightly limits photosynthesis. For instance, in Mediterranean species stomatal conductance is the most important factor limiting photosynthesis under mild water stress. If water stress increases, however, stomatal and mesophyll conductance co-limit photosynthesis, while mesophyll conductance is the most important limitation, followed by biochemical limitations, under severe drought (Flexas *et al.*, 2014). Regardless of the pathway limiting carbon fixation and the specific sensitiveness to these photosynthetic constrains, the more intense and long is the drought period the greater will be the reduction of the assimilated carbon and hence, the availability of the newly assimilated carbon for demanding process, e.g. respiration, growth, defense and exudates (Dietze *et al.*, 2014). Thus, when

carbon supply is limited, carbon-consuming process may rely on the available non-structural carbohydrates (NSC) reserves, which may also trigger changes in the allocation of new assimilates (Hartmann *et al.*, 2013*b*; Mitchell *et al.*, 2013).

While photosynthesis may cease under extreme drought, respiration needs to be sustained to satisfy minimum metabolic demands. In contrast to photosynthesis, respiration tends to be relatively insensitive to drought and does not decline proportionally (Atkin and Macherel, 2009). Usually, more than half of the carbon assimilated in photosynthesis is lost in respiratory processes necessary for growth and maintenance (Flexas *et al.*, 2006) but, under water stress, this balance may change as both increases or decreases in respiration have been reported (Flexas *et al.*, 2006; Atkin and Macherel, 2009; Pinkard *et al.*, 2011; Rowland *et al.*, 2015). In Mediterranean climates summer is the driest (lowest rainfall) and hottest season, thus temperature need to be considered as another drought-component. Respiration rates increase with temperature and thus the interaction with soil water scarcity, that usually decreases carbon gain, may result in a faster NSC depletion and accelerating mortality (Adams *et al.*, 2009; Zhao *et al.*, 2013). In addition, contrary to drought (or annual rainfall), global warming is one of the most robust climate change projections (IPCC 2013) and hence, even at locations where the frequency of drought in terms of precipitation deficits does not increase, it does in terms of moisture deficits from which arises the concept of “hotter droughts” (Allen *et al.*, 2015).

Carbon resources depletion as water deficit progresses could potentially limit growth. However, carbon source activity is only one of the main pathways that can regulate sink activity (tissue growth). Temperature, soil moisture and soil nutrients can act as direct plant growth control and can stimulus molecular signals that end up regulating sink activity (Fatichi *et al.*, 2014; Körner, 2015). In response to these stressors, growth, given its high sensitivity to cell turgor, necessary for cell division and tissue elongation (Tang and Boyer, 2002; Sala and Hoch, 2009) is often the first process (prior to assimilation) to diminish. Moreover, carbon sink size and activity regulate photosynthetic activity via gene expression and sugar-mediated regulation of photosynthetic enzymes (Aspinwall *et al.*, 2015). Specifically under drought stress, asynchronies

between photosynthesis and growth cessation in response to water deficit may cause an accumulation of carbon when water availability is not enough to sustain the minimum turgor for growth but photosynthesis continues, even if at low levels (McDowell *et al.*, 2013*a*; Limousin *et al.*, 2013; Dickman *et al.*, 2015). Mitchell et al. (2014) defined the 'carbon safety margin' as the difference between the leaf water potential at which growth is zero and the water potential at which net assimilation ceases. In their study, Mitchell et al. (2014) showed how narrower carbon safety margins in *Pinus radiata* relative to *Eucalyptus globulus* were associated with faster starch depletion in all organs. However, this wider carbon safety margin in *E. globulus* was not associated to longer life spans in this species. The complexity increases when different NSC components and different tissues are taken into account. For instance, several recent studies show that soluble sugars tend to remain constant or increase under drought (Mitchell *et al.*, 2014; Mencuccini, 2014; Dietze *et al.*, 2014), likely because they are involved in osmoregulation and overall hydraulic integrity (Sevanto *et al.*, 2014; O'Brien *et al.*, 2014). In addition, sucrose concentration has been related to the ability of plants to refill embolised vessels and hence recover xylem hydraulic conductivity (Salleo *et al.*, 2009; Secchi and Zwieniecki, 2011; Trifilò *et al.*, 2014). The interaction between NSC dynamics and the whole plant hydraulic system is still far from being fully understood (Anderegg *et al.*, 2015).

In addition to stomatal control of water loss by transpiration (Sperry *et al.*, 2002), at longer time scales plants can maintain an adequate water balance by modifying the ratios between the surfaces devoted to plant water uptake, water transport and water loss. Well known examples include the reduction of total leaf area, hence reducing the ratio of leaf to sapwood or absorbing root area, or allocating more resources to the root system (increasing the root to shoot ratio) in order to facilitate access to deeper water sources (Chaves *et al.*, 2003; Maseda and Fernández, 2006). Leaf area reductions under drought, however, may not necessarily increase the performance of the remaining foliage. Poyatos et al. (2013), for instance, showed in Scots pine that extreme reductions in leaf area were associated with enhanced physiological sensitivity to water deficits at the tree level and were not enough to avoid mortality. As well as stomatal

closure, severe leaf area adjustments may limit carbon uptake at the tree level during and after the stressful period (McDowell *et al.*, 2008; Galiano *et al.*, 2011).

The mechanism(s) of drought-induced mortality

The study of plant responses to drought to understand why some species succumb while other species survive during drought is a long-standing question (Bossel 1986, Franklin et al. 1987, Manion 1991, Martínez-Vilalta et al. 2002). Based on prior knowledge, McDowell et al. (2008) made an effort to present drought-induced mortality mechanisms in trees in a coherent, hydraulic framework. Since then, the physiological mechanisms of mortality under drought have become a hot topic, with large efforts devoted to understand mortality processes. McDowell et al. (2008) hypothesized that the two main physiological mechanisms underlying tree die-off were hydraulic failure and carbon starvation, which could also interact (amplify or be amplified by) the impact of biotic attacks. According to McDowell et al. (2008) hydraulic failure is the point at which whole-plant water transport is impeded due to excessive cavitation. Thus, hydraulic failure occurs when transpiration reaches critical values in response to water deficit or high water demand that generate excessive tension in the xylem. As a result, this tissue gets embolised, hydraulic conductivity is reduced and the plant eventually desiccates (Sperry *et al.*, 1998, 2002). The tension at which hydraulic failure occurs depends on species-specific xylem vulnerability to declining water potentials (vulnerability curves). On the other hand, carbon starvation is the situation in which carbon supply from photosynthesis, carbon stocks or autophagy fails to meet minimum metabolic needs or is not accessible to be used for these purposes (McDowell, 2011).

In the context of the McDowell et al. (2008) framework, the dominance of either of the hypothesized physiological mechanisms of mortality relates to drought-intensity and duration, but also to plants' ability to regulate their water status. In particular, to the classic classification between iso/anisohydric species (Jones, 1998; Tardieu and Simonneau, 1998), understood as two endpoints along a continuum of stomatal regulation of leaf water potential (Klein, 2014). In

this framework, the more isohydric species, those that maintain higher leaf water potentials (Ψ_{leaf}) by reducing stomatal conductances (g_s) as soil dries during drought, are the ones that would be more susceptible to die through carbon starvation. This is because stomatal closure would reduce water losses but it would also constrain carbon uptake. During stressful periods, isohydric plants are expected to be more dependent on their available carbon stocks. By contrast, in anisohydric species stomatal sensitivity to Ψ_{leaf} is lower than in relative isohydric plants and thus they allow Ψ_{leaf} to decrease as the soil dries. The advantage of the anisohydric strategy is that plants may be able to sustain carbon assimilation for longer. In contrast, however, they may be more vulnerable to hydraulic failure than isohydric species, as they operate at lower water potentials and, possibly, with narrower hydraulic safety margins.

The McDowell et al. (2008) framework has become the benchmark for later studies on drought-related mechanisms of mortality in plants. As a result, the focus has been placed on stomatal behavior as a key trait defining the strategy of plants to minimize mortality risk and, at the same time, determining the most likely physiological mechanism of mortality (hydraulic failure vs. carbon starvation). This simplification may be useful in some cases, but it may be problematic when comparing species with contrasted strategies to face drought stress. As we have seen before, plant responses to drought are complex and involve several interrelated traits, and stomatal behavior is only one component of the strategy (Klein, 2014; Martínez-Vilalta *et al.*, 2014). In addition, stomata are complex systems that respond to several factors besides to Ψ_{leaf} (Tardieu *et al.*, 1996; Mcadam and Brodribb, 2014; Brodribb *et al.*, 2014), hence assuming that the iso/anisohydric regulation of water potential is able to fully explain stomatal behavior may be misleading.

The McDowell et al. (2008) framework predicts that relatively anisohydric species are more prone to hydraulic failure than relatively isohydric species because of their 'later' stomatal closure during drought. By contrast, relatively isohydric species would be more susceptible to die by carbon starvation because 'earlier' stomatal closure makes them more dependent on their carbon pools. However, the iso/anisohydric classification is based on the stomatal response to leaf water potential or, more strictly, on the capacity to maintain

relatively high (close to zero) and stable leaf water potentials (Tardieu and Simonneau, 1998). This classification does not consider the relationship between stomatal sensitivity to water potential and xylem hydraulic vulnerability (Klein, 2014; Martínez-Vilalta *et al.*, 2014) nor, perhaps more importantly, stomatal responses through time. These aspects are important, firstly, because there are large variations across species in xylem vulnerability to cavitation (Choat *et al.*, 2012), with anisohydric species frequently being more resistant than isohydric species (Martínez-Vilalta *et al.*, 2003; Plaut *et al.*, 2012). Secondly, because the same stomatal conductance at a given water potential may have very different implications for water potential regulation in different species depending on their xylem hydraulic vulnerability to embolism (Martínez-Vilalta *et al.*, 2014). Finally, because the iso/anisohydric modes of water potential behavior should be associated with shorter and longer periods of stomatal opening and positive carbon uptake, respectively, for them to have any impact on the likelihood of carbon starvation; an assumption that has been seldom tested.

Approaches to study drought-induced plant mortality

Tree mortality studies include a multidisciplinary research community ranging from physiology and ecology to vegetation modeling and forest management (Allen *et al.*, 2015). The variety of approaches is reflected in equally diverse methodologies focusing on different aspects of tree mortality. Thorough studies on tree morphological and physiological responses to drought and their effect on tree-mortality are fairly difficult and rare in natural conditions due to the stochasticity of drought and our inability to predict the timing of die-off events. In this sense, experimental studies in controlled conditions are particularly interesting due to their ability to generate extreme droughts that induce mortality either in the field or in the greenhouse (or laboratory). Among these, field studies in controlled or semi-controlled conditions are the most realistic ones as trees are not subjected to artificial constrains (e.g. limitations of the root system development) and the integrity of the ecosystem is maintained. However, this kind of studies is usually quite expensive and relatively rare in forest ecosystems. More easily affordable are greenhouse experiments, which allow for precise climate control but also to standardize some vegetation

aspects such as tree age or size. One of the main criticisms to these experimental studies is that usually they are conducted on small saplings developed in pots, which is far from reality and limits the extrapolation of results to real forest settings. Growing plants into the ground generally results in more realistic conditions, as it increases plants' ability to explore water sources and likely increases their endurance when exposed to drought. This is important because drastic declines of plants' physiological integrity may mask some relevant physiological process, such as carbon mobilization.

Recent increase in the scientific literature on tree mortality provides us with extremely valuable knowledge about past or ongoing decay process worldwide. Coexisting species with contrasted vulnerabilities to drought merit special attention, as they may provide the key to understand the potential impact of future changes in climate and because these species are expected to exhibit different strategies to cope with drought. Therefore, understanding the role of the traits defining these strategies may clarify the mechanisms determining drought-induced mortality in plants. At the same time, however, and without playing down the importance of comparisons across species, the complexity due to contrasting strategies and the plethora of traits and mechanisms involved may hinder in some cases the attribution of the relative importance of each trait on the whole plant response. In that regard, intra-specific studies may be a good complement. Although differences in drought resistance within species can be large, either in the field or under controlled conditions (Cavender-Bares and Bazzaz, 2000; Martínez-Vilalta *et al.*, 2009; Moran *et al.*, 2015), overall strategies to face drought tend to be similar. Hence, intra-specific studies may facilitate disentangling the influence of different traits on drought-survival and on the mechanisms underlying drought-induced mortality.

General objectives of the thesis

In this thesis I aim at contributing to the understanding of the mechanisms of drought-induced mortality in trees by characterizing the impact of different droughts on the carbon and water economies of species with contrasted stomatal behavior, and analyzing how stomatal responses relate

with differences in drought-resistance between species and among individuals within a given species. I also analyze the basis of the hydraulic framework proposed by McDowell et al. in 2008, and adopted ever since, by assessing if the classic distinction between iso- and anisohydric species is useful to advance our understanding on the mechanisms underlying tree mortality under drought stress. The specific objectives of this thesis are to:

(1) determine if differences in stomatal regulation between species in terms of iso/anisohydric behaviors are associated to different modes of physiological failure under drought, and how they relate to the susceptibility to low water availability, warmer temperatures or both;

(2) test the common assumptions that relates: (i) relatively lower (more negative) water potentials in anisohydric species with higher stomatal conductances and longer periods of carbon uptake under drought, and (ii) relatively higher (closer to zero) water potentials in isohydric species with wider hydraulic safety margins and, hence, lower risk of hydraulic failure.

(3) to understand how morphological and physiological characteristics of individual plants and their plasticity in response to drought explain, and to what extent, time until death within species, and rank the importance of different traits.

Study systems

To address targets (1) and (2) we use two classic models of drought-induced mortality in plants: the piñon-juniper system in SW USA (particularly *Pinus edulis* vs. *Juniperus monosperma*) and the holm oak system in NE Spain (*Quercus ilex* vs. *Phillyrea latifolia*). Piñon-juniper woodlands have been severely affected by drought-induced mortality over the last two decades, sometimes amplified by bark beetle attacks (Mueller *et al.*, 2005; Breshears *et al.*, 2005, 2009*b*; Gaylord *et al.*, 2013). *P. edulis* is more vulnerable to drought, while co-occurring *J. monosperma* largely survive even under extreme events, e.g. during 2000-2003 drought period (Figure 1.1) (Breshears *et al.*, 2005, 2009*b*; Allen *et al.*, 2010).

Piñon and juniper are considered iso- and anisohydric species, respectively, and were used by McDowell et al. (2008) as the model species of the two ends of the spectrum in their hydraulic framework. Piñon-juniper woodlands provide an opportunity to test the relationship between contrasted stomatal behavior and differences in drought resistance. In the second chapter of this thesis, I take advantage of an ecosystem-scale experiment in a piñon-juniper woodland dominated by *Pinus edulis* and *Juniperus monosperma* in northern New Mexico, USA.

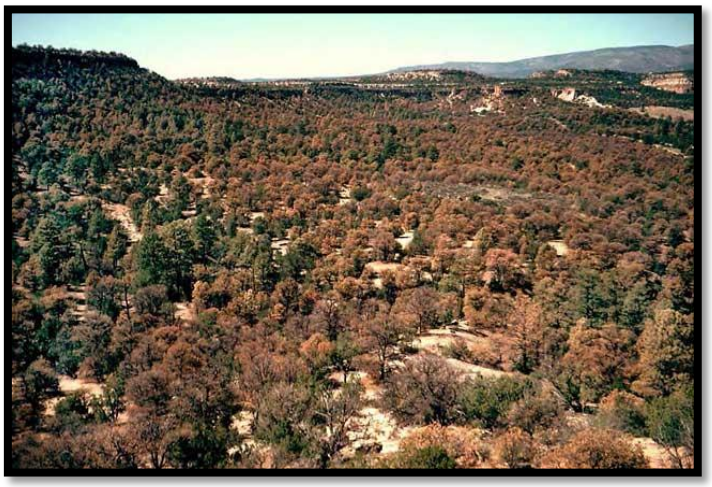

Figure 1.1.
Piñon pines in New Mexico in 2002 stressed from drought and an associated bark beetle outbreak. Photo by Craig D. Allen, USGS.

In this manipulative (partially controlled) experiment in the field we assayed plant responses to increasing temperatures, reduced rainfall or both factors combined. The warming treatment was implemented using Open Top Chambers to regulate air temperature, and reduced rainfall was achieved by installing thermoplastic polymers covering ~45 % of the total plot area (Figure 1.2).

Figure 1.2.
Detail of the ecosystem-scale experiment in a piñon-juniper woodland conducted at Los Alamos Survival/Mortality Experimental located on Frijoles Mesa at 2175 m a.s.l. in Los Alamos County, New Mexico (35°49′5″N 106°18′19″W). Open Top Chambers surrounding piñon-juniper trees and thermoplastic polymers installed on the ~45 % surface area of the plot.

The third chapter 3 of the thesis focuses on Mediterranean holm oak forests and, in particular, on the comparison between *P. latifolia* (a tall shrub or small tree) and *Q. ilex*, one of the most representative Mediterranean trees (Figure 1.3, left and right images, respectively) (Rodà *et al.*, 1999). Although differences in water potentials as the soil dries are not as extreme between these species as in the piñon-juniper case, *Q. ilex* and *P. latifolia* have been also studied as examples of iso- (*Q. ilex*) and anisohydric species (*P. latifolia*). In addition, differences in drought resistance between species have been also reported under both natural and experimental conditions (Lloret and Siscart, 1995; Peñuelas *et al.*, 1998, 2000; Lloret *et al.*, 2004*a*; Ogaya and Peñuelas, 2007), and the physiological factors underlying these differences have been partially explored (Martínez-Vilalta *et al.*, 2002*a*; Ogaya and Peñuelas, 2007).

Figure 1.3.
Specimens of *P. latifolia* (left) and *Q. ilex* (right) (www.floracatalana.net).

Likely in the piñon-juniper example, the comparison between these species is particularly interesting in the context of the drought-induced mortality mechanisms but also critical to understand possible species replacements under 'hotter droughts' projections. In chapter 3 we set-up a manipulative

drought experiment in a greenhouse were *P. latifolia*, *Q. ilex* (and *Pinus sylvestris*) small trees were planted into the ground to study their responses to recurrent drought periods of different length and the mechanisms underlying drought-induced mortality (Figure 1.4).

Figure 1.4.
Q. ilex and *P. latifolia* drought-experiment. Plants were planted into the ground of a polytunnel greenhouse located in the experimental facilities of the Institute of Agricultural, Food Research and Technology (2º10'3"N, 41º37'56"E, 203 m asl; Caldes de Montbui, Spain). The left picture was taken in June 2013, two years after the beginning of the experiment. The picture on the right is later in 2014, when some *Q. ilex* trees had dried-up after suffering three periods of extreme drought, while all *P. latifolia* trees were still totally or partially green.

In the same study system, *P. sylvestris* trees were planted to study the intra-population variability in drought responses and survival (chapter 4, objective 3). Scots pine is a widely distributed temperate tree with the southern (and dry) distribution limit in the Iberian Peninsula. Scots pine dieback process associated to drought and/or warming (e.g. Figure 1.5) have been described in Spain (Martínez-Vilalta and Piñol, 2002; Hódar *et al.*, 2003; Galiano *et al.*, 2010) and in other regions (Allen *et al.*, 2010; Rigling *et al.*, 2013).

Figure 1.5.
Mixed forest of *Q. ilex* and *P. sylvestris* in Prades Mountains, Catalonia (Spain) in 2012. In the upper canopy, Scots pines dead trees indicate the decline process of this species in the area (Photo courtesy of R. Poyatos).

Some studies have reported that oak species are replacing the more vulnerable pine species in southern and central Europe, and that this process is driven by multiple factors including drought (Rigling *et al.*, 2013; Carnicer *et al.*, 2014). However, pines, including our target species, show a plastic response to water availability and/or warming, in particular regarding their stomatal control and the adjustment of leaf-to-sapwood area ratios (DeLucia *et al.*, 2000; Poyatos *et al.*, 2007; Martínez-Vilalta *et al.*, 2009). Thus, the vulnerability of xeric populations of this species even under current climatic conditions and the plasticity of its drought responses make this species an excellent candidate to study how trait differences among individuals may translate into differences in survival time under extreme drought and may illuminate the physiological mechanisms underlying such differences.

Chapter 2

Responses of two semiarid conifer tree species to reduced precipitation and warming reveal new perspectives for stomatal regulation

Núria Garcia-Forner, Henry D. Adams, Sanna Sevanto, Adam D. Collins, Lee T. Dickman, Patrick J. Hudson, Melanie J.B. Zeppel, Michael J. Jenkins, Heath Powers, Jordi Martínez-Vilalta & Nate G. McDowell

Published in Plant, Cell and Environment

ABSTRACT

Relatively anisohydric species are predicted to be more predisposed to hydraulic failure than relatively isohydric species, as they operate with narrower hydraulic safety margins. We subjected co-occurring anisohydric Juniperus monosperma and isohydric Pinus edulis trees to warming, reduced precipitation, or both, and measured their gas exchange and hydraulic responses. We found that reductions in stomatal conductance and assimilation by heat and drought were more frequent during relatively moist periods, but these effects were not exacerbated in the combined heat and drought treatment. Counter to expectations, both species exhibited similar g_s temporal dynamics in response to drought. Further, whereas *P. edulis* exhibited chronic embolism, *J. monosperma* showed very little embolism due to its conservative stomatal regulation and maintenance of xylem water potential above the embolism entry point. This tight stomatal control and low levels of embolism experienced by juniper refuted the notion that very low water potentials during drought are associated with loose stomatal control and with the hypothesis that anisohydric species are more prone to hydraulic failure than isohydric species. Because direct association of stomatal behavior with embolism resistance can be misleading, we advocate consideration of stomatal behavior relative to embolism resistance for classifying species drought response strategies.

Keywords: drought, increased temperature, global change, mortality, iso- vs. anisohydric behavior, stomatal conductance, hydraulic conductivity, hydraulic failure, carbon starvation.

INTRODUCTION

Drought-induced forest mortality has become a major focus of attention in plant ecological research (Allen *et al.*, 2010). Plant responses to drought include adjustments at different timescales and have been characterized according to different schemes (e.g. Chaves *et al.*, 2003; Maseda and Fernández, 2006; Choat *et al.*, 2012). A useful framework classifies plants based on stomatal regulation of leaf water potential in response to changes in atmospheric moisture demand and soil water supply (isohydric vs. anisohydric species; Stoker, 1956; Larcher, 1975; Jones, 1998; Tardieu and Simonneau, 1998). The iso- vs. anisohydric dichotomy has been given a central role in theories explaining the physiological causes of drought-induced mortality, and has been proposed as a predictive trait of the specific underlying mechanism of mortality (McDowell *et al.*, 2008; Plaut *et al.*, 2012).

Relatively isohydric plants respond quickly to declining water availability and rising atmospheric moisture demand by closing their stomata in order to control water losses and avoid excessively low leaf water potentials that could cause cavitation and, ultimately, hydraulic failure. The hypothesized cost to this strategy is a negative carbon balance due to an inability to maintain photosynthetic rates during drought (McDowell *et al.*, 2008; Galiano *et al.*, 2011). Moreover, when declining water availability is accompanied by elevated temperature, increased respiration rates could raise the likelihood of carbon starvation (Adams *et al.*, 2009, 2013). At the other end of the continuum, anisohydric plants show less strict stomatal regulation in response to drought, and their leaf water potentials more directly track the fluctuations in soil water availability and atmospheric moisture demand. In these species, xylem may operate with narrower safety margins (the difference between the minimum xylem pressure a stem experiences and the pressure at which it would lose some fraction of its hydraulic conductivity, e.g. 50% loss), and they have been hypothesized to be exposed to greater risk of hydraulic failure than isohydric plants (McDowell *et al.* 2008). Although recent research shows that carbon starvation and hydraulic failure are highly interrelated processes that should be studied concurrently (McDowell, 2011; Sala *et al.*, 2012; Sevanto *et al.*, 2014), the link between stomatal regulation and the likelihood of different modes of

mortality is still an open question with important implications for our ability to understand and model plant drought responses (McDowell *et al.*, 2013*a*).

The use of the iso-/anisohydric dichotomy to characterize drought responses in general and the process of drought-induced mortality in particular can be problematic for several reasons. Firstly, this categorization reflects two theoretical extremes, while the stomatal behavior of many plants is better represented as occurring along a spectrum between these two endpoints (Klein, 2014), and it is likely to be more flexible than implied by a dichotomic classification. Several studies have shown that the iso- vs. anisohydric characterization may vary within species as a function of soil water availability (Franks *et al.*, 2007; Zhang *et al.*, 2011; Domec and Johnson, 2012). Secondly, the iso-/anisohydric classification, which was originally proposed in the context of short-term diurnal stomatal responses, rests on the frequently untested assumption that a rapid stomatal response implies the maintenance of relatively constant leaf water potentials over much longer periods. This is not necessarily the case, depending on the relative vulnerability of stomata and xylem to declining water potentials (Martínez-Vilalta *et al.*, 2014). The use of iso-/anisohydry in this context may conflate species differences in stomatal regulation behavior with differences in resistance to drought-induced embolism, which calls for alternative ways of comparing stomatal responses across species (Klein 2014). In addition, different mechanisms of stomatal closure in conifers (based on high abscisic acid concentrations vs. very low leaf water potentials; Brodribb and McAdam, 2013; Brodribb *et al.*, 2014) may complicate the relationship between stomatal regulation and leaf water potential dynamics across species.

Most studies use the relationship between stomatal conductance and either leaf water potential or vapor pressure deficit (VPD) to characterize stomatal behavior. Some studies have shown that higher stomatal sensitivity in response to drying soil (Zhao *et al.*, 2013) or narrower carbon safety margins, defined as the difference between leaf water potential when growth is zero and leaf water potential when net photosynthesis is zero (closed stomata, Mitchell *et al.*, 2014), can lead plants to a negative carbon balance and faster depletion of their reserves. At the same time, the same stomatal conductance at a given

water potential or VPD value may have very different implications depending on the xylem hydraulic vulnerability of the species and fails to account for the fact that leaf water potentials (particularly midday values) are affected by the vulnerability to embolism. The hydraulic connectivity to the soil is another key factor that can complicate the interpretation of correlations between stomatal conductance and water potential or VPD. Plaut *et al.* (2012) and Sevanto *et al.* (2014) demonstrated that pre-dawn leaf water potentials may not reflect soil moisture content during drought in piñon pine (*Pinus edulis*) due to plant hydraulic isolation from the soil. Finally, studies of drought responses in plants have frequently focused on soil water availability as the major stress driver. These studies have shown that stomatal sensitivity (timing of closure during drought) and the magnitude of decrease in hydraulic conductivity under similar drought conditions ranges widely between and within species, depending on hydraulic architecture and root properties (Rogiers *et al.*, 2012*b*; Will *et al.*, 2013). However, drought has two components: reduced soil water availability and increased atmospheric water demand, and stomata respond to both. Vapor pressure deficit increases non-linearly with temperature, generally increasing atmospheric water demand and transpiration at a given stomatal conductance (g_s) (Oren *et al.*, 1999; Breshears *et al.*, 2013). As a result, warming has been shown to exacerbate the effects of drought (Williams *et al.*, 2013). This is important in the context of climate change, because the confidence in future projections is much higher for temperature and VPD than for rainfall and soil water content (IPCC, 2013) and, hence, changes in the former may be more reliable drivers to predict changes in vegetation.

In the present study, we used an ecosystem-scale experiment in a piñon-juniper woodland (dominated by *Pinus edulis* and *Juniperus monosperma*) in northern New Mexico, USA, to test the hypothesis that relatively isohydric plants are less prone to hydraulic failure than relatively anisohydric plants because of their earlier stomatal closure during drought. Experimental treatments were used to simulate different climatic conditions including ambient, reduced precipitation, increased temperature and the combination of both. Piñon-juniper woodlands have been a model system to study drought-related mortality (Breshears *et al.*, 2005, 2009*b*; McDowell *et al.*, 2008; Plaut *et al.*, 2012, 2013;

Limousin *et al.*, 2013). *P. edulis* has been characterized as a relatively isohydric species and *J. monosperma* as relatively more anisohydric (West *et al.*, 2007; Plaut *et al.*, 2012). Additionally, *P. edulis* is more vulnerable to drought-induced xylem embolism than *J. monosperma* (Linton *et al.*, 1998; Willson *et al.*, 2008). Our main objectives here were to: (1) determine the individual and combined effects of temperature and soil moisture on plant hydraulics and gas exchange of coexisting *P. edulis* and *J. monosperma*, and (2) analyze stomatal regulation of these two plant species with contrasting hydraulic resistance, and how this regulation relates to their differential vulnerability to drought. We expect the effects of increased temperature (Heat) and reduced precipitation (Drought) to be additive (or even multiplicative), so that the combined treatment (Heat & Drought) would have the greatest impact on plant performance, with lower stomatal conductance and photosynthesis rates and higher embolism levels. Differences in stomatal regulation between species will differ depending on whether we express stomatal conductance as a function of absolute water potential, as a function of the distance to a "dangerous" plant water potential (e.g., hydraulic safety margin), or directly as a function of percent loss of hydraulic conductivity in the xylem. We assessed the relevancy of these three representations for understanding plant responses to drought in the context of predicting tree mortality. Finally, per McDowell *et al.* (2008) we hypothesize that the anisohydric *J. monosperma* will be more prone to hydraulic failure than the isohydric *P. edulis*, and this will be reflected in narrow safety margins.

MATERIAL AND METHODS

Site description and experimental design

The study was conducted at the Los Alamos Survival/Mortality Experiment located on Frijoles Mesa at 2175 m a.s.l. in Los Alamos County, New Mexico (35°49'5"N 106°18'19"W). Mean annual temperature (25-year mean 1987-2011) is 9.2 ºC, January being the coldest month (-2ºC on average) and July the warmest month (20ºC). Mean annual precipitation (1987-2012) is 415 mm of which roughly 50 % falls during the North American Monsoon season from July to September (Los Alamos Weather Machine http://environweb.lanl.gov/weathermachine/). The site is dominated by piñon

pine (Pinus edulis Engelm.) and juniper (Juniperus monosperma (Engelm.) Sarg.); shrubby gambel oak (Quercus gambelii Nutt.) and an occasional ponderosa pine (Pinus ponderosa C. Lawson) occurs in the vicinity. Soils are Hackroy clay loam derived from volcanic tuff with a typical profile of 0 to 8 cm of sandy loam, 8 to 35 cm of clay and 35 to 150 cm Bedrock (Soil Survey Staff, Natural Resources Conservation Service, United States Department of Agriculture http://websoilsurvey.nrcs.usda.gov/). Soil depth at the site ranges from 40 to 80 cm.

A manipulative experiment was established at the site in spring of 2012 using open top chambers and a drought structure to impose the treatments. A total of 63 trees, 32 *J. monosperma* and 31 *P. edulis*, were randomly selected and assigned to one of the five treatment combinations : (1) control (C), with no heating and no precipitation exclusion; (2) control chamber (CC), trees located inside open top chambers with temperature regulated to match outside air temperature and no rain exclusion; (3) drought (reduced precipitation, D), with ~45 % precipitation interception; (4) heat (H), with a chronic temperature increase of ~5 ºC; and (5) heat & drought (HD), both treatments at the same time. On average, trees in the D and HD treatments were located 10.6 m and 11.0 m from the nearest edge of the drought structure, respectively. This equals a distance of 4.9 and 4.1 times tree height for each treatment. All the trees in C and D treatments lacked chambers, whereas open top chambers were installed surrounding CC, H and HD trees. In total, 18 chambers of different sizes were built, with some chambers including multiple trees (up to five) when the spatial arrangement of trees did not allow building of separate chambers. Ambient temperature was monitored on site (sensors: CS215 Temperature and Relative Humidity Probe, Campbell Scientific, Logan, UT, USA) and used as a reference for chamber temperature control. Similar sensors were installed inside each chamber at two heights, 1 m and 2/3 of canopy height; and chamber temperature was determined from the average. Precipitation exclusion for D and HD treatments was accomplished by means of thermoplastic polymer troughs covering ~45 % of total plot area. Start date for all treatments was June 11th 2012.

Five to nine individuals per species and treatment were monitored, with size ranging from 0.5 to 5.5 m tall and 1 to 5 m of canopy width. Physiological data were collected monthly during spring to fall 2012 and 2013 with a total of seven campaigns per year. The two first physiological campaigns of 2012 were carried out before the treatments began. Meteorological data were recorded using a Campbell Scientific CR1000 datalogger at a maximum frequency of every 30 minutes throughout the experimental period for all parameters except precipitation, which was measured continuously. Meteorological sensors included an AIO 102778 Weather Sensor, (Climatronics, Bohemia, NY, USA) for air temperature, relative humidity, wind speed and direction and barometric pressure, Campbell Scientific CS215 for additional measurements of air temperature and relative humidity, LI-200S Pyranometer (Li-Cor, Lincoln, NE, USA) for global radiation, Li-Cor LI-190SB Quantum Sensor for photosynthetically active photon flux density, and TR-525USW-R3 Tipping Bucket Rain Gauge (Texas Electronics, Dallas, TX, USA). Soil water content (SWC) was measured periodically at 10 to 60 cm depth using Diviner 2000 probes (Sentek Sensor Technologies, Stepney, SA, Australia). The SWC values reported here are the averages for the top 40 cm of soil, as this was the minimum soil depth in the study area.

Water potentials and leaf gas exchange

All sampling campaigns lasted two consecutive days during which water potentials and gas exchange were measured for all trees. Two twigs per tree were collected at two times: before sunrise to measure predawn water potential (ψ_{pd}) and between 11:30 and 13 h (solar time) on the same day to measure midday water potential (ψ_{md}). Twigs were immediately placed in plastic bags and stored in a refrigerator until they were measured (within 1-2 hours) at the field site using a Scholander-type pressure chamber (PMS Instruments, Albany, OR, USA). Daily change in water potential ($\Delta\psi$) was calculated as the difference between ψ_{pd} and ψ_{md}. Instantaneous determinations of leaf stomatal conductance (g_s) and net assimilation rate (A_N) were conducted using a Li-Cor LI-6400 infrared gas-exchange analyzer system. These measurements were carried out at mid-morning, when highest stomatal conductance could be expected, under the following conditions: 380 ppm of CO_2 concentration (as the

average of ambient air fluctuation between 360-400 ppm), 1500 µmol m^{-2} s^{-1} light-saturating photosynthetic photon flux density (PPFD), block temperature fixed to 20 or 25 ºC depending on the air temperature (to reduce the temperature gradient between inside and outside the leaf chamber), and relative humidity on full scrub (as ambient air humidity was very low and this procedure allowed greater stability). Environmental conditions outside the chambers during measurement varied between 13 and 33 ºC for temperature and 750 - 1800 µmol m^{-2} s^{-1} for PPFD. Measurements were taken once steady state gas exchange had been maintained for at least 2 min, on sun-exposed shoots on the southern hemisphere of the canopy. Leaf area of measured foliage was determined using a Li-Cor LI-3100C area meter and used to correct gas exchange rates.

Percentage loss of hydraulic conductivity

Percentage loss of xylem hydraulic conductivity was estimated from the vulnerability curves measured in a subset of our experimental trees (n=3 per species per treatment) from August to October 2013 (14-16 months after treatments began) in a companion study (Zeppel *et al.,* in prep; Figure S1 Appendix I). Branches were cut in the field and wrapped in plastic bags. Once in the laboratory they were cut under water and allowed to rehydrate in a refrigerator for 24 hours before processing to avoid any potential artifacts (Wheeler *et al.*, 2013). Water potentials after rehydration were roughly 0.02 MPa higher than predawn water potentials, indicating xylem integrity. Vulnerability curves were generated using the air injection method (Cochard *et al.*, 1992) and fitted with a Weibull function (Neufeld *et al.*, 1992):

$$PLC = 100 - 100 \cdot e^{[-(Pw/a)^{\wedge}b]} \qquad \text{Eq.2.1}$$

where PLC is the percentage loss of hydraulic conductivity, P_w is the applied pressure that corresponds to the negative value of the plant water potential, and a and b are fitted parameters. From equation (2.1) we can estimate: 1) the water potential corresponding to 50 % loss of conductivity (ψ_{50}= -b); 2) the air-entry point, ψ_e, an estimation of the xylem tension at which pit membranes are overcome and embolism starts to spread (Domec and Gartner 2001); and 3) the hydraulic failure threshold, ψ_{max}, an estimate of the maximum tension of the

xylem before failing and becoming non-conductive. ψ_e and ψ_{max} were estimated following (Domec and Gartner, (2001) and are linear approximations of the applied pressures at the air entry point and at complete embolism respectively. In our study, they correspond to average PLC values of approximately 10 and 90 %, respectively. As no significant treatment effects were detected at the species level, all treatments' level data were pooled to make composite vulnerability curves for each species. Therefore, average values of a and b by species were used in this study to estimate PLC from ψ_{md} values measured over the study period. In order to characterize hydraulic safety margins (ψ_{sf}), we subtracted ψ_e from ψ_{md} (Meinzer *et al.*, 2009). Positive ψ_{sf} values indicate that the ψ_{md} of the sample is above ψ_e and therefore PLC would be expected to be ~0 %. Negative values indicate the likely presence of embolism; the more negative the value the greater the level of embolism. The results were qualitatively identical if other definitions of safety margins were used, e.g. ψ_{50} or ψ_{max} instead of ψ_e (data not shown).

Statistical analysis

We used general linear mixed models to study the time series of ψ_{pd}, ψ_{md}, ψ_{sf}, A_N, g_s, PLC and SWC. Sampling date, heating (yes or no), drought (yes or no) and their interaction were used as explanatory variables in the fixed part of the models. Similar models were used to study the response of these variables (ψ_{pd}, ψ_{md}, ψ_{sf}, A_N, g_s and PLC) to soil water content. Tree nested into chamber was included as a random factor in all statistical models. For this purpose all outside chamber trees were considered to be in the same (fictitious) chamber (no chamber). Similar mixed models with drought, heating and their interaction as fixed factors were used to assess the relationships between response variables: $\Delta\psi$ versus ψ_{pd}, g_s versus ψ_{sf}, and g_s versus PLC. When analyzing the relationship between g_s and ψ_{sf} and PLC we only used data from campaigns for which PPFD > 1250 μmol m^{-2} s^{-1} and air temperature > 18 ºC, to avoid g_s depression due to suboptimal light and temperature conditions.

Prior to all analyses, data were log or square root transformed to achieve normality whenever required (see Appendix I, Tables S1-S13). A different model was fitted for each species in all statistical tests except for seasonal

variation of SWC where both species were considered together. Our model selection procedure always started from the saturated model and progressively removed the variables with the lowest explanatory power until the minimal adequate model with the lowest Akaike Information Criterion (AIC) was obtained. Models within two AIC units of the best fitting model were considered equivalent in terms of fit and the simplest one was selected. All analyses were carried out using the R Statistical Software version 3.0.2 (R Development Core Team, 2012), using the function lme of the nlme package for Linear and Nonlinear Mixed Effects Models.

RESULTS

Over the study period, temperature was above the 25 year average and precipitation varied considerably between studied years (Figure 2.1). Annual precipitation in 2012 and 2013 was 226 and 426 mm, respectively, compared with the 25 year average of 415 mm. 2013 was wetter than 2012 but 30 % of rainfall was concentrated in just one week of September (Figure 2.1c) thus most sampling conducted in 2013 was also during a relatively dry period compared to historical conditions. Soil moisture varied between 3.8 and 43.4 % in control treatments, with an average around 18%. A large peak in SWC was observed after the heavy rains of September 2013 (Figure 2.1d). Winters were cold with sporadic snowfalls from November to April. The two growing seasons studied were warm with average temperature (May - October) of 20.2 and 19.0 ºC in 2012 and 2013, respectively, compared with the 15.7 ºC 25 year average for these months. High temperature and evaporative demand occurred in the dry pre monsoon period, with maximum values around 35 ºC and 4 kPa (Figure 2.1a, b). Treatment trees showed a consistently lower SWC than controls but differences among treatments were relatively small due in part to the regional dry conditions. Only the interaction between heating and date was significant ($P<0.001$), although distinctive periods with significant treatment effects could not be identified (Figure 2.1d). There were no differences in temperature and VPD between C and CC treatments ($P=0.26$ and 0.19, respectively). Daily average temperature was roughly 4.4 ºC higher in H and HD chambers than in D and controls (Figure 2.1a). Higher temperatures in H and HD treatments

were also reflected in an increased evaporative demand of about 0.54 kPa daily mean from May to October (Figure S2 Appendix I).

Overall, H and D treatments resulted in lower ψ_{pd}, ψ_{sf}, g_s and A_N, but the differences were not significant for all dates (Figures 2.2 and 2.3). In general the differences were clearer (and significant) during moderately wet periods (spring, autumn), whereas they decreased under extremely dry conditions or under extremely wet periods such as September 2013.

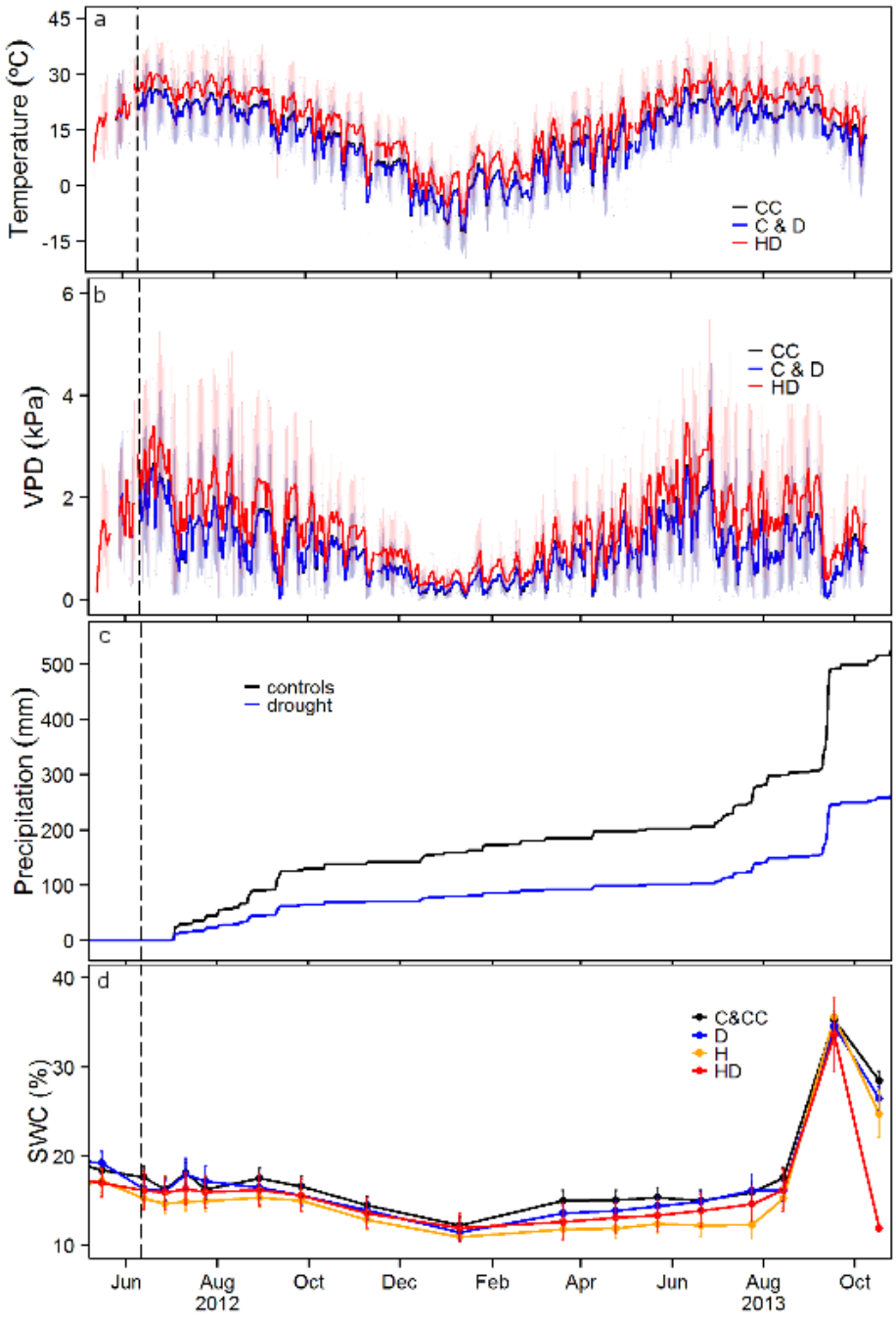

Figure 2.1.
Meteorological conditions during the course of the experiment from June 2012 to October 2013. Panels: a) temperature; b) vapor pressure deficit (VPD) cumulative precipitation; c) cumulative precipitation and d) soil water content (SWC). In panels (a) and (b) solid lines represent daily mean values of the air outside the chambers (no heating) (C&D), inside control chambers (CC), and inside heated chambers (HD) (H omitted due to overlapping); whereas shaded lines indicate maximum and minimum daily values. Panel c shows cumulative precipitation at the SUMO meteorological station (ambient) and as calculated in the reduced rainfall treatments (D& HD).Panel d shows the average SWC from 0 to 40 cm depth. Different colors indicate different treatments. Vertical lines indicate heating treatment beginning in panels a and b, and the first rainfall interception date in c and d.

Between species, drought effects were more noticeable (more dates with significant differences) in *J. monosperma* than in *P. edulis* (Table1). Significant effects (P<0.05) were more frequently associated with drought than heat treatments, particularly in *J. monosperma* (Tables S1-S5 Appendix I). Most of the differences detected between treatments for PLC over time in *J. monosperma* have little biological significance since PLC was typically less than 7% (except June 2013, Figure 2.2c). Interestingly, the interaction between the sampling date and drought and warming, HD treatment, had no additional effect on *P. edulis* for any of the variables studied (i.e., its effect was not different from that of D or H treatments alone), and it only affected the interaction between sampling date and ψ_{pd}, A_N, and g_s (P<0.05) for *J. monosperma*. In some cases plants subjected to the combined HD treatment were closer to the controls (C + CC) than either D or H plants (Figures 2.2, 2.3).

Table 2.1. Number of days with significant treatment effects from drought (D)and heat (H) to controls (C&CC) or their interaction (HD) relative to H and D (not to controls),on predawn water potential (ψ_{pd}),hydraulic safety margin (ψ_{sf}), Percent loss of hydraulic conductivity (PLC), stomatal conductance (g_s), and net assimilation rate (A_N). The + and - symbols indicate positive and negative effects, and n.s. indicates non-significant effects.

	J. monos erma			*P. edulis*		
Variable \ Treatment	D	H	HD	D	H	HD
ψ_{pd}	9 -	4-	0	6-	4-	n.s.
ψ_{sf}	8-	3-	n.s.	2-	1-	n.s.
PLC	7+	3+	n.s.	2+	1+	n.s.
g_s	5-	1-/1+	0	7-	5-	n.s.
A_N	6-	2-	0	5-	5-	n.s.

Neither drought, nor the combined treatment had any significant effect on the physiological variables' (ψ_{pd}, ψ_{sf}, PLC, A_N and g_s) responses to SWC in any of the species. Only heated *P. edulis* trees showed lower ψ_{pd} for a given SWC

(P-value of intercept and slope <0.05, Appendix I Table S6; see also Figure S3a). Stomatal conductance and A_N were also affected by heat in both species (Table S11; Figure S3d,e Appendix I).

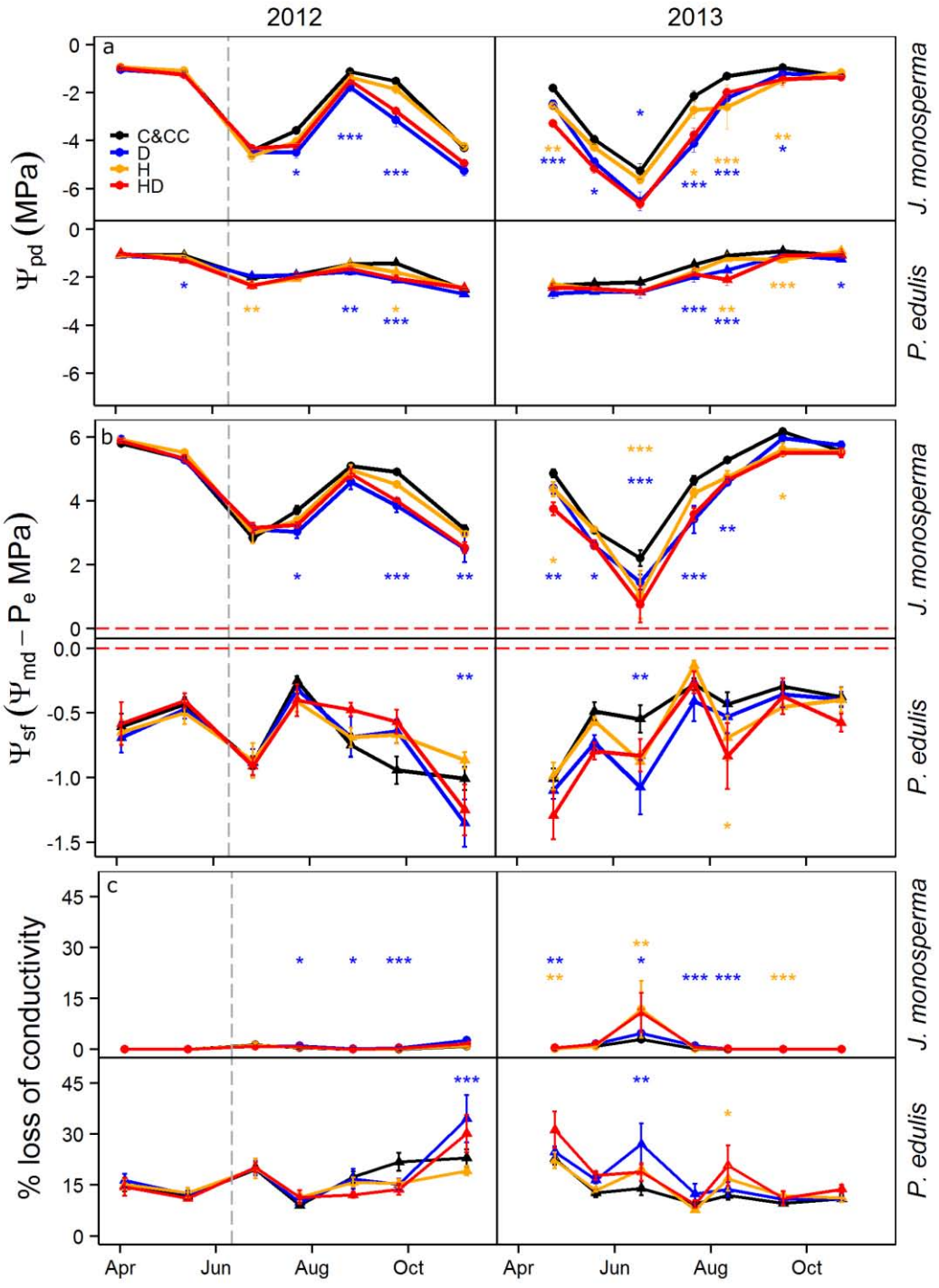

Figure 2.2.
Time series of (a) predawn water potentials (ψ_{pd}), (b) hydraulic safety margin (ψ_{sf}) and (c) percentage loss of hydraulic conductivity (PLC) in branches of *P. edulis* and *J. monosperma* during the experimental period of 2012 and 2013. PLC was estimated from ψ_{md} by hydraulic vulnerability curve (Appendix I, Fig. S1). Means and standard errors are shown. N varies

from five to 13 depending on treatment and species. Vertical dashed lines indicate the date the treatments began and in Fig. 3b red horizontal lines show the point at which ψ_{md} achieves the air-entry point, ψ_e. Asterisks indicate significant differences between treatments (H & D) and controls for a given date(*: 0.01<P<0.05, **: 0.001<P<0.01, ***: P<0.001).

Predawn water potentials (ψ_{pd}) tracked the changes in environmental conditions, particularly SWC and VPD (Figure 2.2), and the average values ranged from -0.9 to -6.6 MPa in *J. monosperma* and from -0.9 to -2.7 MPa in *P. edulis*. ψ_{pd} were highest in spring and autumn, and plants achieved the most negative water potentials in the dry pre-monsoon season. In 2013, spring was drier than autumn, and it was reflected in the Ψ_{pd} of both species (Figure 2.2a). Midday water potentials (ψ_{md}) were correlated with Ψ_{pd} in both species ($R^2_{juniper}$=0.87 and $R^2_{piñon}$=0.23, P<0.001 in both cases).

Vulnerability curves measured in this study showed higher hydraulic resistance at all pressures in *J. monosperma* than *P. edulis* with an average ψ_{50} of -10.8 MPa and -4.4 MPa respectively (Figure S1 Appendix I). When ψ_{md} values were related to air-entry water potentials, the corresponding hydraulic safety margins (ψ_{sf}) reflected similar temporal dynamics between species but very different absolute values: ψ_{sf} was always positive for *J. monosperma* (implying PLC < 10% in this species), whereas it was negative throughout the study period for *P. edulis* (Figure 2.2b; note that the scale is different for each species). These safety margins result in a PLC range from 10 to 40 % in *P. edulis* whereas *J. monosperma* shows barely detectable hydraulic conductivity losses except during the driest season in 2013 (Figure 2.2c). In *J. monosperma* ψ_{pd} and ψ_{sf} remained nearly constant at high soil moisture levels and dropped sharply when SWC decreased below 20 %. A similar pattern was shown by *P. edulis*, although the decline was less steep in this species (Figure S3a, b; Tables S6-S7 Appendix I).

Stomatal conductance (g_s) dynamics were consistent with ψ_{pd} patterns for the two species. However, in spite of large differences in absolute ψ_{pd} values between species, the isohydric *P. edulis* and the anisohydric *J. monosperma* showed similar seasonal stomatal behavior, closing their stomata at similar times in early summer under dry conditions and showing a fast recovery after monsoon rains (Figure 2.3a). Despite similar temporal patterns, absolute A_N

values were slightly higher in *J. monosperma* than *P. edulis*, as shown by the fact that the slope of the regression between *P. edulis* and *J. monosperma* A_N values was slightly, but significantly, lower than one (95% confidence interval = 0.81 - 0.97); see Appendix I Figure S4.

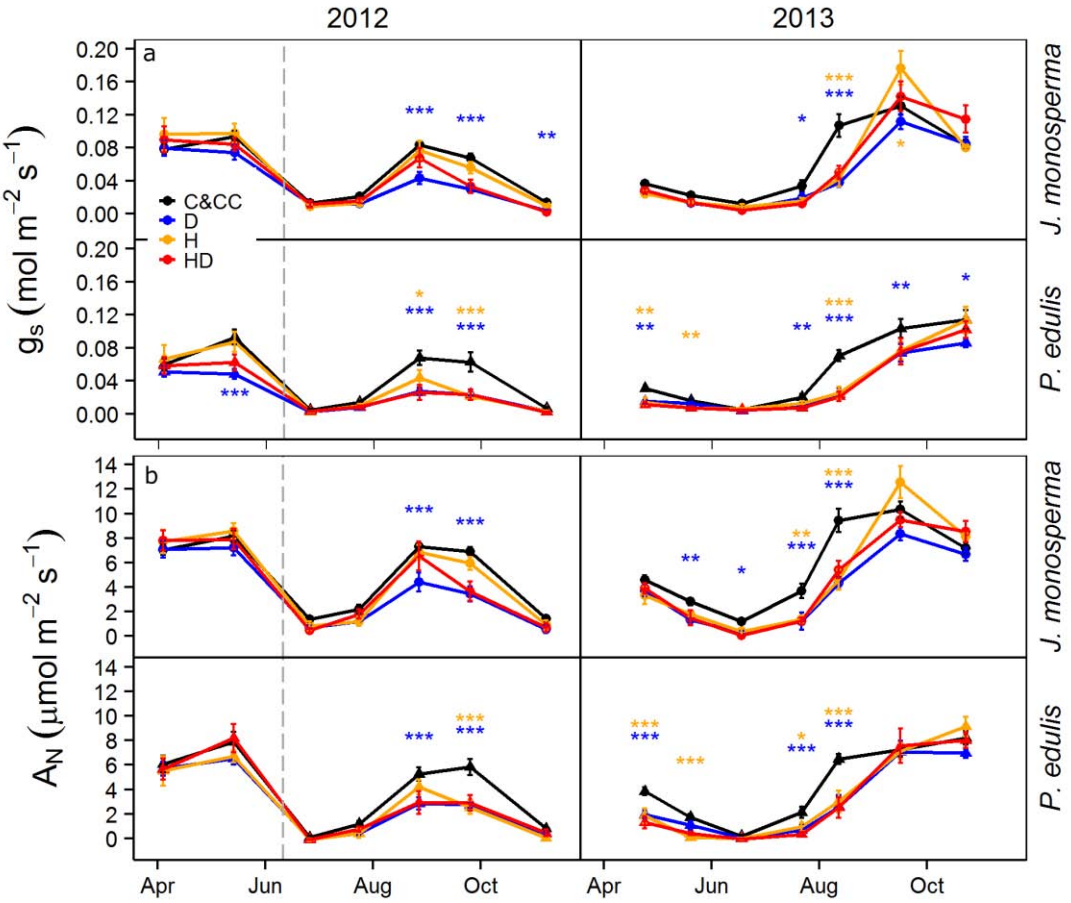

Figure 2.3.
Time series of (a) stomatal conductance (g_s) and (b) net assimilation rate (A_N) in leaves of *P. edulis* and *J. monosperma* during the experimental period of 2012 and 2013.Means and standard errors are shown. N varies from five to 13 depending on treatment and species. Vertical dashed lines indicate the date the treatments began. Asterisks indicate significant differences between treatments (H & D) and controls for a given date(*: 0.01<P<0.05, **: 0.001<P<0.01, ***: P<0.001).

However, this difference declined during relatively dry periods, and A_N rapidly approached ~0 in both species as drought developed (Figures 2.3b; S4). Similar to A_N, absolute g_s values were slightly lower in *P. edulis* (Figure S5 Appendix I); and in this case the difference between species was greater in heated trees (P<0.05). Net assimilation rate and stomatal conductance appeared sensitive to SWC over the entire range of SWC variation, but the

decline in A_N and g_s accentuated when SWC dropped below 20 % (Appendix I Figures S3d and e; Tables S9-10).

The difference between predawn and midday water potentials (Δψ), a measure of the water potential reduction through the plant associated with whole-plant water transport at midday, decreased in both species in response to drying soil (as indicated by declining ψ_{pd}) ($R^2_{juniperus}$=0.34 and R^2_{pinus}=0.64, P<0.001 in both cases; Figure 2.4, Table S11 Appendix I). Δψ decline in *P. edulis* was steeper than in *J. monosperma*. However, this relationship was unaffected by treatments in either species.

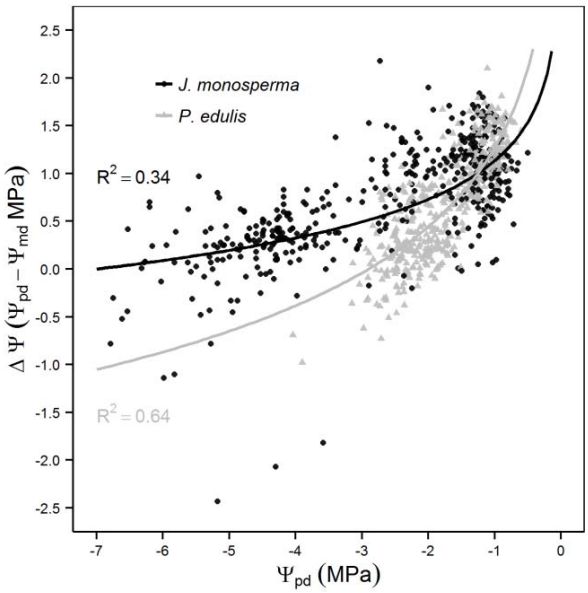

Figure 2.4.
Relationship between the predawn to midday difference in water potential (Δψ) and predawn water potential (ψ_{pd}) in branches of *P. edulis* and *J. monosperma* (solid grey triangles and black circles, respectively).Data corresponds to values measured in all trees during the different campaigns carried out through the experiment (N=435 and 419 for *J. monosperma* and *P. edulis* respectively). Data from different treatments are pooled together. Power regression fits are depicted for both species.

Stomatal conductance was also examined as a function of hydraulic measures for those dates with optimum values of PPFD and temperature (Figure 2.5). In *J. monosperma*, g_s decreased steeply with narrowing ψ_{sf} (P<0.001, R^2=0.67; Figure 2.5a, Table S12 Appendix I), and this relationship was similar across treatments. A similar behavior was observed in *P. edulis*, but in this case ψ_{sf} explained less than 10% of stomatal conductance variability (P<0.001, R^2=0.07). For this species the only significant treatment effect indicated that droughted (D) plants had slightly lower g_s for a given ψ_{sf} than controls (P<0.05; Figure S6a Appendix I). There was a strong negative relationship between stomatal conductance and percent loss of xylem hydraulic conductivity (PLC) for *J. monosperma* across treatments (R^2=0.75; Table S13

Appendix I), although the range of variation of g_s occurred within a mere 10 % variation in PLC (from 0 to 10 %; Figure 2.5b). *P. edulis* drought (D) trees showed lower g_s values when PLC was 0 (P-value of intercept difference <0.05). A clear reduction of stomatal conductance with increasing PLC was also observed in *P. edulis*, although in this case the model explained only 7% of variance in g_s ($P<0.05$, $R^2=0.07$). The previous results implied that, although stomatal closure occurred at much higher (less negative) water potentials in *P. edulis* (as expected), hydraulic safety margins were always wider in *J. monosperma* (Figure 2.2b), even under extremely dry conditions, due to the high sensitivity of its stomata to increasing PLC.

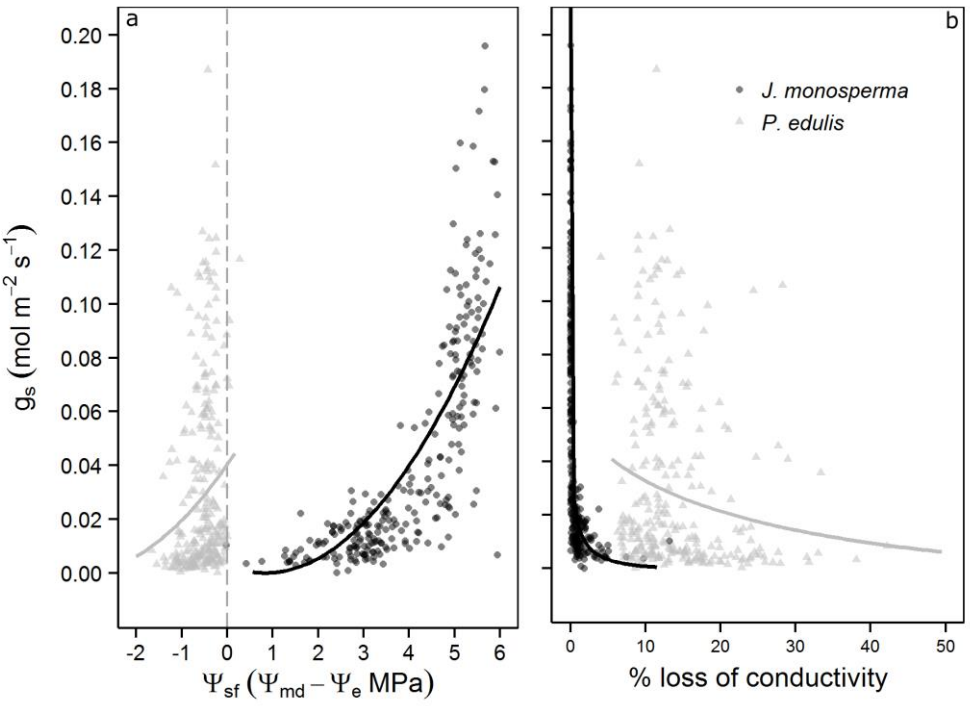

Figure 2.5.
Relationship between stomatal conductance (g_s) and hydraulic safety margin (ψ_{sf}; a) and between g_s and percentage loss of hydraulic conductivity (PLC; b) in *P. edulis* and *J. monosperma* (solid grey triangles and black circles, respectively). In Fig. 5a, the vertical dashed line indicates the point at which the ψ_{md} reaches the air-entry point, ψ_e. Data correspond to values measured in all trees during the different campaigns carried out through the experiment (N=280 and 269 for *J. monosperma* and *P. edulis*, respectively). Solid lines are species-specific linear models for juniper (black) and piñon (grey).

DISCUSSION

Effects of drought and warming on plant hydraulics and gas exchange

Stomatal and hydraulic responses to heat and reduced precipitation treatments clearly illustrate that low water availability and an increase in temperature can have a negative impact on tree performance regardless of the species' strategy to face drought. As expected, drought and heat treatments impacted plant performance resulting in lower water potentials, g_s and A_N rates than controls (Fig. 2.2 and 2.3). Treatment effects were not always significant and differences in SWC were small due to regionally dry conditions in 2012 and 2013. But, ψ_{pd} was lower in D and HD trees relative to the controls, supporting the effectiveness of the drought treatment and suggesting that similar SWC may simply reflect higher water use in the control treatments.

Significant differences between treatments were more frequent under moderate ambient temperatures and water availability, likely because even control trees were severely water-limited throughout much of the study period such that treatment effects often disappeared during the driest part of the year (cf. Zhao *et al.* 2013) and conversely, even drought treatments had abundant water during periods of anomalously high precipitation (SWC ~40 %), such as in September 2013. This is in agreement with a previous study conducted in a nearby area (Mesita del Buey, ~8 km distant) showing that water is not available for plant extraction at SWC < 18 % on the clay loam portion of the soil (Breshears *et al.*, 2009*a*). This result is also consistent with the threshold-like responses to SWC observed for some physiological parameters in this study for SWC ~20 % (Figure S3 Appendix I). Interestingly, measured SWC fluctuated around 18 %, close to this SWC threshold, for most of the study period and regardless of treatment (Figure 2.1d).

The combined treatment, heat and drought, is the most realistic scenario according to IPCC (2013) projections of increasing drought (in terms of frequency and intensity) and warmer temperatures. Our hypothesis was that this treatment would have the largest impact on plants' performance. However, the interaction between drought and heat did not exacerbate stress beyond that experienced by trees in either the heat or drought treatments and thus we reject our initial hypothesis. This is likely because homeostatic regulation of water use resulted in all experimental treatments reaching the SWC threshold of 20% at approximately the same times (Figures 2.1d and S3 Appendix I), suggesting

that immediate synergistic effects on plants hydraulics and stomatal control in response to an increase in temperature and a lower level of soil water content cannot be assumed. Other studies accounting for the effects of both temperature and water availability have shown that high VPD associated with warmer temperatures intensifies the effects of drought (Williams *et al.*, 2013; Will *et al.*, 2013; Duan *et al.*, 2014), and that the soil moisture content at which whole plant C balance became negative increases with temperature (Adams *et al.*, 2009; Zhao *et al.*, 2013). It remains to be established to what extent the lack of interaction between reduced precipitation and warming observed in our study is due to the extremely dry ambient conditions during our study period. This interaction may be easier to detect in moister environments or in other variables not measured here.

Anisohydric species are not necessarily more prone to hydraulic failure

The marked seasonality of temperature and precipitation in the study area, together with our study treatments, provided a wide range of environmental conditions, from reasonably favorable with elevated soil water content and moderate temperature to extremely dry conditions under low soil water content and high temperatures. Over this seasonal and experimental drought gradient *P. edulis* water potentials showed the expected isohydric behavior, with relatively low temporal variation in ψ_{pd}, whereas *J. monosperma* presented a typical anisohydric pattern (Figure 2.2a, West *et al.*, 2007; Plaut *et al.*, 2012; Limousin *et al.*, 2013). This contrasting behavior in terms of water potential dynamics did not result in clear differences in the temporal dynamics of g_s or A_N between species (Figure 2.3). Stomata closed and constrained A_N at similar times and under similar environmental conditions in both species, albeit at very different leaf water potentials (Figures 2.3 and 2.5). This difference is likely related to different mechanisms of stomatal closure in the two conifers studied here. Whereas stomatal closure in pines seems to be characterized by high abscisic acid (ABA) concentrations, in junipers stomatal closure may occur at relatively low ABA levels, presumably due to low guard cell turgor associated with their particularly negative leaf water potentials (Brodribb and McAdam, 2013; Brodribb *et al.*, 2014). Interestingly, our observations coupled with these different mechanisms of stomatal closure imply that low water potentials are not

necessarily associated with loose stomatal regulation, one of the key assumptions of the iso-/anisohydric paradigm. Although g_s and A_N were slightly higher in the relatively anisohydric *J. monosperma* than in *P. edulis* (Figures S4, S5 Appendix I), it is unclear whether this small difference has important biological implications. Our results are consistent with previous studies showing that gas exchange of anisohydric species is not necessarily less constrained than isohydric species during drought (Quero *et al.*, 2011), calling into question the generality of the hypothesis that anisohydric species are less prone to the carbon starvation process (McDowell *et al.* 2008).

Surprisingly, tight control of ψ_{md} and earlier response to drying soil in *P. edulis* (steeper relationship between ψ_{md} and ψ_{pd}) was not enough to avoid excessive hydraulic tensions that cause embolism in this species (Sperry *et al.*, 2002; McDowell *et al.*, 2008). In fact ψ_{md} was beyond the air entry point (P_e, Meinzer *et al.*, 2009) throughout the entire study period in *P. edulis*, implying chronic embolism, whereas hydraulic safety margins were always positive for *J. monosperma*, indicating avoidance of embolism (Figure 2.2b, 2.5a). Two main causes explain the contrasting pattern of embolism we observed in these two species over the course of the study. Firstly, *J. monosperma* is highly resistant to cavitation (low ψ_{50}, Figure S1 Appendix I), as reported previously for this species (Linton *et al.*, 1998; Willson *et al.*, 2008; Plaut *et al.*, 2012), and is well-recognized for its greater drought tolerance and survival ability during a previous severe drought that caused widespread mortality of co-occurring *P. edulis* (Breshears *et al.*, 2005, 2009*b*). Secondly, although stomatal closure occurs at much lower water potentials in *J. monosperma* than in *P. edulis*, when stomatal response is presented as a function of hydraulic safety margins (Figure 2.5a) or PLC (Figure 2.5b), it becomes clear how conservative stomatal behavior actually is in juniper. Our results show that in *J. monosperma*, stomatal conductance is curtailed as soon as xylem tensions approached the air entry point (P_e), avoiding any significant xylem cavitation. This result is not consistent with the hypothesis that anisohydric species will risk embolism during drought and thus are more likely to experience hydraulic failure than isohydric plants (McDowell *et al.* 2008).

More generally, our results challenge the notion that the regulation of leaf water potential per se can be used to establish the most likely physiological mechanism of drought mortality in these conifers. *P. edulis* and *J. monosperma* have long been recognized as examples of isohydric and anisohydric trees (Lajtha and Barnes, 1991; West *et al.*, 2007; Plaut *et al.*, 2012). More recently, the differing stomatal behavior of these two species has been used to hypothesize that isohydric species (piñon) are more likely to experience carbon starvation than anisohydric species (juniper), which are more likely have hydraulic failure at mortality than isohydric species (McDowell *et al.*, 2008; Breshears *et al.*, 2009*b*). However the iso vs. anisohydric characterization of plant species is typically based on a descriptive observation of stomatal response or leaf water potential dynamics without regard to species differences in embolism resistance (Linton *et al.*, 1998; Willson *et al.*, 2008, Figure S1 Appendix I) or other relevant plant attributes related to stomatal closure mechanisms (Brodribb and McAdam, 2013; Brodribb *et al.*, 2014), maintenance of turgor in leaves (Meinzer *et al.*, 2014) or phloem transport (Nikinmaa *et al.*, 2013; Sevanto *et al.*, 2014). Our findings demonstrate that conflation of stomatal behavior with these other elements, and particularly with embolism resistance in *P. edulis* and *J. monosperma*, has misled hypothesis development for drought-induced mortality in trees. Consequently, iso- vs. anisohydric characterization of stomatal behavior, as typically based on observations of leaf water potential dynamics and/or stomatal conductance, should not form the basis of assumptions or hypotheses for the physiological mechanism of drought-induced mortality among tree species. Instead, we advocate consideration of stomatal behavior relative to embolism resistance for predicting the physiological process by which trees die from drought (cf. Klein, 2014; Martínez-Vilalta *et al.*, 2014).

In conclusion, our study highlights the complexity of characterizing stomatal regulation and the importance of how variables are expressed when assessing the physiological implications of such regulation. We examined stomatal responses through a wide range of drought conditions in two model species, the relatively isohydric *P. edulis* and relatively anisohydric *J. monosperma* and conclude that the latter can be considered to have either a

lower stomatal control (the classical view, if g_s is related to absolute water potentials), a higher stomatal control (if g_s is related to hydraulic safety margins) or a similar behavior (if the temporal dynamics of g_s or its response to SWC are considered) compared to the former species. This discrepancy arises from the fact that the original classification between iso- vs. anisohydric plants is based strictly on their capacity to regulate leaf water potentials (Stocker, 1956; Jones, 1998; Tardieu and Simonneau, 1998). Nonetheless, this classification fails to account for the large differences in vulnerability to embolism among species (Choat *et al.*, 2012; Ogasa *et al.*, 2013) and within species (Anderegg, 2015). Moreover, different species may operate over very different ranges of water potentials even under similar environmental conditions, reflecting differences in stomatal closure mechanisms (Brodribb *et al.*, 2014), rooting depth, xylem anatomy (Zeppel *et al.*, in prep), leaf turgor regulation (Meinzer *et al.*, 2014) and phloem transport (Nikinmaa *et al.*, 2013). These distinctions in hydraulic behavior are important and we show that they have very relevant implications for how we understand the mechanism of drought-induced mortality in iso- vs. anisohydric species (cf. McDowell *et al.* 2008). We argue that a more integrative approach incorporating stomatal and xylem responses with declining water potential (cf. Klein 2014; Martínez-Vilalta *et al.* 2014) would be a step forward in classifying drought response strategies and predicting physiological mechanisms of mortality.

ACKNOWLEDGMENTS

We would like to thank the research assistant Jessica Wilks who was involved in this study. This study was supported by DOE-Office of Science, Office of Biological and Environmental Research, the Spanish Ministry of Economy and Competitiveness (MINECO) via competitive grant CGL2013-46808-R, NGF was supported by an FPI scholarship from the MINECO associated to grant CGL2010-16373, MZ was supported by an Australian Research Council Early Career Researcher fellowship (DECRA). HDA was supported by Los Alamos National Laboratory LDRD Director's Fellowship.

Chapter 3

Isohydric species do not necessarily show lower assimilation during drought

Núria Garcia-Forner, Carme Biel, Robert Savé, Jordi Martínez-Vilalta

(*in preparation*)

Abstract

Stomata are key structures in the study of drought-induced plant mortality because of their ability to regulate carbon and water flows between leaves and the atmosphere. Strong regulation of leaf water potential (isohydry) is commonly linked to 'early' stomatal closure under drought, which in turn is believed to imply lower hydraulic risk at the expense of reduced carbon assimilation. Hence, the iso/anisohydric classification has been widely used to assess drought-resistance and mortality mechanisms across species, but the underlying assumptions have been rarely tested. These assumptions include a direct correspondence between the iso/anisohydric water potential regulation and stomatal behavior across species, and similar vulnerability to xylem embolism in iso- and anisohydric species. Our main objective is to assess the physiological mechanisms that underlie differences in drought resistance between *Phillyrea latifolia* and *Quercus ilex* under controlled, experimental conditions. These two species coexist in Mediterranean forests and are examples of anisohydric and isohydric behaviors, respectively. Specifically, we hypothesize that lower water potentials in *P. latifolia* will not necessarily be associated with narrower hydraulic safety margins, not with higher stomatal conductance or longer periods of positive gas exchange. Our results confirm the stronger regulation of leaf water potential in *Q. ilex*, but this behavior did not imply lower hydraulic impairment, due to lower resistance to xylem embolism in this species. We found similar temporal patterns of stomatal conductance and assimilation between species. If anything, the anisohydric *P. latifolia* tended to show lower assimilation rates than *Q. ilex* under extreme drought. The fact that *P. latifolia* was as carbon-constrained as *Q. ilex* was also indicated by similar growth rates and carbon reserves dynamics in both species. Our study warns against making direct connections between leaf water potential regulation, stomatal behavior and the mechanisms of drought-induced mortality in plants.

Keywords

Holm oak forest, stomatal behavior, carbon constrains, hydraulic risk, drought-resistance.

INTRODUCTION

Plants are in constant need for water to sustain cell metabolism and the turgor necessary for cell division and tissue expansion (Tang and Boyer, 2002; Sala and Hoch, 2009). Water and nutrients are acquired in roots and transported by the transpiration stream from roots to the other plant organs (Tyree and Zimmermann, 2002). Both water transport integrity and metabolic activity need to be assured in order to maintain physiological activity and, eventually, prevent mortality under stress (Sala *et al.*, 2012; Nardini *et al.*, 2014). Intense or recurrent droughts may disrupt xylem and phloem transport (Tyree and Zimmermann, 2002; Sevanto *et al.*, 2014; Dickman *et al.*, 2015), reducing plant production (Gulías *et al.*, 2002; Galmés *et al.*, 2007; Ogaya *et al.*, 2014) and eventually leading to plant death (McDowell, 2011). The effect of a given drought on plant performance depends on the length and intensity of the stress but also on the species-specific strategy to face water shortage (Martínez-Vilalta *et al.*, 2003; Galmés *et al.*, 2007; McDowell *et al.*, 2008; Quero *et al.*, 2011; Vilagrosa *et al.*, 2014; Pivovaroff *et al.*, 2015). The costs and implications of these strategies need to be evaluated to establish if some of them make some species more resistant to extreme drought than others (Hartmann *et al.*, 2015).

Plant strategies to cope with water shortage involve a complex set of traits related to water and carbon economies. These traits show strong interactions and can be relevant at different organizational levels and time-scales (Mencuccini, 2014). Some of the drought responses that allow plants to keep an adequate water balance attempt to increase water uptake and/or decrease water losses (Regier *et al.*, 2009). For instance, in the mid-term plants can increase resource allocation to the root system (Markesteijn and Poorter, 2009; Nippert and Holdo, 2015), reduce their leaf area (Bréda *et al.*, 2006; Ogaya and Peñuelas, 2006; Pinkard *et al.*, 2011; Limousin *et al.*, 2012) or modify their life cycle (Taeger *et al.*, 2014; Adams *et al.*, 2015) to improve their water balance. At shorter time scales and at tissue and organ levels the affected processes (and the resulting interactions) may include stomatal behavior, xylem and phloem transport or source-sink carbon balance (Mencuccini, 2014). Among these, stomatal closure plays a central role on plants' response to drought stress by reducing plant transpiration and avoiding

excessive xylem tensions that could reduce or impede hydraulic transport (Sperry, 2000; Brodribb *et al.*, 2003).

Stomata conductance is also directly linked with the plant carbon economy by controlling CO_2 uptake and thereby, assimilation. If carbon acquisition is constrained by stomatal closure (e.g., under drought), carbon-related process such as cell metabolism may become dependent on carbon reserves and/or their availability (Sala *et al.*, 2010). Frequently, it is assumed that those species that operate at relatively low water potentials (Ψ_w) (anisohydric) close stomata more slowly than species maintaining relatively high Ψ_w (isohydric) and, therefore, are able to sustain carbon assimilation for longer under drought (McDowell *et al.*, 2008; Domec and Johnson, 2012). Nevertheless, stomatal responses are complex and are also affected by vapor pressure deficit (Zhang *et al.*, 2011; Rogiers *et al.*, 2012*b*), light intensity (Guyot *et al.*, 2012) and hormonal signals, particularly abscisic acid (ABA) concentrations (Tardieu and Simonneau, 1998; Brodribb and McAdam, 2013; Brodribb *et al.*, 2014). Klein (2014) showed in a study on 70 plant woody species across the iso-/anisohydric spectrum that differences in stomatal sensitivity to Ψ_w were smaller than differences in xylem sensitivity (by comparing the Ψ_w at which 50 % of stomatal conductance or hydraulic conductivity were lost). In addition, the impact on water potential regulation of a given stomatal sensitivity to Ψ_w will depend also on the vulnerability of the hydraulic system of the plant (Martínez-Vilalta *et al.*, 2014).

In a previous study, Garcia-Forner et al. (2015) compared the responses of *Pinus edulis* and *Juniperus monosperma* subjected to experimental drought in SW USA, and found very little differences between species in the time they reached ~0 stomatal conductance, despite the fact that the two species operate at very different water potentials and are considered paradigmatic examples of iso- and anisohydric behavior. Thus, keeping relatively high (close to zero) Ψ_w may not necessarily imply a cost in terms of carbon assimilation under drought. If that was true, isohydric species would not necessarily show greater dependence on their stored carbohydrates nor would be more prone to death through carbon starvation (*sensu* McDowell et al. 2008). In addition, stomatal closure at lower (more negative) water potentials in the juniper (anisohydric

species) did not result in higher hydraulic impairment in this species, due to its higher resistance to xylem embolism (Garcia-Forner *et al.*, 2015). It is thus important to establish whether these results extend to other species with contrasted iso-/anisohydric behavior and clarify the implications of water potential regulation in terms of stomatal responses and the physiological mechanisms of plant mortality under drought.

Forest die-off and an increase of crown defoliation have been reported in several areas across the Mediterranean basin, and it has been associated to an increase in average temperatures and a decrease in water availability (Carnicer *et al.*, 2011). An increase in plant mortality and reduced seedling recruitment could trigger shifts in vegetation composition (Mueller et al. 2005, but see Lloret et al. 2012). Holm oak (*Quercus ilex*), an evergreen, isohydric tree (e.g., Quero et al. 2011) dominating large forest areas in the Mediterranean basin, has been shown to strongly reduce growth and increase stem mortality rates in response to reduced precipitation (Lloret and Siscart, 1995; Peñuelas *et al.*, 1998, 2000; Lloret *et al.*, 2004*b*). By contrast, the coexisting species *Phillyrea latifolia* shows lower minimum water potentials (Ogaya *et al.*, 2014) and it is able to maintain water transport and photosynthesis at lower water potentials than *Q. ilex* (Martínez-Vilalta et al. 2002). Accordingly, field studies have shown lower drought-induced stem mortality in *P. latifolia* than in coexisting *Q. ilex*, as well as higher recruitment of the former species (Saura-Mas *et al.*, 2015). Similar results have been obtained in response to experimental throughfall reductions (Ogaya *et al.*, 2003; Ogaya and Peñuelas, 2007). However, longer term experiments have shown that *Q. ilex* populations have a high capacity to acclimate to experimentally reduced water availability (Barbeta *et al.*, 2013; Rosas *et al.*, 2013), highlighting the need for further studies characterizing the mechanisms that could trigger a shift in the composition of Mediterranean holm oak forests.

In this study we compare physiological responses to extreme drought of *P. latifolia* and *Q. ilex* saplings in a greenhouse experiment. These two Mediterranean species are considered models of anisohydric and isohydric behavior, respectively. Our main objectives are to assess whether the differences observed in the field are maintained when the two species are

grown under identical, controlled environmental conditions; and to study the physiological mechanisms that underlie species differences in drought resistance. In particular, we hypothesize that lower water potentials in *P. latifolia* (1) will not imply that this species operates closer to hydraulic failure, and (2) that they will not be necessarily associated with higher stomatal conductance or longer periods of positive gas exchange (assimilation). As a result, we expect similar growth and NSC dynamics between species.

MATERIAL AND METHODS

Plant material and experimental design

The study was conducted in a polytunnel greenhouse located in the experimental facilities of the Institute of Agricultural, Food Research and Technology (2º10'3"N, 41º37'56"E, 203 m asl; IRTA, Caldes de Montbui, Spain). Three species were initially included in the experiment: *Phillyrea latifolia*, *Quercus ilex* and *Pinus sylvestris*. However, due to large differences in species' resistance to drought (all pines died within a few months of the treatment onset) we decided to present the results in two separate papers, one focused on the pine drought responses (Garcia-Forner et al., in review), and the present one focusing on *Phillyrea latifolia* and *Quercus ilex*. For these two later species the study lasted from 2011 to 2014.

In April 2011, 50 saplings (7 years old and ~ 1.5 m tall, grown in individual pots) per species were transplanted into the ground at random locations within a regular grid inside the tunnel. Individual plants were separated 1.5 m. Soils are farmlands with sandy loam texture and a minimum depth of 80 cm, and were plowed (subsoiled) before planting the trees. The acclimation period in the greenhouse (no treatment) lasted one year during which the water regime (applied twice per week) followed the monthly rainfall pattern at Prades Mountains (41º19'58.05''N, 1º0'52.26''E, 1015 m asl; NE Spain), where the two study species coexist, reduced to 80 % to account for differences in soil depth, shallower in Prades.

After one year of acclimation, 6 and 8 *Q. ilex* and *P. latifolia* trees, respectively, were assigned to the control (C) treatment and the remaining 44

and 42 trees per species, respectively, were assigned to the drought (D) treatment. The temporal development of the study includes six experimental periods: acclimation period, from April 2011 to May 2012; first drought period, from May 11 to October 2, 2012; recovery period, from October 3, 2012, to May 24, 2013; second drought period, from May 25 to September 7, 2013; unintended flooding on September 7-9, 2013; and the third drought period from the flooding until the end of 2014 (Figure 3.1). Control trees were watered during the four years following the pattern explained above, while this watering regime was applied to drought trees only during the acclimation period and the recovery period. During drought periods, D trees received no watering (and the tunnel structure excluded rainfall). Exceptional rains caused a flooding in the study area in September 2013 (cloud symbol, Figure 3.1), which resulted in running water entering our tunnel greenhouse. In practice, the period immediately after the flooding can be thus considered a second recovery period after a water input pulse.

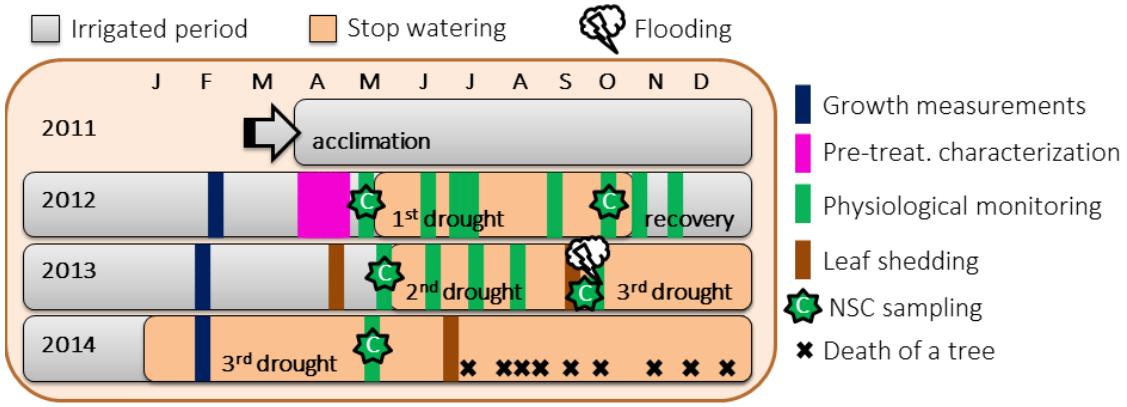

Figure 3.1.
Experimental design and timing of different measurement campaigns. Monthly information from 2011 to 2014 is shown. Experimental design is divided in 6 periods: acclimation, 1st drought, recovery, 2nd drought, unintended flooding (cloud symbol) and 3rd drought. Acclimation and recovery periods are shown in grey and drought periods in brown. Vertical lines indicate when different measurements were taken: growth measurements (basal diameter and twig diameter and length), dark blue; pre-treatment species characterization (P-V curves, light and CO_2 response curves), pink; physiological monitoring (gas exchange, chlorophyll fluorescence and water potentials), green; and leaf shedding, brown. Symbols filled with a *C* letter indicate sample collection for non-structural carbohydrates. Black crosses indicate when a tree dies (mortality was only observed in *Q. ilex*).

Overview of morphological and physiological measurements

During the acclimation period all trees were characterized morphologically (first blue line, Figure 3.1). An additional physiological characterization (pink rectangle, Figure 3.1) was performed in a subset of five trees per species, in which we measured photosynthetic curves in response to light and CO_2. Pressure-volume (P-V) curves were also established in a subset of trees (N = 5-6 individuals per species) during the acclimation period and in spring and fall 2012. Tree growth was evaluated once per year in all trees (in winter) and leaf shedding was also evaluated in spring and autumn 2013 and in spring 2014. Leaf water potentials (predawn and midday), leaf gas exchange and chlorophyll fluorescence were monitored from 2012 to 2014 (Figure 3.1): once during the acclimation period (May 2012), five times during the first drought, twice during the recovery period in 2012, once prior to the second drought period, three times during the second drought period, a week after the 2013 flooding and, finally, eight months after the third drought period had started (May 2014). Leaf dark respiration was not measured in 2012.

In 2012 physiological measurements were performed in a subset of 30 trees per species (5C + 25D trees). The following years all trees were measured but half of the D trees were subjected to an additional treatment that did not interference with the current study. These trees are not considered here. Thus, in 2013 and 2014 we include all C trees plus 23 D trees per species (from which 13 were also tracked in 2012). In the same subsets of trees branches were collected to measure non-structural carbohydrates (NSC) in spring and fall over the three study years (except for fall 2014). All these measurements are described in detail in the next sections.

A visual evaluation of the condition of each tree was conducted throughout the experimental period to assess tree aboveground death, defined as the time when all leaves were brown and dry and there was no green phloem in the trunk. The frequency of the assessments was approximately weekly, but it intensified during the most stressful periods and towards the end of the experiment.

Meteorological and soil moisture measurements

Ambient temperature (T) and relative humidity (RH) were monitored in the tunnel greenhouse at 1.5 m height with two EHT Temperature/RH sensors (Decagon Devices Inc., Pullman, Washington, USA). Four SD222 photosynthetic active radiation (PAR) sensors (Macam Photometrics Ltd., Livingstone, UK) were installed at 3 m height across the length of the greenhouse. Temperature, relative humidity and PAR were recorded every 15 minutes with an Em50 datalogger (Decagon Devices Inc.; for temperature and RH) and a CR10X datalogger (Campdell Scientific Inc., Logan, UT, USA; for PAR).

Soil water content (SWC) was monitored in 2012 with a total of twelve 10HS Soil Moisture Probes (Decagon Devices Inc.) installed at 25 cm depth and at a distance of 30 cm from randomly assigned trees (four next to droughted trees and two next to control trees for each species). These probes were substituted by 18 EC-5 Soil Moisture Probes (Decagon Devices Inc.) at the end of 2012. Nine probes per species were installed nearby 6 D trees and 3 C trees, at the same soil depth as before. SWC data was recorded every 30 minutes using a CR1000 datalogger (Cambdell Scientific Inc.). All meteorological data and soil water content was monitored from December 2011 to September 2014.

Morphological measurements

In March 2012, we measured the height (H) and stem diameter (DBH) at 5 cm from the soil of all trees. Trees' sapwood area (A_S) was calculated from stem diameter (no hardwood was observed). At this point total leaf area per plant (A_L) was estimated by multiplying total foliated branch length by mean leaf density and mean individual leaf area. Mean leaf density was estimated by counting the number of leaves in 20 cm long sections of two representative branch segments per tree. In these same segments individual leaf area was estimated by measuring midrib length in a subsample of two leaves per segment and using the relationships between midrib length and leaf area determined previously in the same experimental trees for each species. Tree-level leaf-to-sapwood area ratio (A_L:A_S) was calculated as the quotient between A_L and A_S. In 2013, two branches per tree were selected to estimate A_L:A_S in

the same manner, and these branch-level measurements were repeated three times between 2013 and 2014.

Stem basal area increment (BAI) and relative growth rate (RGR) in twigs were measured annually. For the latter, three twigs located ~1 m above the ground were selected per tree in winter 2011 and were measured annually to calculate the relative growth rate in basal diameter (RGR.D) and length (RGR.L). These measurements were averaged per tree.

Initial physiological characterization

Pressure-volume curves were generated using the free transpiration method (Galmés *et al.*, 2011) on current-year shoots (~10 cm long) of 5-6 trees per species, and were repeated three times to account for seasonal variability. After collection, shoots were allowed to rehydrate overnight and, afterwards, their water potential and weight were measured repeatedly during air drying until leaves showed signs of damage. Dry weight of the samples was determined after 48 h at 65 ºC. Osmotic potential at full turgor (π_{ft}) and the water potential at turgor loss point (Ψ_{tlp}) were calculated from the plot of $1/\Psi_w$ against the RWC of the sample (Choat *et al.*, 2007).

Light and CO_2 response curves were performed on fully expanded leaves from five trees per species. We used a Li-6400 XT open infrared gas-exchange analyzer system (Li-Cor, Lincoln, NE, USA) fixing chamber conditions to 43 ± 2 % RH and 25 ºC of temperature. For light-response curves, quantum flux density started at 750 µmol m^{-2} s^{-1}, increased until 1500 µmol m^{-2} s^{-1} and then it was slowly reduced to 0. Dark respiration rate (R_d) and the maximum photosynthetic rate (A_{max}) were estimated from these curves. In the CO_2 response curves PPFD was fixed to 1500 µmol m^{-2} s^{-1} and ambient concentration of CO_2 was decreased slowly from 390 to 50 µmol m^{-2} s^{-1} and then increased to 1250 µmol m^{-2} s^{-1} (Galmés *et al.*, 2007). To fit these curves we used individual R_d values from the light response curves. Maximum RuBP saturated rate of carboxylation ($V_{c,max}$), the electron transport rate driving RuBP regeneration (J_{max}) and the triose-phosphate utilization rate (V_{TPU}) were calculated from CO_2 response curves following Farquhar et al. (1980) and von Caemmerer (2000).

Physiological monitoring

Monitoring consisted in seven, four and one campaigns in 2012, 2013 and 2014, respectively, including measurements before, during and after the imposed drought during the first two years (Figure 3.1). At each time leaf samples were cut before sunrise for predawn water potential (Ψ_{pd}) and at noon (solar time) for midday water potential (Ψ_{md}). After harvesting, samples were wrapped and stored in a cooler until measurements were taken within two hours of collection. All water potentials were determined with a pressure chamber (3005 Soil 265 Moisture Corp., Santa Barbara, CA, USA). On the same dates, instantaneous gas exchange and chlorophyll fluorescence were measured using a Li-Cor LI-6400XT open infrared gas-exchange analyzer system equipped with a 6400-40 Leaf Chamber Fluorometer (Li-Cor, Lincoln, NE, USA). Dark respiration (R_d, in 2013 and 2014 only) and maximum and minimum fluorescence in dark adapted leaves were measured before dawn (3-5 am, solar time), and the two latter variables were used to calculate maximum quantum yield (F_vF_m, Baker 2008). Net assimilation rate (A_N) and stomatal conductance (g_s) were determined on the same trees and the same fully expanded leaves at 8-11 am (solar time). Chamber conditions were fixed at 400 ppm CO_2, 1500 µmol photons m^{-2} s^{-1}, 43 ± 3 % RH and 25 ºC block temperature. All measurements were taken once steady state had been achieved.

Non-structural carbohydrates

Non-structural carbohydrates (NSC) in branches were measured five times on the same trees monitored for gas exchange: before (spring) and after (fall) the drought treatment in 2012 and 2013 and after eight months with no watering in spring 2014 (see Figure 3.1). All samples were rapidly microwaved for 90s at 750 Watts to stop enzymatic activity and then dried for 96 h at 65 ºC. Samples were then debarked, ground to fine powder and NSC concentrations were analyzed following the enzymatic procedures described by Hoch et al. (2002), including minor modifications by Galiano et al. (2011). NSC were calculated as the sum of glucose, fructose, sucrose and starch, individually quantified.

Statistical analyses

We used simple linear models to compare parameters extracted from the photosynthetic response curves (R_d, A_{max}, $V_{c,max}$, J_{max}) between species. General linear mixed models were used to study time series of Ψ_{pd}, Ψ_{md}, A_N, g_s, F_vF_m, R_d, leaf shedding and NSC. In all cases, tree was included in the random part of the models, and date, species, treatment and their interactions were considered as fixed factors. We used similar models to fit the relationships between Ψ_{pd} and A_N and g_s. In these models, tree was also included as a random factor and species, treatment and their interaction were considered fixed effects. In all cases model selection was based on Akaike information Criterion (AIC). *Post-hoc* tests were carried out using the function *cdl* from the package *lsmeans* for pairwise comparisons of least squares means. To compare assimilation and stomatal rates between species, average A_N and g_s values measured in one species were regressed against the values of the same variable measured concurrently in the other species, using model II simple linear regression and the major axis method (MA). In these analyses, deviation from the zero intercept and 1:1 slope indicate differences between species. The relationship between stomatal conductance and net assimilation rate was evaluated using the empirical model of Ball, Woodrow & Berry (1987) (cf. Limousin et al., 2013):

$$g_s = g_0 + m\frac{A_N * RH}{C_a} \quad \text{Eq. 3.1}$$

Where *RH* and C_a are the relative humidity and the CO_2 concentration around the leave inside the chamber and g_0 and *m* are the intercept and slope of the regression, respectively. All analyses were carried using the R statistical Software v.3.0.3 (R Development Core Team, 2014), using the functions *lm* from the *nlme* package for linear models and *lmodel2* from the *lmodel2* package for model II regression. Significant differences were considered when $P<0.05$.

RESULTS

Environmental conditions and trees survival

Environmental conditions inside the greenhouse followed typical Mediterranean patterns with maximum temperatures and VPD during summer

and occasional cold spells during winter. Annual averages during the three considered years were ~17 ºC and ~ 2 kPa (day-time), being 2012 the hottest year (Figure S1 Appendix II). Yearly maximum PAR values were observed between June and July, reaching 1350 µmol m^{-2} s^{-1} (Figure S1 Appendix II). Note that PAR inside the greenhouse was approximately 14 % lower than outside the greenhouse (difference calculated for 2012; www.ruralcat.net, Caldes de Montbui meteorological station). Soil water content before the first drought treatment was applied in 2012 was between 24-28 % and decreased to ~21 % in C trees and ~13 % in D trees during the first summer (Figure 3.2). Minimum soil moisture in 2013 was below 10% in D trees of both species. A one-time flooding event in September 2013 caused the recovery of soil moisture in D trees to values close to those of C trees. However, differences between the two treatments developed again quickly and remained very large until the end of the study period (Figure 3.2).

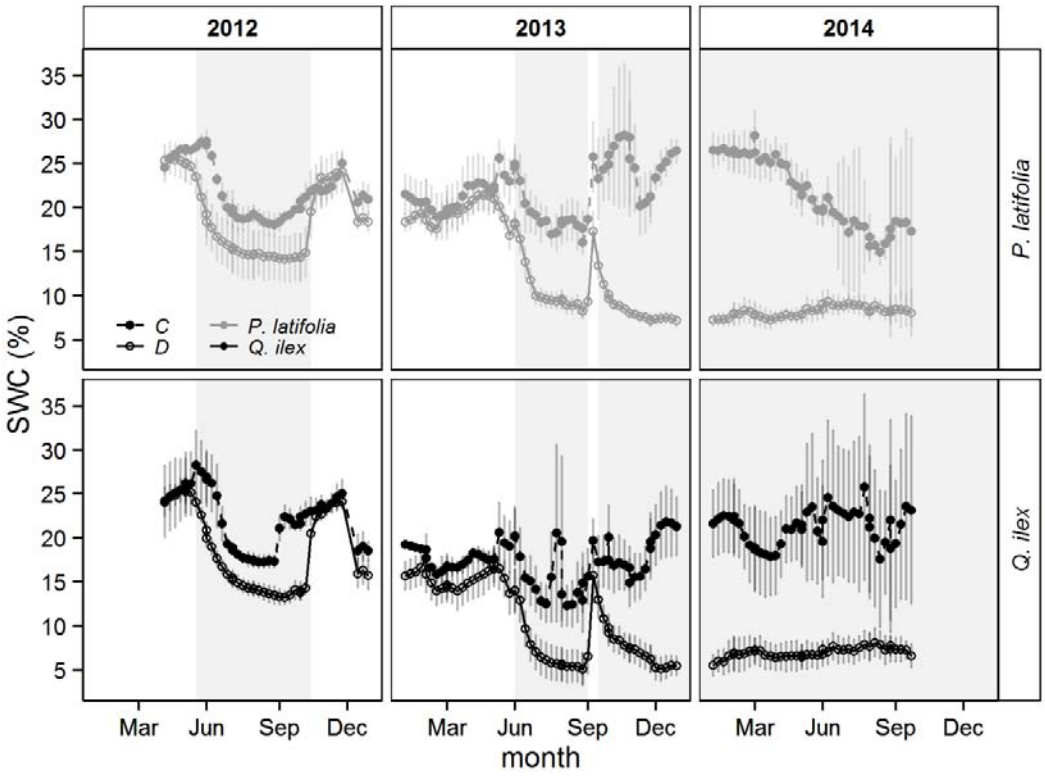

Figure 3.2.
Soil water content at 25 cm depth during the course of the experiment from April 2012 to September 2014. Means and standard error of *P. latifolia* (upper panels, grey) and *Q. ilex* (lower panels, black) are shown. In all cases, empty circles indicate D trees and filled circles denote C trees.

There was no sign of decline from 2011 to 2013 in any of the species. No mortality was detected in *P. latifolia* trees over the study period from 2011 to the end of 2014. By contrast, *Q. ilex* crown desiccation started in 2014 and, by the end of this year (end of the study) 8 % of *Q. ilex* trees (all from the D treatment) had died.

Initial species characterization

There was no difference in photosynthetic response to light and CO_2 between species, except for R_d, which was approximately half in *Q. ilex* compared to *P. latifolia* (P<.01; Table 3.1). Among P-V parameters, *P. latifolia* showed lower minimum absolute π_{ft} and Ψ_{tlp} than *Q. ilex* (Table 3.1). At the beginning of the experiment trees had a DBH of 23.5 ± 0.5 mm and were 169 ± 0.3 cm tall, on average. The size of C trees was similar between species and there was no difference between C and D trees within species; however, *Q. ilex* D trees were slightly but significantly smaller than *P. latifolia* ones (Table 3.2). Tree level A_L was 0.89 ± 0.4 m^2 on average and both A_L and $A_L A_S$ were similar between species and treatments (Table 3.1).

Table 3.1. Summary of the parameters extracted from the photosynthetic response curves (light and CO_2) and the pressure-volume curves at the species level. Average values and standard errors (in parenthesis) of the photosynthetic curves and absolute minimum of the pressure-volume parameters are shown. N is 18 per species for pressure-volume curves (3 times*6 trees) and 6 for the photosynthetic response curves. Letters indicate significance differences between species (P<0.05).

	P. latifolia	***Q. ilex***
R_d (µmol CO_2 m^{-2} s^{-1})	2.11 (0.26)[a]	1.01 (0.21)[b]
$V_{c,max}$ (µmol CO2 m^{-2} s^{-1})	64.58 (8.24)	63.19 (8.28)
J_{max} (µmol e^- m^{-2} s^{-1})	94.65 (9.26)	91.31 (7.93)
V_{TPU}	6.97 (0.60)	6.67 (0.69)
A_{max} (µmol CO_2 m^{-2} s^{-1})	10.98 (1.52)	10.47 (1.15)
π_{ft} (MPa)	-1.64	-1.16
Ψ_{tlp} (MPa)	-2.32	-1.60

Dark respiration rate (Rd), maximum RuBP saturated rate of carboxylation ($V_{c,max}$), electron transport rate (J_{max}), triose-phosphate utilization rate (VTPU), maximum assimilation rate (A_{max}), osmotic

potential at full turgor (π_{ft}), water potential at turgor loss point (Ψ_{tlp}).

Table 3.2. Morphological and hydraulic characteristics of control (C) and drought (D) trees of each species. Morphological measurements were conducted prior to spring 2012 in all trees. Numbers in parenthesis indicate standard errors and letters are shown when significant differences between groups were detected (P<0.05).

	P. latifolia		***Q. ilex***	
Variable	**C**	**D**	**C**	**D**
DBH (mm)	23.9 (2.0)^{ab}	25 (0.8)^{a}	21.7 (1.4)^{ab}	22.3 (0.6)^{b}
A_L (m^2)	1.00 (0.04)	0.94 (0.07)	1 (0.2)	0.8 (0.06)
A_L:$A_{S,tree}$(m^2cm^{-2})	0.25 (0.05)	0.19 (0.01)	0.27 (0.05)	0.20 (0.02)
Height (cm)	167.2 (6.1)^{ab}	178.2 (3.7)^{a}	171.4 (14.4)^{ab}	160.3 (5.5)^{b}

Physiological time courses

Overall, in 2012 and 2013 Ψ_{pd}, Ψ_{md}, A_N, g_s and F_vF_m were higher in spring prior to drought onset and decreased as soil dried during the summer (Figures 3.3 and 3.4). Drought recovery depended on the studied variable and year. The only measurement campaign performed in 2014 (May) showed similar or lower water potentials, A_N, g_s and F_vF_m compared to those measured at the peak of stress in D trees during the previous years. In *P. latifolia* C trees R_d increased significantly in 2014 up to values higher than those observed in July 2013 (Table S5 Appendix II; Figure 3.4c).

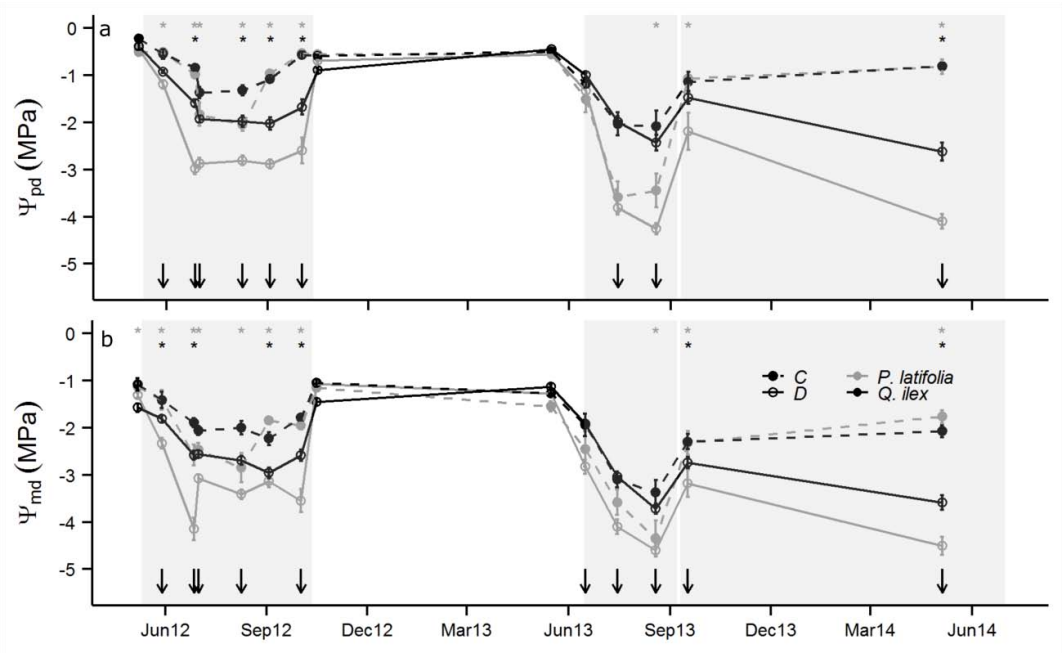

Figure 3.3.

Time course of (a) predawn water potential (Ψ_{pd}) and (b) midday water potential (Ψ_{md}) in leaves of *P. latifolia* (grey) and *Q. ilex* (black) during the experimental period. Means and standard errors are shown. In both species solid circles and dashed lines indicate C trees and empty circles and solid lines indicate D trees. Asterisks indicate significant differences within species between treatments (C vs. D) and arrows indicate significant differences between species for D trees.

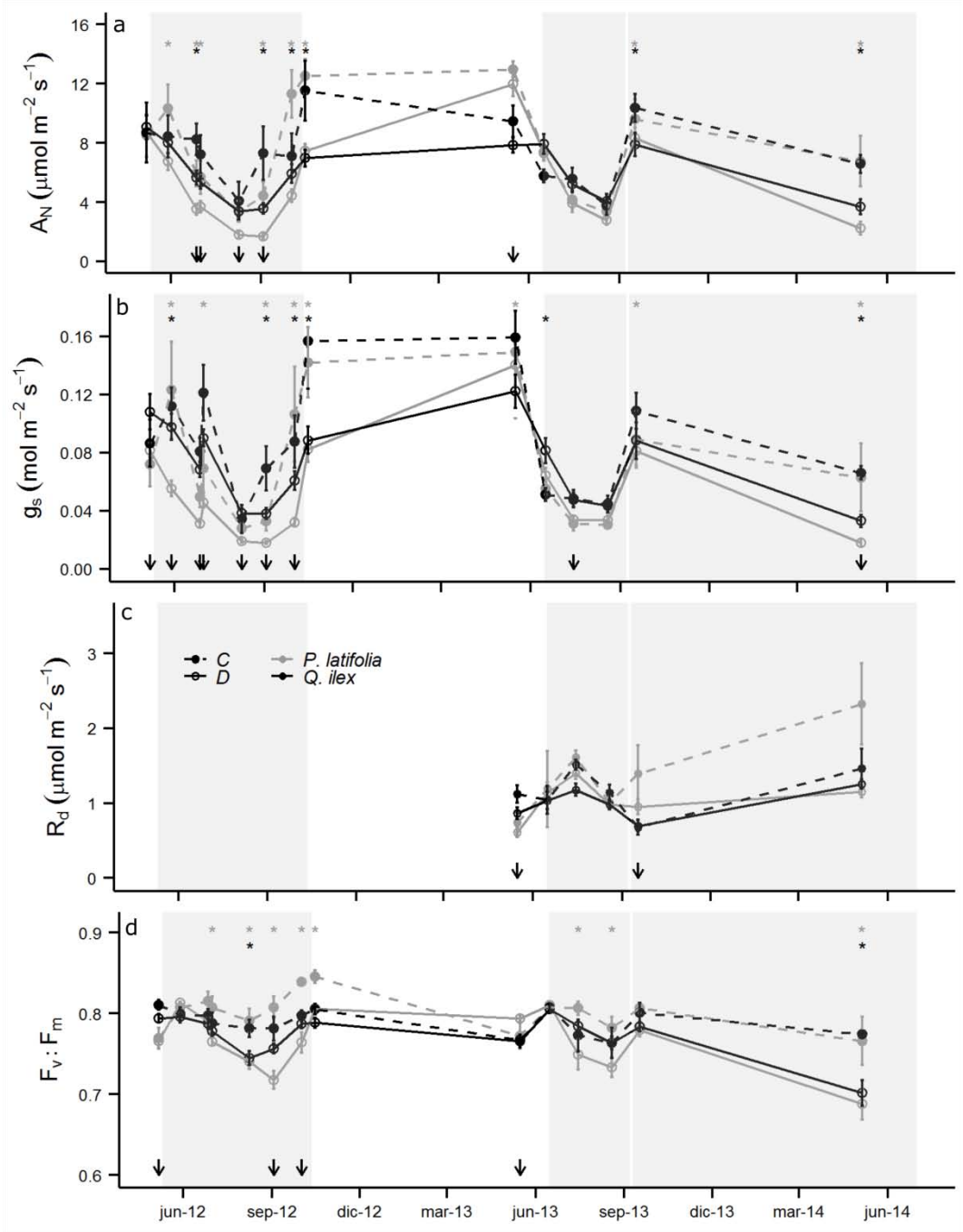

Figure 3.4.
Time course of (a) net assimilation rate (AN), (b) stomatal conductance (gs), (c) dark respiration rate (Rd) and (d) maximum quantum yield (FvFm) in leaves of P. latifolia (grey) and Q. ilex (black) during the experimental period. Means and standard errors are shown. In both species solid circles and dashed lines indicate C trees and empty circles and solid lines indicate D trees. Asterisks indicate significant differences within species between treatments (C vs. D) and arrows indicate significant differences between species for D trees (or between

species grouping C and D trees in panel c; due to lack of treatment effects in this case).

Significant differences between species for D tress (arrows in Figures 3.3 and 3.4) were noticeable over the experimental period. Water potentials (Ψ_{pd} and Ψ_{md}) were higher in *Q. ilex* (Figure 3.3; Table S1,S2 Appendix II). Amongst D trees, A_N, g_s and F_vF_m were generally lower in *P. latifolia* than in *Q. ilex* but, unlike what happened for water potentials, the differences were not always significant and tended to become less frequent over time (Figures 3.4a,b,d; Data Tables S3,S4,S6 Appendix II). Differences in R_d between species were significant for two dates, albeit in opposite directions (Fig. 4c; Table S5 Appendix II). Note that in this case C and D trees were pooled together because there was no treatment effect on R_d through the study. Significant differences between species for D tress (arrows in Figures 3 and 4) were noticeable over the experimental period. Water potentials (Ψ_{pd} and Ψ_{md}) were higher in *Q. ilex* (Figure 3; Table S1,S2 Supplementary Material). Amongst D trees, A_N, g_s and F_vF_m were generally lower in *P. latifolia* than in *Q. ilex* but, unlike what happened for water potentials, the differences were not always significant and tended to become less frequent over time (Figures 4a,b,d; Data Tables S3,S4,S6 Supplementary Material). Differences in R_d between species were significant for two dates, albeit in opposite directions (Fig. 4c; Table S5 Supplementary Material). Note that in this case C and D trees were pooled together because there was no treatment effect on R_d through the study.

The experimental drought period was shorter in 2013 than in 2012 (105 days compared to the 153 days the previous year). However, minimum average Ψ_{pd} in *P. latifolia* D trees was lower in 2013 (-4.3± 0.4 MPa, P<.0.0001; Fig. 3a). Different water availability between years was not reflected in A_N and g_s, as they both reached values close to 0 for D trees during the peak of the drought in all years (Figures 4a,b). Differences between C and D trees within species were more frequent during the first drought period than during the second for all studied variables (more days with significant differences, shown as asterisks in Figures 3 and 4). Recovery of water potentials after re-watering in 2012 was similar for C and D trees (Figure 3), but g_s, A_N and F_vF_m increased more in C than in D trees, reaching values above baseline (spring) rates (Figure 4). During recovery in 2013, *P. latifolia* D trees showed lower water potentials, A_N and g_s

than C trees. At this time, only Ψ_{md} and A_N were different between treatments (lower in D trees) in *Q. ilex*.

Stomatal and photosynthetic responses

The response of g_s and A_N to declining predawn water potential (Ψ_{pd}) was faster in *Q. ilex* than *P. latifolia* (P-value of the slope difference was <.0001 and 0.0031, for g_s and A_N, respectively; Figure 3.5). There was large gas-exchange variation at high Ψ_{pd} within species. However, the stomatal conductance at high Ψ_{pd} (close to zero) was significantly higher in *Q. ilex* than *P. latifolia* (P-value of the intercept was <.0001). There were no differences between treatments in g_s and A_N response to Ψ_{pd} (Figure 3.5; Tables S7-S8 Appendix II). Through the experiment, average stomatal conductances by date were not different between *P. latifolia* and *Q. ilex* as shown by the fact that the slope of the regression line between the two variables (0.88) was not different from 1 (Figure 3.6a; Table S9 Appendix II). However, the intercept of the relationship was significantly different from 0, with higher values for *Q. ilex* at low g_s. Despite similar g_s patterns, the slope of the regression between the A_N of the two species was significantly different from 1 (95 % confidence intervals of the slope = 0.47-0.76; Figure 3.6b; Table S10 Appendix II). *P. latifolia* showed higher A_N than *Q. ilex* during relatively favorable periods (high A_N) but the opposite happened at low A_N (during stressful periods). Both species showed the same relationship between g_s and A_N (cf. Eq. 3.1) (Table 3.3), but *Q. ilex* showed slightly but significantly higher residual cuticular conductance than *P. latifolia* (Table 3.1 and Table S11 Appendix II).

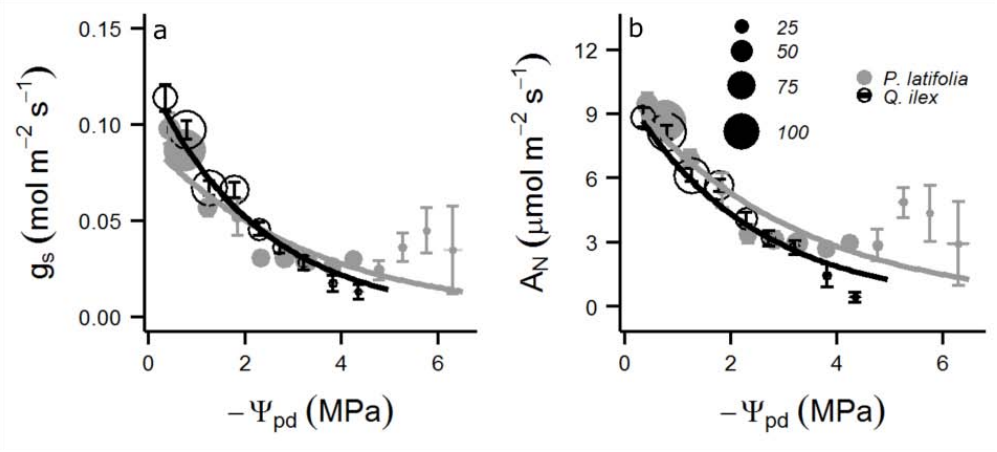

Figure 3.5.
Relationship between predawn leaf water potential (Ψ_{pd}) and (a) stomatal conductance (g_s) and (b) net assimilation rate (A_N). Circles indicate average g_s or A_N binned every 0.5 MPa for *P. latifolia* (grey) and *Q. ilex* (black). Circle size is proportional to the number of data points per bin (between 2 and 109). Grey and black solid lines depict fitted models for *P. latifolia* and *Q. ilex*, respectively.

Table 3.3. Coefficients ± standard error of the Ball, Woodrow & Berry empirical model (Eq. 3.1). Letters indicate significance values between groups.

Species	Treatment	g_o	m
P. latifolia	Control	0.108 ± 0.008^a	0.178 ± 0.007^a
	Drought	0.113 ± 0.009^a	0.165 ± 0.004^a
Q. ilex	Control	0.140 ± 0.009^b	0.159 ± 0.010^a
	Drought	0.138 ± 0.009^b	0.162 ± 0.007^a

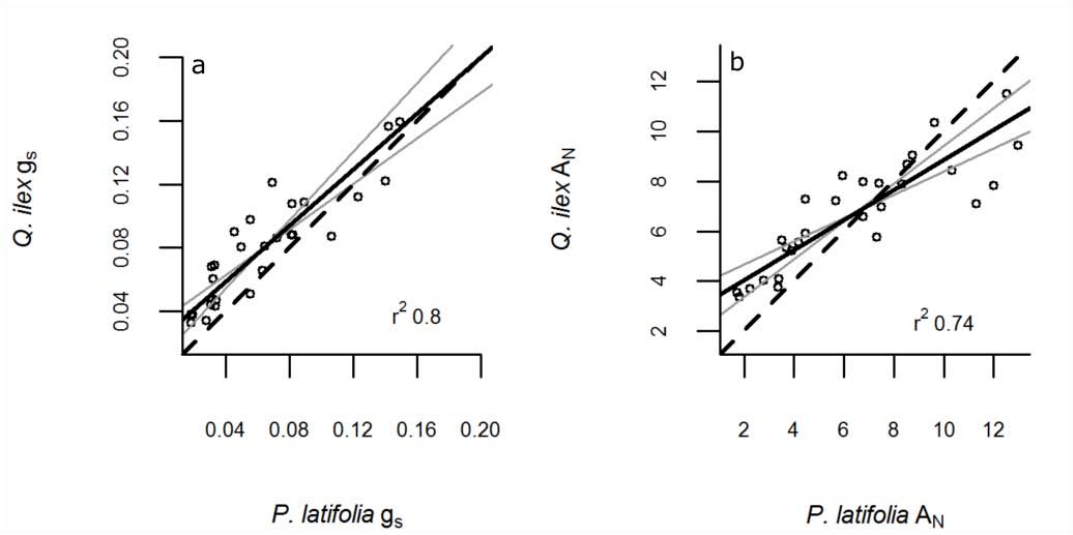

Figure 3.6.
Comparison of (a) stomatal conductance (g_s; in mol H_2O m^{-2}s^{-1}) and (b) net assimilation rate (A_N; in µmol CO_2 m^{-2}s^{-1}) in leaves of *P. latifolia* and *Q. ilex* throughout the study. Average values by date are shown (N = 30). In both panels the dashed line is a 1:1 line, the black solid

line shows the major axis (MA) regression line between species, and the grey solid lines indicate the 95% confidence intervals.

Growth and leaf area dynamics

Both species showed lower growth rates (BAI) in D than C trees in 2012, with a particularly large difference (3.1 ± 0.3 cm^2) for *P. latifolia* (Figure 3.7a; Table S12 Appendix II). A BAI reduction between 2012 and 2013 was noticeable in both species but only for C trees. In 2014, BAI decreased in both species for D trees down to extremely low values. In contrast, BAI increased in C trees of both species to initial (2012) values, probably due to the higher water availability as a result of the September 2013 flooding. Relative growth rate in branches (diameter and length, Figures 3.7b and 3.7c, respectively; Table S13-14 Appendix II) decreased through the years in both species and treatments to almost no branch growth in D trees during 2014.

P. latifolia trees reduced their leaf-to-sapwood area in branches throughout the experiment, but only 2014 values were significantly lower than the initial ones (Figure S2; Table S15 Appendix II). This species exhibited higher A_L:A_S at branch level than *Q. ilex* trees during the whole study. The two species showed similar shedding behavior between C and D trees; however, there was a tendency (P-value between treatments = 0.06) in *P. latifolia* towards higher A_L:$A_{S.br}$ in D than in C trees.

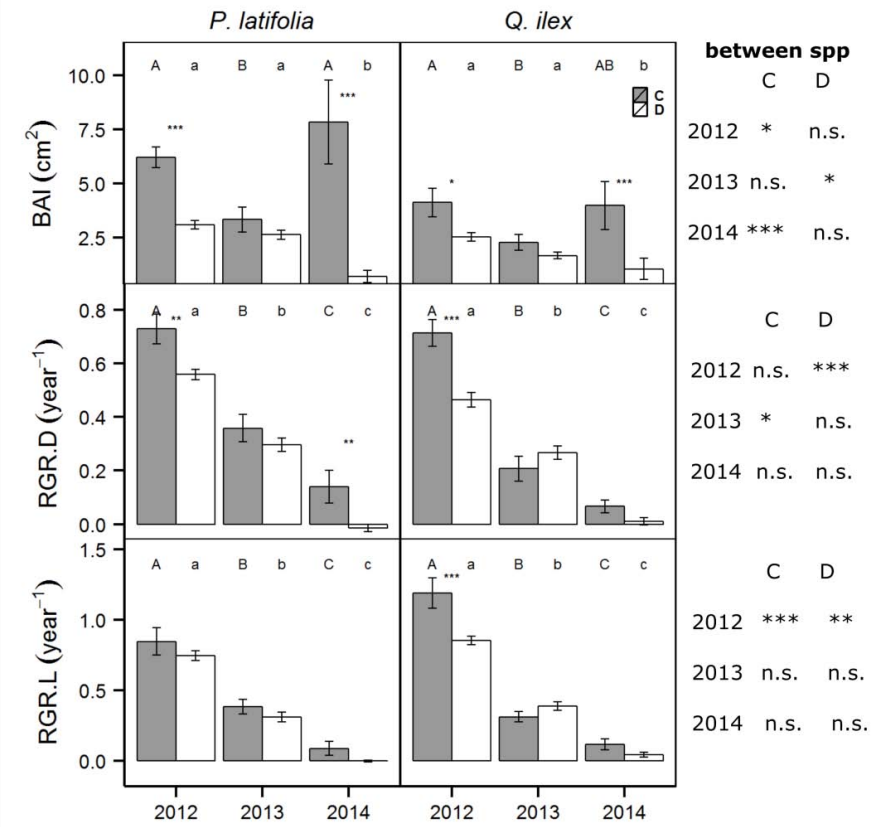

Figure 3.7.
Annual growth rate in *P. latifolia* and *Q. ilex*: (a) Basal area increment, BAI; (b) relative growth rate in shoot diameter, RGR.D and (c) relative growth rate in shoot length, RGR.L. Annual average by species and treatment are shown with the corresponding standard errors (C in grey and D in white). Asterisks indicate significant differences between treatments within species for a given year (*: 0.01<P<0.05, **: 0.001<P<0.01, ***: P<0.001). Letters indicate significant differences (P<0.05) over years for a given species and treatment; uppercase is used for C trees and lowercase for D trees. The tables on the right show, for each variable, the comparison between species as a function of treatment and year.

Non-structural carbohydrates

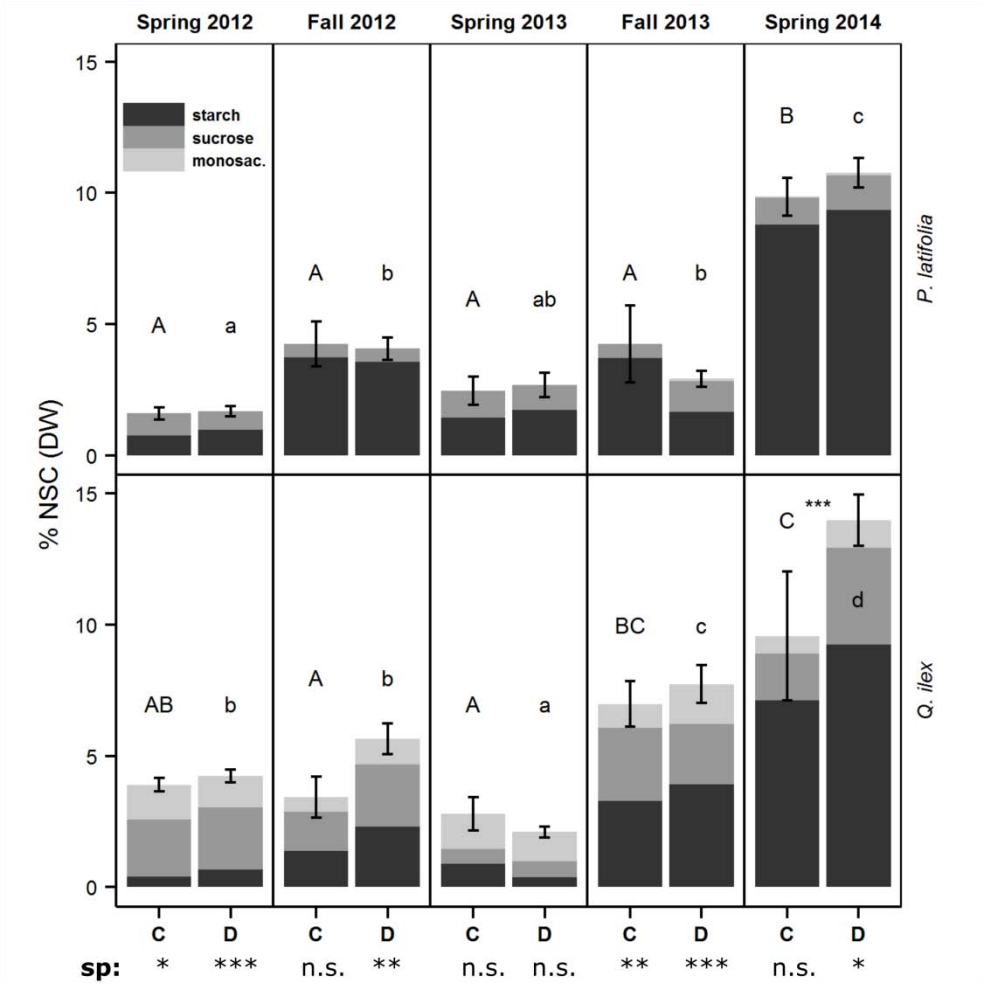

Figure 3.8.
Concentration of non-structural carbohydrates (NSC) in branches of *P. latifolia* and *Q. ilex*. Samples were taken in spring of 2012, 2013 and 2014 and fall of 2012 and 2013 (at the end of the imposed drought). The average and standard errors of the NSC concentration for a given species, treatment and season are shown. Grey scale indicates the concentration of the different components of total NSC (starch, sucrose and monosaccharides). Letters indicate significant differences (P<0.05) over time for a given species and treatment; uppercase is used for C trees and lowercase for D trees. Asterisks at the bottom of the plot indicate significant differences between species for a given date and treatment (*: 0.01<P<0.05, **: 0.001<P<0.01, ***: P<0.001).

Prior to the first drought period was imposed, the concentration of non-structural carbohydrates in branches was higher in *Q. ilex* than *P. latifolia* for both C and D trees (Figure 3.8). In *P. latifolia* D trees, NSC concentrations increased from spring to fall in 2012, but not in 2013; while no differences were observed in C trees (letters, Figure 3.8). In *Q. ilex*, NSC increased after the imposed drought only during 2013 (C and D trees). After eight months with no water supply (Spring 2014) NSC concentrations increased in both *Q. ilex* and *P. latifolia* for C and D trees (although the difference was not significant for *Q. ilex*

C trees) to reach the maximum values observed during the whole study period in all combinations of species and treatment. At this time, NSC concentration in D trees was significantly higher (P<.05) in *Q. ilex* (14.0 ± 1.0 % dry weight) than *P. latifolia* (10.8 ± 0.6 % dry weight); while NSC concentration was similar between species for C trees. The largest increase in both species was in the starch content.

DISCUSSION

Our results confirmed the differences in drought-resistance between *Q. ilex* and *P. latifolia* observed in the field (Ogaya and Peñuelas, 2003, 2007), as substantial *Q. ilex* mortality was observed at the end of the experiment (8 %), while all *P. latifolia* individuals survived. Our study is unique in that previous reports of higher mortality rates in *Q. ilex* than in *P. latifolia* in response to drought focused on stem mortality (Ogaya and Peñuelas, 2007; Barbeta *et al.*, 2013) rather than on individual tree mortality. Differences in drought-resistance between the studied species support the hypothesis that shifts in species composition in Mediterranean holm oak forest may occur with increasing drought frequency and/or intensity (Saura-Mas *et al.*, 2015). It should be noted, however, that in our case three periods of ~ 5, 3.5 and 9 months with no water supply (and increased temperatures due to the greenhouse effect) were needed to induce mortality in *Q. ilex*. These results show how resistant to drought the two study species are, and contrast with the much shorter survival times for *Pinus sylvestris* growing in the same experimental system (Garcia-Forner et al. in review). This situation also contrasts with most experimental studies using potted plants, which tend to underestimate survival in the field. Rainless periods of more than 3-4 months are currently exceptional in the distribution range of the two study species. The discrepancy between these figures and the shorter droughts reported to cause mortality in the field (particularly for *Q. ilex*) likely reflects two facts. Firstly, stem mortality occurs under less extreme conditions than whole individual mortality (Galiano *et al.*, 2012). This is an important aspect in coppiced trees like *Q. ilex* and clearly requires further study. Secondly, soil conditions in our experiment were more favorable to plants (deep farmland soils in a flat plain) than those found in most natural forests.

P. latifolia (anisohydric species) is not more prone to hydraulic failure than Q. ilex

Seasonal Ψ_{pd} variation followed SWC patterns over drought-recovery cycles in D trees, but with very different absolute values by species. As expected (Bombelli and Gratani, 2003; Serrano *et al.*, 2005; Ogaya *et al.*, 2014), *P. latifolia* exhibited the most negative water potentials both years (and also in spring 2014). However, average Ψ_{md} did not decrease below -6.6 MPa, the point of 50 % loss of hydraulic conductivity (P_{50}) estimated for this species in the field (Martínez-Vilalta et al. 2002). Maximum estimated percent loss of hydraulic conductivity (PLC) for *P. latifolia* using these vulnerability curves (Martínez-Vilalta et al. 2002) and Ψ_{md} values measured in this study was 24 %. Published P_{50} values for *Q. ilex* stems vary widely between studies, likely reflecting methodological artifacts (Martin-StPaul *et al.*, 2014). Using the two extreme values reported by Martínez-Vilalta et al. (2002) and Martin-StPaul et al. (2014) using the bench dehydration technique (likely the most robust methodology for establishing vulnerability curves in long-vessel species) the maximum PLC estimates for *Q. ilex* over the study period would range between 17 % and 63 %. These values are higher or similar to those estimated for *P. latifolia*. Higher loss of hydraulic conductivity experienced by *Q. ilex* agrees with field observations and comparative studies (Martínez-Vilalta et al. 2002, Martínez-Vilalta et al. 2003) showing that under the same soil conditions *Q. ilex* experiences greater reductions in plant hydraulic conductance than *P. latifolia*. Moreover, *Q. ilex* showed higher cuticular conductance than *P. latifolia* and maintained leaf area under extreme water stress, presumably increasing its vulnerability at the individual tree level. Overall, these results are consistent with those reported by Garcia-Forner et al. (2015) for *Pinus edulis* and *Juniperus monosperma* in SW USA, and support the notion that anisohydric species, such as *P. latifolia* in this study, are not necessary more prone to hydraulic failure than coexisting isohydric species (*Q. ilex*), as had been hypothesized by McDowell et al. (2008, 2011).

Carbon economy is unrelated to iso- anisohydric behavior in the study species

Although the difference in water potential regulation between *Q. ilex* (isohydric) and *P. latifolia* (anisohydric) is well established, there is less agreement when comparing stomatal behavior and assimilation rates in response to drying soil (and/or other factors), with some studies showing no differences between species (Gratani and Bombelli, 1999; Bombelli and Gratani, 2003; Gratani and Varone, 2004) and others showing higher potential rates and/or seasonal gas exchange rates in *Q. ilex* under well watered conditions but lower when drought stress increases (Filella *et al.*, 1998; Peñuelas *et al.*, 1998; Ogaya and Peñuelas, 2003; Ogaya *et al.*, 2014). In our experimental study on plants subjected to the same environmental conditions during almost four years we observed that g_s decreased faster with declining Ψ_{pd} in *Q. ilex* than in *P. latifolia*. However, this is not the relevant comparison with regards to the plant carbon economy, precisely because both species operate at different water potentials. Instead, it is more informative to compare the temporal dynamics of gas exchange or the relationship between concurrent measurements of g_s or A_N in the two species. When this is done, differences between species are only evident in assimilation (not in g_s) but in the opposite direction as expected: *Q. ilex* D trees display lower assimilation rates than *P. latifolia* D trees under favorable conditions (high soil moisture, low VPD, and mild light and temperatures) but sustain higher assimilation rates when conditions become drier. This is important because it suggests again that water potential regulation may be uncoupled from stomatal control and that isohydric species are not necessarily more carbon constrained compared to anisohydric ones (Quero *et al.*, 2011; Garcia-Forner *et al.*, 2015). Although temporal dynamics of R_d were largely similar between species (Figure 3.4c), higher R_d values of *P. latifolia* under well watered conditions (photosynthetic curves) and in C trees in spring 2014 suggest that *P. latifolia* may have similar or higher carbon demand for respiration than *Q. ilex*.

The fact that the isohydric species in our study (*Q. ilex*) is not more carbon limited than the anisohydric species is also supported by the growth data. Unlike what has been reported in field studies (higher sensitivity of stem

growth to rainfall reductions in *Q. ilex* than in *P. latifolia)* (Ogaya and Peñuelas, 2007; Barbeta *et al.*, 2013) we found similar growth responses to drought at both branch and whole tree levels (BAI) between species. Plant growth is more sensitive to drought stress, particularly to cell turgor, and often decreases before reductions in photosynthesis are observed (Mitchell *et al.*, 2013; Palacio *et al.*, 2014; Körner, 2015). Here, despite differences in minimum water potentials between species, they remained most of the time below the corresponding turgor loss point in both species (-2.3 and -1.6 MPa for *P. latifolia* and *Q. ilex,* respectively), thereby the length of the potential growth period might be similar.

The fact that growth constrains persisted in 2014 but NSC pools, and particularly starch, increased significantly suggests that growth was not limited by carbon assimilation (Körner, 2015) in the study species. An increase in branch NSC concentration under extreme drought could be explained by a combination of two processes: (i) higher assimilation relative to growth and respiration demands or (ii) carbon mobilization from roots under drought (Hartmann *et al.*, 2013*a*). The first one implies that even low A_N can result in NSC accumulation if the proportional reduction in the sinks is higher. This would explain why NSC increase in *Q. ilex* starts earlier (fall 2013) than in *P. latifolia* (Spring 2014). Secondly, carbon mobilization from roots can occur, particularly in resprouter species, which are expected to allocate large carbon pools belowground (Vilagrosa *et al.*, 2014; Zeppel *et al.*, 2015). Regardless of where stored carbon comes from, higher concentrations of NSC are likely to contribute to drought resistance under extreme drought (O'Brien et al. 2014, García-Forner in review) by facilitating the maintenance of turgor and cell metabolism and, possibly, by facilitating xylem refilling (Zwieniecki and Holbrook, 2009; Secchi and Zwieniecki, 2011). In addition, high NSC concentration in both species towards the end of the study period, at a time when *Q. ilex* mortality was already occurring, strongly suggests that drought-induced mortality was not triggered by carbon starvation in our study.

An important caveat of our NSC estimates for *P. latifolia* is that we were not able to quantify sugars from the raffinose family, which can represent a substantial portion of the sugars transported in the phloem of some

angiosperms (Woodruff, 2014). Unfortunatelly, we were not able to find quantitative information in the literature that would allow us estimate the percentage that raffinose could represent in the study species relative to other soluble sugars. In any case, our NSC values for *P. latifolia* should be seen as minimum estimates, which limits our capacity to establish comparisons between species.

Conclusions

Drought-induced mortality involves several processes at different spatiotemporal scales, making it difficult to attribute the cause of death to a single trait or process. The two study species, which frequently coexist in the field and are usually characterized as models of the iso vs. anisohydric behavior in Mediterranean forests, exhibit large differences in drought-induced mortality at the stem and tree levels under both field and greenhouse experimental conditions. Our study confirms their contrasted behavior in terms of water potentials. However, lower water potentials in *P. latifolia* were not associated to higher risk of hydraulic failure in this species. In fact the opposite was true, and hydraulic failure remains the most likely cause of death of *Q. ilex* under extreme drought (Martínez-Vilalta *et al.*, 2003). Likewise, higher water potentials in *Q. ilex* were neither associated with lower stomatal conductance nor with lower assimilation in this species. These results caution against making direct links between water potential regulation, stomatal regulation and the physiological mechanisms of mortality. Multiple pathways could determine the higher resistance of *P. latifolia* trees under drought despite experiencing lower water potentials, including higher resistance to embolism (Martínez-Vilalta *et al.*, 2002*b*, 2003) and a more plastic regulation of water demand by means of leaf loss during continued and recurrent droughts.

Acknowledgements

This research was supported by the Spanish Ministry of Economy and Competitiveness (MINECO) through competitive grants CGL2010-16373 and CGL2013-46808-R. NGF was supported by a FPI scholarship from the MINECO. We would like to thank the field technicians of the Environmental and

Horticulture department in the IRTA for their valuable assistance in the field work.

Chapter 4

Individual traits as determinants of time to death under extreme drought in *P. sylvestris*

Núria Garcia-Forner, Anna Sala, Carme Biel, Robert Savé, Jordi Martínez-Vilalta

Tree Physiology (*under review*)

ABSTRACT

Plants exhibit a variety of drought-responses involving multiple interacting traits and processes, which challenges predictions of drought survival. Careful evaluation of responses within species, where individuals share broadly similar drought-resistance strategies, can provide insight on the relative importance of different traits and processes. We subjected *Pinus sylvestris* saplings to extreme drought (no watering) leading to death in a greenhouse to: 1) determine the relative effect of predisposing factors and responses to drought on survival time; 2) identify and rank the importance of key predictors of time to death, and 3) compare individual characteristics of dead and surviving trees sampled concurrently. Time until death varied over three months among individual trees. Survival time was best predicted by variables related to carbon uptake and carbon/water economy before and during drought. Trees with higher concentrations of monosaccharides before the beginning of the drought treatment and with higher assimilation rates prior and during the treatment survived longer, even at the expense of higher water loss. Dead trees exhibited much lower non-structural carbohydrates (NSC) relative to surviving trees sampled concurrently. Overall, our results indicate that the maintenance of carbon assimilation to prevent acute depletion of NSC content above some critical level appears to be the main factor explaining survival time of *P. sylvestris* trees under extreme drought.

Keywords: carbon and water relations, hydraulic failure, hydraulic conductivity, life span, mortality, non-structural carbohydrates, Scots pine.

INTRODUCTION

Drought-induced forest mortality is a widespread phenomenon (Allen *et al.*, 2010) with potentially large ecosystem-level implications (Anderegg *et al.*, 2013*b*), and it is expected to increase under climate change (Breshears *et al.*, 2009*b*; Peng *et al.*, 2011; Anderegg *et al.*, 2014). Plants exhibit a wide range of morphological and ecophysiological responses to drought both between and within species (Chaves *et al.*, 2003; Bréda *et al.*, 2006). This diversity is the product of diversification and adaptation processes at different scales (Ackerly *et al.*, 2000) and can result in the coexistence of different strategies and corresponding plant traits (e.g. (Martínez-Vilalta *et al.*, 2002*b*; Galmés *et al.*, 2007; Hernández *et al.*, 2010; Moreno-Gutiérrez *et al.*, 2012). Predicting which species are more likely to die under drought has proven difficult, in part because contrasting strategies, multiple traits and processes involved make it difficult to attribute the relative importance of each trait.

Species' or individuals' ability to overcome drought periods depend on multiple factors, including stomatal behavior, vulnerability to xylem embolism, regulation of leaf area, and carbon allocation (Chaves *et al.*, 2003; Maseda and Fernández, 2006). Plants regulate water loss to prevent critical xylem tensions and water transport failure (Maherali *et al.*, 2004; Brodribb and Cochard, 2009; Choat *et al.*, 2012; Urli *et al.*, 2013). They do so via modifications of water supply vs. demand ratios (e.g. leaf-to-sapwood area ratio) and stomatal control (Sperry *et al.*, 2002). However, stomatal closure and severe reductions in leaf area under stressful conditions are likely to reduce carbon uptake during and after drought (McDowell *et al.*, 2008; Galiano *et al.*, 2011). If assimilation is curtailed, the carbon balance may become negative and carbon sinks such as growth, respiration or other metabolic process become dependent on carbon pools and their accessibility (Dietze *et al.*, 2014).

The plethora of traits and mechanisms involved in drought-induced mortality requires a comprehensive framework that incorporates such complexity. The hydraulic framework proposed by McDowell et al. (2008) took such approach, and made explicit the critical link between water and carbon economy under drought. Despite substantial progress, however, the specific

processes involved, and particularly their interaction, are yet to be completely understood (Sala *et al.*, 2010; McDowell, 2011; McDowell *et al.*, 2013*b*). Hydraulic failure has been shown to induce plant mortality (Anderegg *et al.*, 2012; Mitchell *et al.*, 2013; Hartmann *et al.*, 2013*a*). Stomatal control can delay hydraulic failure by reducing water loss in leaves, but it occurs at the cost of carbon supply via photosynthesis, potentially leading to reductions of stored non-structural carbohydrates (NSC) (Breshears *et al.*, 2009*b*; Hartmann *et al.*, 2013*b*; Dickman *et al.*, 2015). NSC provide critical sources of carbon for respiration, supply solutes to drive water movement and turgor maintenance (Sevanto *et al.*, 2011, 2014; O'Brien *et al.*, 2014), and may be involved in xylem refilling after embolism formation (Secchi and Zwieniecki, 2011). Different traits and their respective responses will affect the rate at which different responses occur, thus making it very difficult to determine the specific critical components of tree physiology needed to model mortality (Hartmann *et al.*, 2015).

Most studies conducted so far on the mechanisms of drought-induced mortality have focused on comparisons across species or ecotypes (Anderegg and Anderegg, 2013; Herrero *et al.*, 2013; Galvez *et al.*, 2013; Matías and Jump, 2014; Pratt *et al.*, 2014; O'Brien *et al.*, 2014). However, intra-population differences in drought resistance can be large, both in the field and under controlled conditions (Cavender-Bares and Bazzaz, 2000; Martínez-Vilalta *et al.*, 2009; Moran *et al.*, 2015), and there are at least two reasons why focusing on these differences is important. Firstly, differences in drought resistance have critical ecological implications: differences in survival time of a few days may translate into life or death under field conditions, where drought duration is generally uncertain but finite (e.g., Martínez-Vilalta *et al.*, 2002*a*; Adams *et al.*, 2009). Secondly, because of phylogenetic constraints, broad drought resistance strategies are similar among individuals within species or populations, thus providing an opportunity to explore the physiological consequences of trait variation on the physiological mechanisms underlying drought-induced mortality. Interestingly, Sevanto et al. (2014) showed that even within a single species (*Pinus edulis*), mechanisms of drought-induced mortality may vary causing some individuals to die much faster than others. The key question is

not necessarily why some species succumb to drought faster than others but, more generally, why some individual plants succumb faster than others.

Here we investigate tree survival under extreme, experimental drought from an individual tree perspective, using *Pinus sylvestris* as a model species. Previous studies indicate that carbon limitation is likely to be an important process during mortality of this species (Galiano *et al.*, 2011; Poyatos *et al.*, 2013; Aguadé *et al.*, 2015*a*). We tested several morphological and physiological attributes related to water and carbon economy as predictors of individual differences in drought resistance, measured as time to death. Our main objectives were to: (1) determine the relative effect of predisposing factors (individual morphological and physiological traits measured under well watered conditions) and differential responses to drought stress on survival time; (2) identify and rank the importance of key predictors of time to death at the individual level; and (3) compare the individual characteristics (wood properties, carbon pools and biomass allocation) of dead and surviving trees sampled concurrently. We hypothesized that initial differences among individuals (i.e. predisposing factors) are amplified during drought and eventually determine the likelihood of mortality. Secondly, based on previous results for *P. sylvestris*, variables related to carbon assimilation and storage will be important predictors of time to death in this species.

MATERIAL AND METHODS

Plant material and experimental design

The study was conducted in a polytunnel greenhouse in the Institute of Agricultural, Food Research and Technology (2º10'3"N, 41º37'56"E, 203 m asl; Caldes de Montbui, Spain). Soils are farmlands with sandy loam texture and a minimum depth of 80 cm, and were subsoiled (deep plowed) before planting the trees. In April 2011, a total of 150 saplings of *Pinus sylvestris*, *Quercus ilex* and *Phillyrea latifolia* grown in pots were transplanted to the ground at random locations within a grid inside the greenhouse (plants were 1.5 m apart). Despite identical conditions and treatments (see below), only *P. sylvestris* experienced mortality during the experimental period of this study, and therefore we focus only on this species.

A total of 49 *P. sylvestris* saplings (five years old and ~1.5 m tall) from the same provenance (Bioriza S.L. nursery) were watered twice a week for one year prior to treatment implementation. This pretreatment period, longer than usual for an experimental trial, was intended to ensure acclimation to site conditions and appropriate root expansion into the ground. Watering regimes followed the monthly rainfall patterns at Prades Mountains (41º19'58.05''N, 1º0'52.26''E, 1015m asl; NE Spain) with the typical dry summers of the Mediterranean climate, but reducing total volume by 20 % to account for differences in soil depth, which is shallower in Prades (Figure S1a Appendix III). Prades Mountains are located close to the Southern limit of *P. sylvestris* distribution, where drought-induced decline has been reported (Martínez-Vilalta and Piñol, 2002; Poyatos *et al.*, 2013).

The study started in April 2012 and lasted until early October 2012. A drought treatment (no further irrigation) was implemented from 11 May to 23 July. Different measurement campaigns were conducted throughout the study (Figure 4.1). In April and early May, before the drought treatment, we took plant morphological (tree height, diameter, sapwood area and total leaf area per plant; Figure 4.1 blue-dashed line) and physiological measurements (twig water potentials, sapwood NSC concentration in branches, and leaf gas exchange and chlorophyll fluorescence; Figure 4.1 purple-dotted lines; explained below). Thereafter, five of the 49 trees and the remaining 44 trees were assigned to a control (C) and a drought (D) treatment, respectively. Drought trees received no watering (the tunnel structure excluded rainfall), whereas control trees were watered following the Mediterranean rainfall pattern explained above for the rest of the experiment. For logistical reasons and to avoid interference between treatments, control trees were located at one end of the greenhouse and separated from the rest of the trees by a waterproof trench (80 cm deep). During the treatment period twig water potential, leaf gas exchange and chlorophyll fluorescence were measured three more times. In mid-July, during summer stress peak, we also measured native xylem hydraulic conductivity in branches (Figure 4.1, green-dashed line). After the drought treatment period, all trees were watered with two liters of water and subsequently subjected to the ongoing watering regime of the controls. Recovery was evaluated 15 days after

restoring irrigation, when physiological measurements were repeated for the last time on the remaining live trees.

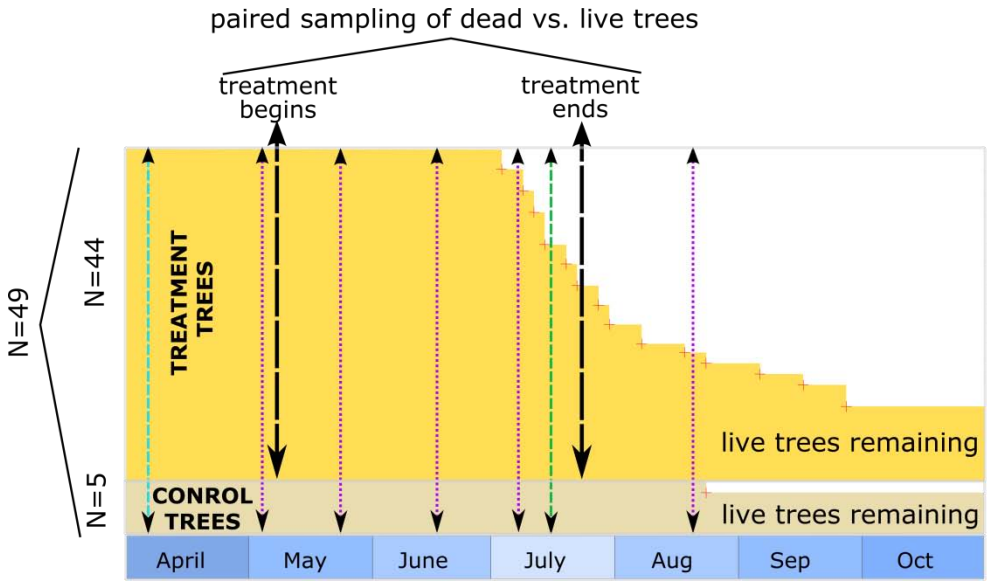

Figure 4.1.
Experimental design and timing of different campaigns. Black-longdashed lines indicate treatment beginning and ending. Vertical colored lines indicate when different measurements were taken, including measurements prior and during experimental drought: pre-drought morphological characterization (height, diameter, sapwood area and total leaf area per plant), blue-dashed line; physiological campaigns (gas exchange, fluorescence and water potentials), purple-dotted lines; xylem hydraulic conductivity and the ratio leaf-to-sapwood area in branches, green-dashed line. Note that samples for non-structural carbohydrates determination at the beginning were taken during the first physiological campaign. Paired samplings of dead vs. live trees were carried out throughout the treatment period (see the top of the figure) during death events (indicated by red crosses). Dead-live samplings included measurements of wood density, biomass and carbon allocation.

The condition of each tree during the experiment was visually evaluated every 2-3 days until the end of the study in October 2012. We defined five plant states based on color and needle turgor, leaf shedding and phloem greenness. State number five indicated a healthy tree with high canopy density, green needles and no needle shedding. A tree was considered dead (state number 0) when all its leaves were brown and stem phloem was dry (no green tissue). The re-watering period was useful to confirm that trees in this state were not able to recover even after generous re-watering.

Individual differences at the time of death were assessed through a paired sampling between dead and live D trees (excluding C trees) during the treatment period (no irrigation, Figure 4.1). Every time a D tree died, the dead

tree and its closest and healthiest neighbor (in the drought treatment) according to the last visual evaluation were harvested. All biomass compartments were collected and samples were taken to measure wood density and NSC in different tissues (branches, stem and roots). Overall, 10 pairs of dead and live trees were harvested (we refer to live trees as 'censored' trees later on because they were harvested and, thus, disappeared from the sample before the end of the study). The experimental drought ended when 10 live-dead tree pairs had been sampled, after which watering was reestablished as explained above. The drought period lasted 78 days, while survival was evaluated during 147 days since the beginning of the study (Figure 4.1).

Meteorological and soil moisture measurements

Ambient temperature (T) and relative humidity (RH) were monitored in the greenhouse at 1.5 m height with an EHT Temperature/RH sensor (Decagon Devices Inc., Pullman, Washington, USA). Photosynthetic active radiation (PAR) was determined as the average of four SD222 sensors (Macam Photometrics Ltd., Livingstone, UK) installed at 3 m height (above the mean canopy height) across the length of the greenhouse. Weather variables were recorded every 15 minutes with an Em50 data logger (Decagon Devices Inc.; for temperature and RH) and a CR10X data logger (Campdell Scientific Inc., Logan, UT, USA; for PAR).

Soil water content (SWC) was monitored with six 10HS Soil Moisture Probes (Decagon Devices Inc.) at 25 cm depth, at 30 cm from randomly assigned trees (four D + two C trees). SWC data was recorded every 30 minutes using a CR1000 data logger (Cambdell Scientific Inc.). All meteorological data and soil water content was monitored from December 2011 to October 2012.

Morphological measurements

In February 2012, 10 months after transplant, we measured 2011 twig growth in all trees to evaluate their acclimation to the greenhouse. The leader stem and two lateral twigs 50 cm from the top were selected per tree to

measure basal diameter (growth.D) and length (growth.L) of the shoots. Measurements were averaged per tree before analysis.

In April 2012, before the initiation of shoot growth, we measured tree height (H) and stem diameter at 5 cm from the soil (D_m; the average of two perpendicular measurements). Tree sapwood area (SA) was calculated from stem diameter (including bark). Total leaf area per plant (LA) was estimated by multiplying total foliated branch length for each age cohort by mean needle density and mean individual needle area for that cohort. Mean needle density was estimated by counting the number of needles in 5 cm long sections of two representative segments of each cohort per tree. In these same segments individual needle area was estimated by measuring length and width in a subsample of 6 needles per segment. The relationship between needle dimensions (length and width) and needle area had been previously determined in these experimental trees. Leaf-to-sapwood area ratio (LA:SA) was calculated as the quotient between LA and SA.

During the dead-live paired sampling all biomass fractions were measured (10 trees per group). Aboveground woody biomass was divided into stem and branches. A trench of 40*30*30 cm was dug around each harvested tree and all roots and soil were collected. Based on the first dead-live paired sampling when whole tree roots were extracted, this volume was sufficient to contain all of the root system of each tree. Root ball and coarse roots (> 2 mm) attached to the root ball were separated from the soil by hand and dry-cleaned of soil. The soil was mixed, weighted, and 4 to 5 kg set aside for air drying and subsequent processing. Each subsample was sieved through a 2 mm mesh and the remaining roots were separated by diameter (> 2 and < 2 mm). Belowground biomass was the sum of the root ball, coarse and fine roots. A section of the stem (~2 cm) at 12 cm from the ground was cut upon harvesting to measure wood density (oven-dried mass divided by green volume, in g cm^{-3}), with green volume estimated by the water-displacement method (Ilic *et al.*, 2000).

Physiological monitoring

Physiological measurements were conducted in a random subsample (selected a priori) of 30 trees (25 D + 5 C) due to time constraints, and were repeated on the same subsample of trees every two to three weeks (Figure 4.1). At each time, twig samples were cut before sunrise and at noon (solar time) for predawn (Ψ_{pd}) and midday water potential (Ψ_{md}) measurements, respectively. Samples were kept cool and humid in plastic bags inside a cooler and measured within two hours of collection (we ensured that water potentials did not change during this time period). Water potential was determined with a pressure chamber (3005 Soil Moisture Corp., Santa Barbara, CA, USA). Net assimilation rate (A_N), stomatal conductance (g_s), maximum quantum efficiency or yield (FvFm), quantum efficiency of photosynthetic electron transport through photosystem II (PhiPS2), quantum efficiency of CO_2 assimilation (PhiCO2), electron transport rate (ETR) and non-photochemical quenching (NPQ) were determined in fully expanded leaves. Instantaneous gas exchange and chlorophyll fluorescence measurements were performed between 8 and 11 h, solar time, using a Li-Cor LI-6400XT open infrared gas-exchange analyzer system equipped with a 6400-40 Leaf Chamber Fluorometer (Li-Cor, Lincoln, NE, USA). Maximum and minimum fluorescence in dark adapted leaves (F_m and F_o, respectively) were measured between 3-5 h solar time during the same day and on the same leaves as those used for mid-morning measurements. This data was used to calculate FvFm in dark adapted leaves, NPQ, PhiCO_2 and PhiPS2. Chamber conditions were fixed at 400 μmol CO_2 m^{-2} s^{-1}, 1500 μmol photons m^{-2} s^{-1}, 43 ± 3 % relative humidity and 25 ºC block temperature. Measurements were taken once steady state gas exchange was achieved. Instantaneous water use efficiency (WUE, mmol CO_2 mol H_2O^{-1}) was calculated as the quotient between A_N and transpiration rate. Assimilation rate at the tree level (A_{tree}) was calculated for the pretreatment date as the product of A_N by the estimated plant leaf area (LA; determined as explained above).

Non-structural carbohydrates measurements

Non-structural carbohydrates were measured before the onset of the drought treatment in branch sapwood (on the same 30 trees under physiological monitoring) and during each paired dead-live sampling in the sapwood of branches, main stems and roots. For branches, we analyzed 2011 shoots; for

main stems, 2 cm-long sections of the trunk were cut at 10 cm from the ground; for roots, we unearthed a taproot from the root ball of each tree until fine roots (~2 mm diameter) were located and collected. All samples were wrapped in plastic bags and stored in a cooler over ice until processed in the laboratory within one hour. Plant material was microwaved for 90 s at 650 Watt to stop enzymatic activity and oven-dried for 96 hours at 65 ºC. All samples were debarked and ground to fine powder. NSC reserves were analyzed as in Hoch *et al.* (2002) with minor modifications by Galiano *et al.* (2011). NSC reserves were defined as the sum of starch, sucrose and monosaccharides (glucose and fructose). Sucrose and monosaccharides constitute the low molecular weight sugars (LMW). All NSC values are expressed as percent dry matter.

Xylem hydraulic conductivity measurements

In mid-July, under summer stressful conditions of high temperature and vapor pressure deficit, all individuals under physiological monitoring that had not been harvested thus far (*N* = 23 trees, 18 D and 5 C) were selected to measure xylem hydraulic conductivity (K_h) and the ratio of leaf-to-sapwood area in branches (LA:SA.br). Branches of 4-5 mm diameter were collected between 8-9 h (solar time), wrapped in plastic bags with a damp cloth and transported to the laboratory in a cooler. Native hydraulic conductance was determined in the same morning with a Xyl'em Embolism Meter (Bronkhorst, France). One segment of ~5 cm length per branch was cut under water, debarked at the proximal and distal ends (0.5 cm) and the proximal end attached to the Xyl'em manifold to measure the water inflow rate generated by a hydrostatic pressure head of ~60 cm. Water was deionized and degassed. Values were standardized to 20 ºC to account for temperature variation in the lab and remove viscosity. We calculated native hydraulic conductivity ($m^4\ MPa^{-1}\ s^{-1}$) as the ratio between the flow through the segment and the pressure gradient ($\Delta\Psi$ = 6 kPa), multiplied by segment length. Sapwood (K_S) and leaf-area (K_L) specific hydraulic conductivity ($m^2\ MPa^{-1}\ s^{-1}$) were determined, respectively, by dividing K_h by the cross-sectional area of the debarked segment and the area of all leaves distal to the segment.

Statistical analyses

We used simple linear models to assess pretreatment differences between resistant and susceptible trees, including: shoot growth in diameter (growth.D) and length (growth.L), tree height (H), basal stem sapwood area (SA), total leaf area per tree (LA), LA:SA ratio, total non-structural carbohydrates (NSC), starch, sucrose, monosaccharides and low molecular weight sugars (LMW) in branches. General linear mixed models were used to study the time course of predawn (Ψ_{pd}) and midday (Ψ_{md}) twig water potentials, net assimilation rate (A_N), stomatal conductance (g_s), instantaneous water use efficiency (WUE), the maximum quantum efficiency (FvFm), quantum efficiency of photosystem II (PhiPS2), quantum efficiency of CO_2 assimilation (PhiCO2), electron transport rate (ETR) and non-photochemical quenching (NPQ). For both linear and general linear mixed models only trees subjected to the drought treatment were included. Trees were classified depending on their drought response as susceptible or resistant, and the corresponding dichotomic variable was included as a fixed factor. All D trees that died during the study period (until early October 2012) were considered susceptible, while all surviving trees at the end of the study plus all censored trees (live trees sampled during the dead-live paired sampling) were grouped into the resistant category. Censored trees were considered resistant because they were the healthiest individuals adjacent to dead trees at the time of the paired sampling. The term resistant is relative and used to simply distinguish censored and alive trees from those that were dead when the study ended. Note that, at worst, including censored trees in the resistant category would tend to underestimate differences between live and dead trees. In mixed models, date and the interaction between date and the variable coding for resistant vs. susceptible trees were also included in the fixed part of the model. Sampling prior to drought implementation (pretreatment) was used as the reference date in models, so that all temporal differences are referred to these initial conditions. Tree was included as a random factor in mixed models.

To study how plant morphological and physiological characteristics affect time to death under extreme drought we used accelerated failure time models (AFT), which can deal with censored data. A log-logistic error distribution was applied to assess treatment differences in survival probability between C and D

trees. In addition, we modeled survival probability through time as a function of different predictor variables, excluding watered control trees. A total of 44 AFT models were fitted, one for each predictor variable. These predictors included all pretreatment variables (growth.D, growth.L, H, D_m, SA, LA, LA:SA, K_S, K_L, NSC, starch, sucrose, monosaccharides and LMW sugars) and three new explanatory variables extracted from each of the time series for Ψ_{pd}, Ψ_{md}, A_N, g_s, WUE, FvFm, PhiPS2, PhiCO2, ETR and NPQ. For each tree and measured variable we calculated the initial (.i) value corresponding to the pre-drought status, the stressed value (.st) measured at the peak of stress during the drought period (the minimum value of the time series in all cases except for NPQ) and the relative variation (.rv) calculated as:

$$x.rv = | (x.st - x.i) / x.i | , \quad \text{Eq. 4.1}$$

where *x* designates each measured variable. To facilitate the comparison of the AFT results across predictor variables, which had very different distributions, results were standardized by calculating the difference in (modeled) median survival time between the 1st and 3rd quartiles for each variable. The median survival time (S_{50}) was defined as the number of days required for survival probability to reach 0.5 (i.e., the time it takes for half of the population to die).

Finally, general mixed models were used to assess differences between live and dead trees from the paired sampling. For wood density, above and belowground biomass and the ratio between below and aboveground biomass, survival (live or dead) was included as a fixed factor, and tree nested into survival time (number of days alive from the start of the drought) was included in the random part of the model. We analyzed the carbohydrate content of living and dead trees at the end of the study using different models due to the high frequency of 0 values in the monosaccharides and starch fractions. We modeled total NSC and LMW sugars using general linear mixed models and starch using a generalized linear mixed model with binomial distribution. In both cases, survival, tissue and their interaction were fixed factors and tree nested into survival time were introduced in the random part of the model.

All analyses were carried out with the R statistical Software v.3.0.3 (R Development Core Team, 2014), using the functions *lm* from the *nlme* package

for linear models, *lmer* and *glmer* from lme4 package for mixed linear and generalized models, respectively, and *survreg* function from survival package for survival models. Significance for all statistical analyses was accepted at $P < 0.05$.

RESULTS

Meteorological conditions, soil moisture and tree survival

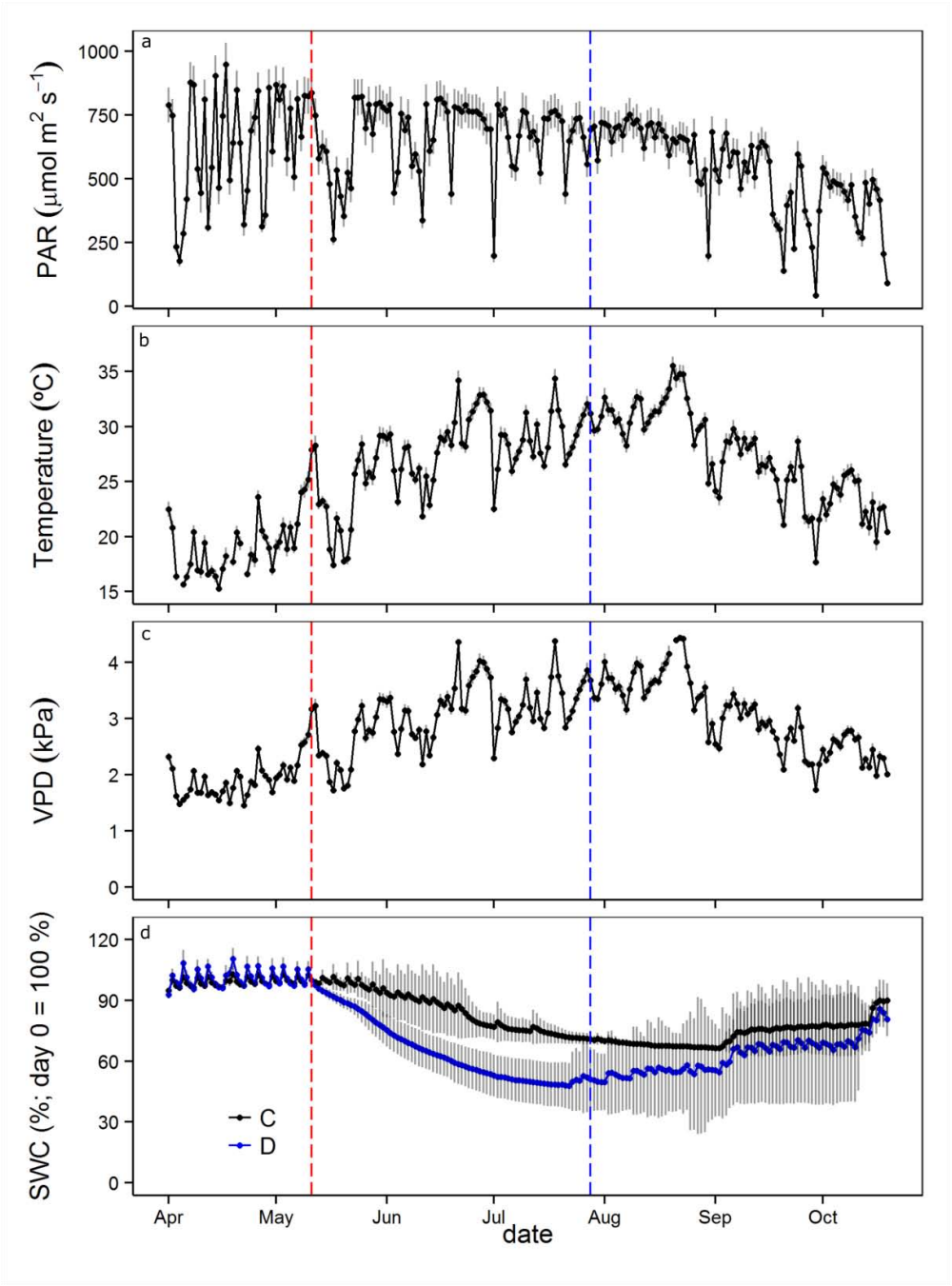

Figure 4.2.
Climatic and soil conditions in the greenhouse during the course of the experiment (May to October 2012), including: daytime average of a) photosynthetic active radiation (PAR), b) temperature, and c) vapor pressure deficit (VPD); and daily average of d) soil water content (SWC) in percentage change relative to the beginning of the treatment. In all panels solid points and solid lines represent average values; whereas grey lines indicate SE in *a*, *b* and *c* panels and standard deviation in panel *d*. Different colors in panel *d* indicate different treatments, control (C) and drought (D). Vertical lines indicate drought beginning (red line) and re-watering date (blue line).

During the study (including pretreatment period) annual average temperature and VPD were 18 ºC and 1.76 kPa, respectively. During the

experimental drought period average daytime temperature was 25.6 ºC and average daytime VPD was 2.8 kPa (Figure 4.2). PAR inside the greenhouse was approximately 14 % lower than outside the greenhouse (www.ruralcat.net, Caldes de Montbui meteorological station) with a day-time average of 616 µmol $m^{-2}s^{-1}$ during the experimental period (Figure 4.2a). Average soil water content prior to the drought treatment was 25.6 ± 1.6 %. Upon treatment implementation, SWC decreased sharply by 48 % and 28 % of the initial water content for D and C trees, respectively, before re-watering them in late July (Figure 4.2d). Minimum SWC was 11 and 21 % for D and C, respectively.

By the end of the study, four of the five C trees were alive (one died at the end of August), while 29 of the 44 D trees succumbed to drought after almost five months (Figure 4.3; Figure S2 Appendix III). A total of 9 trees (4C + 5D) were still alive at this time (note that 10 live trees were harvested during the experimental period), but they ended up dying over the course of the next six months. Reduced water availability had a significant impact on the survival probability (accelerating factor of 0.77; *P*<.01), shortening the predicted median survival time after the treatment onset from 211 days in C trees to 97 days in D trees (Figure 4.3).

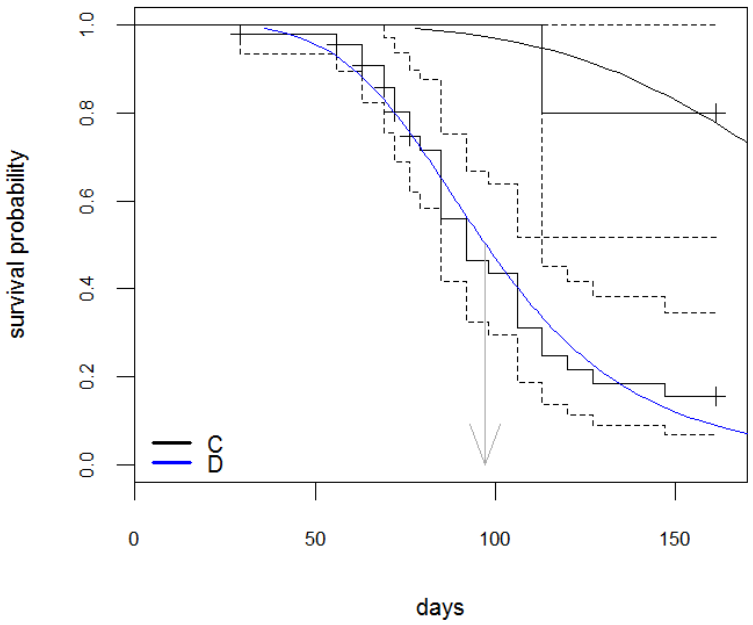

Figure 4.3. Estimated survival function for control (C) and drought (D) trees. Each estimate is accompanied by the corresponding 95 % confidence interval (dashed lines). Solid lines indicate log logistic fits from AFT models with treatment (control or drought) as factor.

Pre-drought characteristics of resistant vs. susceptible trees

Pre-treatment (after ca. one year of acclimation) shoot growth (growth.D and growth.L) and tree size (H and SA) were similar between resistant and susceptible trees (Table 4.1). However, resistant trees showed higher leaf area than susceptible trees both in absolute terms (LA) and relative to sapwood area (LA:SA). Pre-treatment values were similar between C and D trees for all variables except LA:SA, which was higher in C trees (Table 4.1).

Non-structural carbohydrate concentration in branches prior to the onset of the treatment was similar between resistant and susceptible trees (Table 4.1) and in both cases NSC content was close to the 7.2 % shown by C trees. Similar results were obtained when NSC were analyzed by fractions (starch, sucrose, monosaccharides or LMW sugars). Sucrose was the major component of NSC, accounting for 76 ± 3 % of the total carbohydrate content on average.

There were significant pre-treatment differences in the physiological performance of resistant and susceptible trees. Resistant trees showed higher water potentials, g_s, and assimilation rates per unit leaf area (A_N) and per tree (A_{tree}) than susceptible trees (Table 4.1). All trees, including susceptible trees for which Ψ_{pd} indicated no water stress (~ -0.5 MPa), showed low A_N and g_s (Table 4.1) relative to typical values for well watered plants (see Discussion), although WUE was higher in susceptible than resistant trees. PhiPS2 was low for all C and D trees but significantly lower in susceptible trees relative to resistant ones.

Table 4.1. Pretreatment mean values of morphological and physiological variables measured in control, resistant and susceptible trees. Numbers in parenthesis indicate SE and letters indicate P values <0.05 between resistant and susceptible trees. Sample size is 5 for C trees, 10 for resistant trees and 15 for susceptible ones for carbohydrates and time series variables; and 15 and 29 (resistant and susceptible, respectively) in the other cases.

	Control	**Resistant (D)**	**Susceptible (D)**
growth.D (mm)	3.7 (0.3)	4.3 (0.2)	4.0 (0.1)
growth.L (mm)	14.3 (1.2)	14.2 (0.8)	12.9 (0.6)
H (cm)	152.2 (2.6)	152.0 (1.8)	147.2 (2.5)
SA (cm^2)	4.7 (0.4)	5.9 (0.4)	5.6 (0.2)
LA (cm^2)	5021.2 (976.2)	3862.6 (292.7)[a]	3085.7 (221.4)[b]
LA:SA (cm^2 cm^{-2})	1062.9	663.2 (44.5)[a]	545.3 (30.0)[b]

	(191.5)		
NSC (% DW)	7.2 (0.4)	7.5 (0.5)	7.6 (0.7)
Starch (% DW)*	1.1 (0.3)	1.4 (0.3)	0.9 (0.2)
Sucrose (% DW)	5.7 (0.5)	5.5 (0.4)	6.1 (0.6)
Monosacc. (% DW)	0.4 (0.1)	0.6 (0.1)	0.5 (0.04)
LMW (%DW)	6.1 (0.5)	6.1 (0.4)	6.7 (0.6)
A_N (mol CO_2 m^{-2} s^{-1})	3.6 (1.3)	5.4 (0.6)[a]	2.7 (0.6)[b]
A_{tree} (mol CO_2 s^{-1})	1.9 (0.3)	2.0 (0.9)[a]	0.9 (0.2)[b]
g_s (mmol H_2O m^{-2} s^{-1})	33.2 (12.6)	44.4 (5.3)[a]	20.4 (5.2)[b]
Ψ_{pd} (MPa)	-0.5 (0.1)	-0.5 (0.2)[a]	-1.2 (0.2)[b]
Ψ_{md} (MPa)	-1.5 (0.1)	-1.4 (0.2)[a]	-2.0 (0.3)[b]
WUE (mmol CO_2/molH_2O)	6.0 (1.3)	5.4 (0.2)[a]	7.8 (1.0)[b]
PhiPS2	0.20 (0.02)	0.20 (0.01)[a]	0.15 (0.01)[b]
NPQ	3.74 (0.78)	3.45 (0.76)	3.69 (0.94)
FvFm	0.77 (0.02)	0.80 (0.01)	0.72 (0.03)

* P values from the Wilcoxon pairwise test used when normality could not be assumed.

Physiological time courses of resistant vs. susceptible trees

Predawn water potentials decreased as the soil dried but pre-treatment differences between resistant and susceptible trees persisted over time, with averages ranging from -0.5 to -2.1 MPa and from -1.2 to -3 MPa, respectively (Figure 4.4a). In contrast, the initial differences in Ψ_{md} between the two groups of trees tended to decline over time and became non-significant 15 days after the treatment started. A similar trend was experienced by A_N and g_s, with differences between resistant and susceptible diminishing over time (Figure 4.4d,e). At the end of June and early July, g_s and A_N were nearly 0 or even negative for susceptible trees, although no significant differences were found between tree groups. Pre-treatment differences in WUE between resistant and susceptible trees shifted during the drought treatment, with WUE decreasing sharply in susceptible trees to negative values while resistant trees maintained WUE above 1.35 mmol CO_2 mol H_2O^{-1} throughout the study period (Figure 4.4f). In all trees pre-treatment FvFm values of ~0.75 were maintained until ~50 days after treatment initiation, when FvFm diverged, with approximately constant values in resistant trees (similar to C trees) but decreasing in susceptible trees.

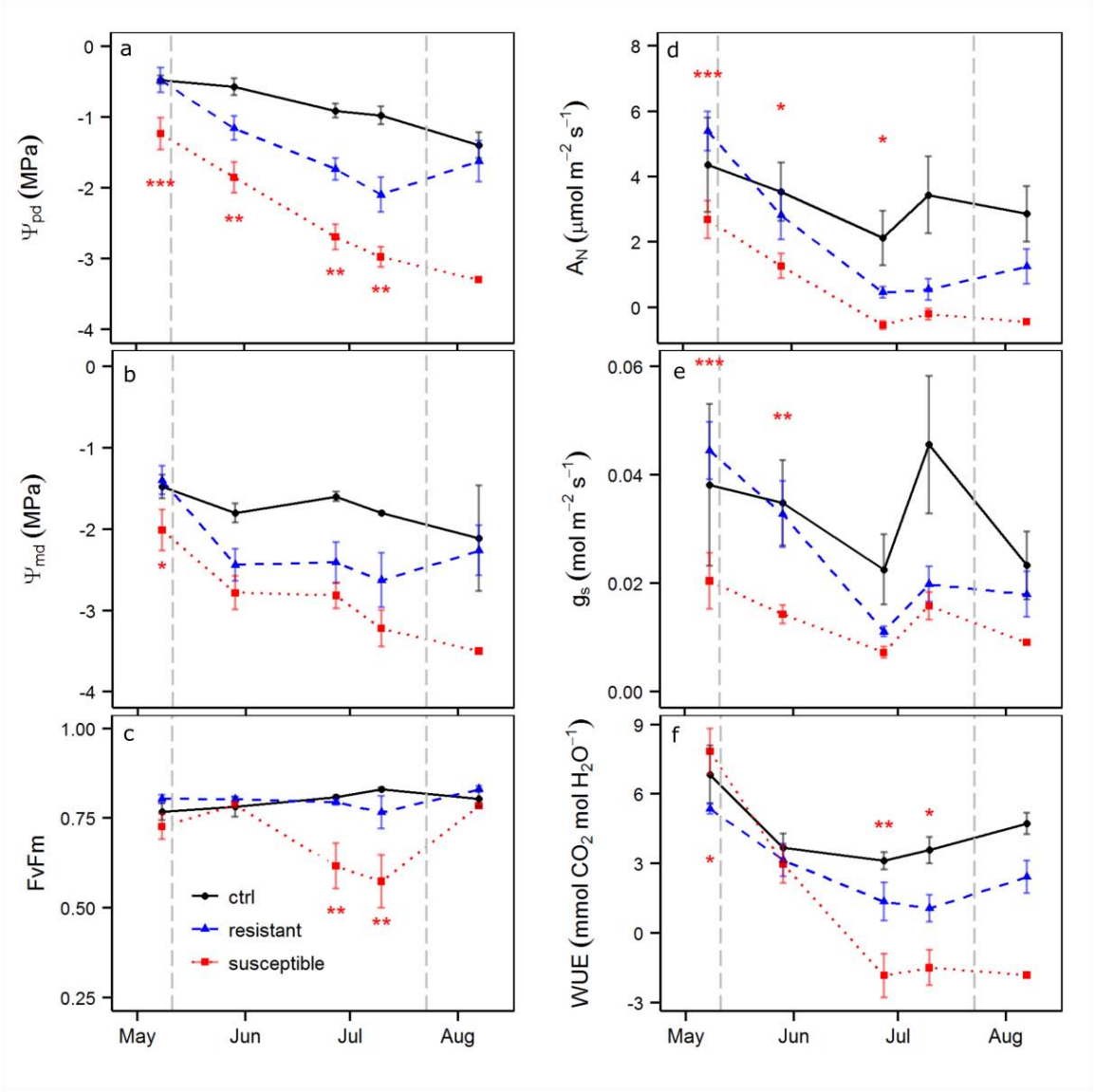

Figure 4.4.
Time courses of (a) predawn water potential (Ψ_{pd}), (b) midday water potential (Ψ_{md}), (c) maximum quantum yield (FvFm), (d) net assimilation rate (A_N), (e) stomatal conductance (g_s) and (f) water use efficiency (WUE). All parameters were measured on leaves, except water potentials that were measured on twigs. Means and SE are shown. N is constant for C trees (4, dead C tree not included), but varies from 10 to 4 in resistant trees and from 15 to 1 for susceptible trees due to the mortality and destructive sampling. Vertical dashed lines indicate the date when watering was stopped (left) and the date when it was re-established (right). Asterisks indicate significant differences between resistant and susceptible trees for a given date (*: 0.01<*P*<0.05, **: 0.001<*P*<0.01, ***: *P*<0.001).

Stomatal conductance decreased as the soil dried in both resistant and susceptible trees. However, resistant trees exhibited higher g_s at any given Ψ_{pd} (Figure 4.5; P =.009, Table S1a Appendix III). Similar results were obtained when Ψ_{md} was used instead of Ψ_{pd} (Table S2, Figure S3 Appendix III). In both

cases, the slope of the g_s response to declining water potential was similar between resistant and susceptible trees.

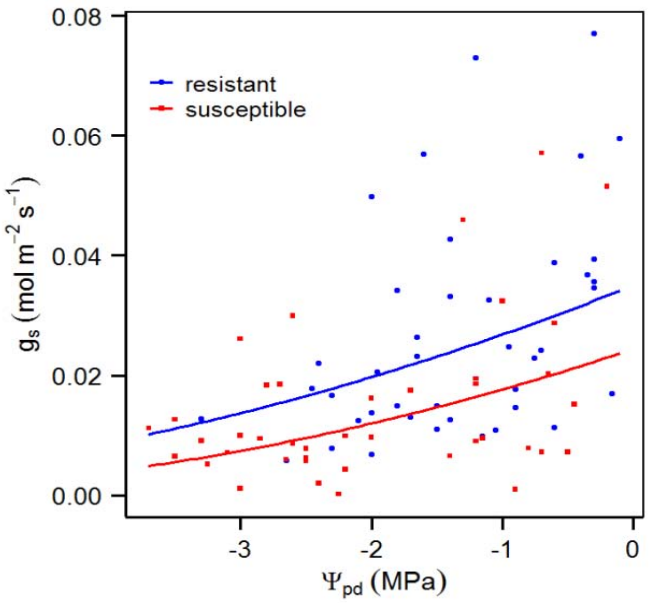

Figure 4.5. Relationship between stomatal conductance (g_s) and predawn water potential (Ψ_{pd}). Data correspond to values measured in the droughted trees (resistant and susceptible) during the study period. Solid lines depict the fitted models (Table S1).

Xylem hydraulic conductivity during drought treatment

Native hydraulic conductivity measured in mid-July showed large variability across groups. However, differences between resistant and susceptible trees were large and significant, with both K_S and K_L being more than twice, on average, in resistant than in susceptible ones (Table 4.2). Native conductivity in resistant trees was 87 % (K_S) and 65 % (K_L) of the corresponding value for C trees, whereas these values declined to 30 % (K_S) and 24 % (K_L) of C trees for susceptible individuals. Branch-level leaf-to-sapwood area ratio was not different between C, resistant and susceptible trees (Table 4.2), contrary to the pre-treatment patterns observed at the whole-tree level (Table 4.1).

Table 4.2. Sapwood specific hydraulic conductivity (K_S), leaf specific hydraulic conductivity (K_L) and the ratio between leaf-to-sapwood area (AL:AS.br) in branches of control, resistant and susceptible trees measured towards the end of the drought period. Numbers in parenthesis indicate SE and letters indicate P values <0.05 between resistant and susceptible trees. Sample size is 5 for C trees, 6 for resistant trees and 12 susceptible trees.

	Control	Resistant (D)	Susceptible (D)
K_S (m^2 MPa^{-1} s^{-1})	7.6×10^{-5} (2.6×10^{-5})	6.6×10^{-5} (2.4×10^{-5})^a	2.3×10^{-5} (5.8×10^{-6})^b
K_L (m^2 MPa^{-1} s^{-1})	6.6×10^{-8} (3.6×10^{-8})	4.3×10^{-8} (1.1×10^{-8})^a	1.6×10^{-8} (3.5×10^{-9})^b

AL:AS.br (cm^2 cm^{-2})	1560.8 (326.1)	1712.5 (499.3)	1848.8 (341.6)

Survival (AFT) models

Of the 44 variables tested only 18 had a significant effect on survival (shown in Figure 4.6). Carbon uptake-related variables (A_N, FvFm, PhiPS2, PhiCO2 and ETR) played an important role on increasing survival time. Particularly, A_N and FvFm were the best predictors of survival time (higher R^2), with higher values (.i, .st) and lower variation relative to the initial value (.rv) increasing survival in all cases. Although the overall highest R^2 corresponded to the A.rv model (R^2 = 0.28), the largest effect in terms of magnitude (a delay of more than 70 days in S_{50}; R^2 = 0.24) corresponded to A.st, the minimum A at the peak of the stress. The effect of pretreatment assimilation (A.i) was slightly smaller, resulting in an increase of 34 days in predicted median survival time. The second group of variables with greater impact on S_{50} included those related to carbon and water economy (g_s, WUE and LA). Higher water use efficiency at the stress peak delayed S_{50}, and high initial (pre-treatment) and stress peak g_s delayed S_{50}, suggesting that maximizing carbon uptake rather than minimizing water loss delayed mortality. This result was further supported by the significant and positive effect of the initial LA and LA:SA values, which explained approximately 20 % of variance in survival. None of the variables derived from water potential time courses had a significant effect on S_{50}. Importantly, when initial Ψ_{pd} was included as a covariate in the A.st and gs.st survival models, the effect of A and g_s on S_{50} remained highly significant (P<0.001 and P=0.009, respectively), indicating their independent effect even when accounting for initial differences in water availability between trees. The concentration of monosaccharides in branches before the treatment had a positive effect on survival time (R^2 = 0.21; P<0.001), increasing median survival time by 26 days. Similarly, specific hydraulic conductivity measured during the drought treatment (K_S and K_L) also had a positive effect on survival time (P=0.004), although the magnitude of the effect was lower than that of monosaccharides. Finally, shoot growth in length (growth.L) during the acclimation period was also significantly and positively correlated with time to death, although the explained variance was low (R^2=0.09; P=0.04).

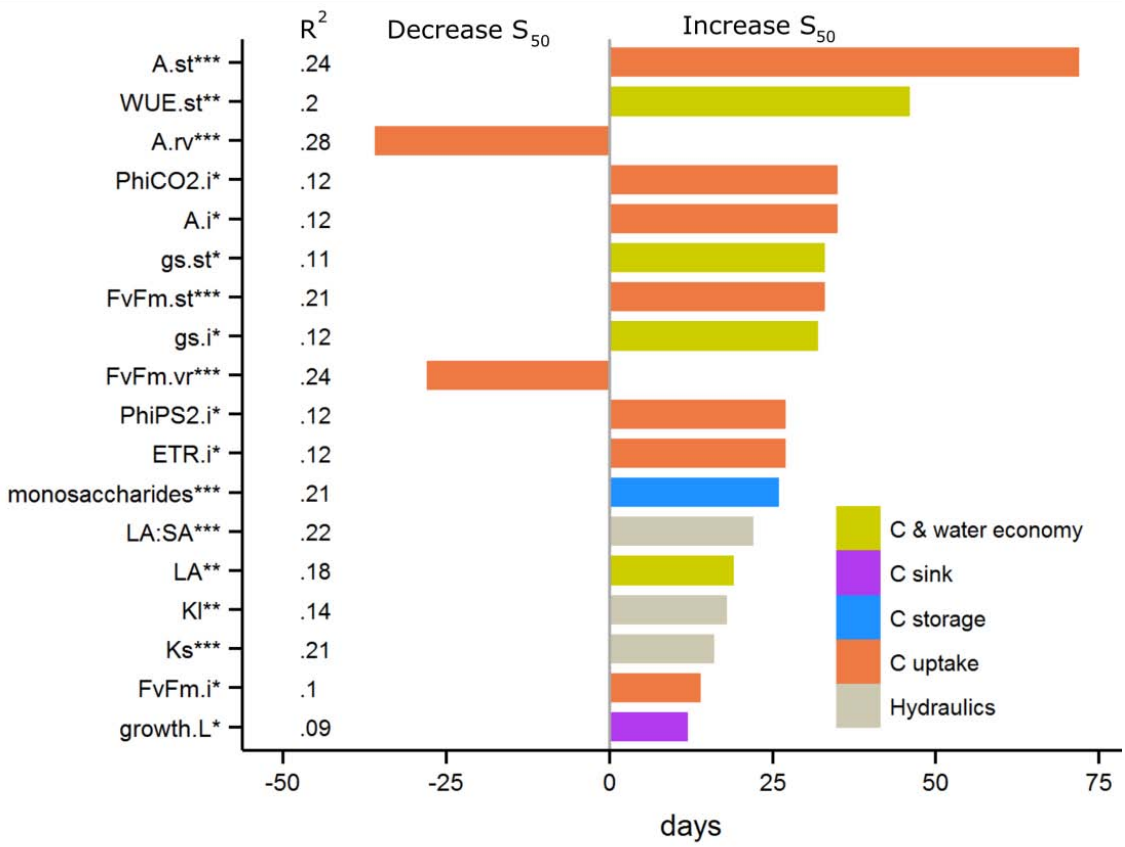

Figure 4.6.
Accelerate failure time (AFT) model results for significant variables. The effect of each explanatory variable on median survival time has been standardized by the intra-population variation for each variable (variation between 1st and 3rd quartiles). Vertical line on 0 days corresponds to the median survival time of the D trees when the value of the 1st quartile of each variable is used as predictor on the AFT model. Horizontal bars show the positive or negative effect when the 3rd quartile of each variable is used. N varies between 18 and 44 trees depending on the predictor variable.

Paired comparisons of dead vs. live trees

Belowground biomass was 50 % higher in live trees (P<0.001; Figure 4.7a). Aboveground biomass tended to be higher in live trees but differences were not significant (P=0.06). Hence, dead trees showed lower ratio of belowground to aboveground biomass than living ones (P=0.01; Figure 4.7b). Fine root biomass and stem wood density were similar between the two groups (P=0.52 and P=0.39, respectively; Figures 4.7c and 4.7d).

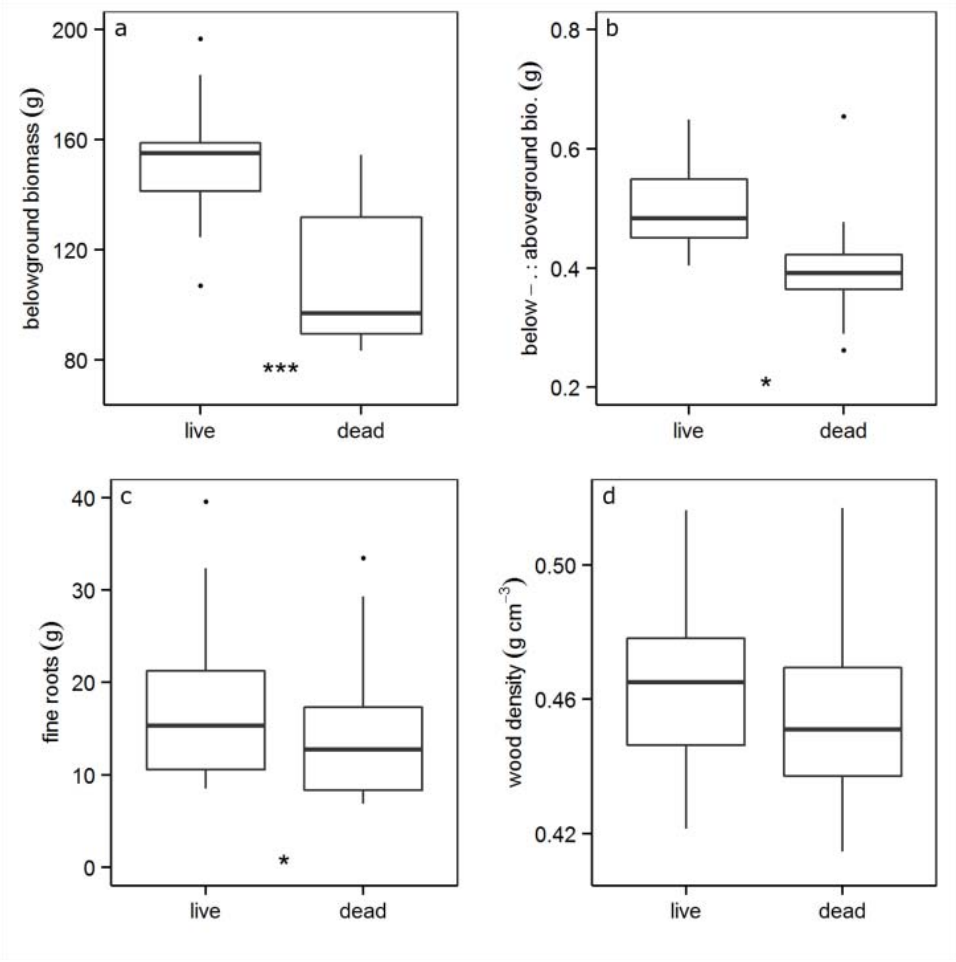

Figure 4.7.
Differences between dead and live trees in (a) belowground biomass, (b) ratio of below:aboveground biomass, (c) fine roots biomass and (d) wood density. Asterisks indicate significant differences between live and dead trees (*: 0.01<*P*<0.05, **: 0.001<*P*<0.01, ***: *P*<0.001).

NSC concentrations decreased relative to pre-drought values in branches (~7 %) (Table 4.1). Total NSC concentration was much lower in dead than in surviving individuals in all tissues (*P*<0.001, Figure 4.8). The same was true for LMW sugars (*P*<0.001), with a major contribution of sucrose to this fraction. In contrast, starch content tended to be lower in living trees, where the proportion of 0 values was significantly higher in all tissues (*P*<0.001).

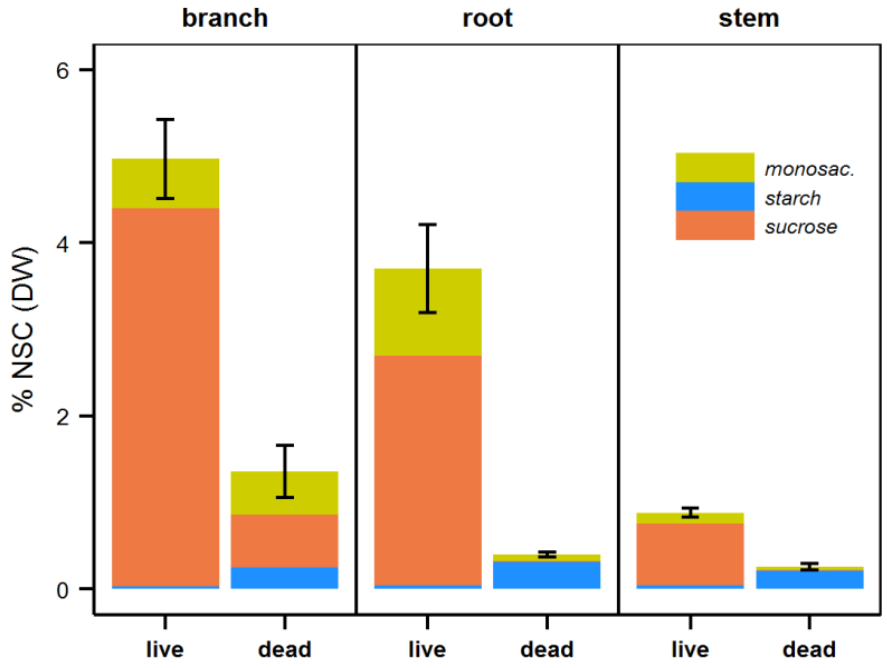

Figure 4.8.
Non-structural carbohydrates content in different tissues of live and dead trees sampled concurrently (paired sampling). Sample size is 10 in both groups. Error bars indicate SE of the total NSC.

DISCUSSION

While all trees had the same origin and were subjected to similar environmental conditions, time until death varied by more than three months. Both, pretreatment characteristics and responses during drought were relevant to explain differences in survival time among individuals. Most importantly, we found that trees with higher assimilation rates before and during the extreme drought were able to survive longer, even at the expense of higher water loss. These results indicate that carbon uptake was critical to prolong survival, and suggest that mechanisms of mortality not only relate to evolved, species-specific drought-resistance strategies (Hartmann, 2011; Klein, 2014), but also to dynamic adjustments at the individual level that occur prior and during drought, including fine tuning of stomatal behavior and carbon allocation (e.g., below- vs. aboveground).

Magnitude and variability of survival times

Our study simulated natural conditions enabling root expansion into the ground during the acclimation period, thus avoiding effects of pot size on root development during the experiment, and providing a better analogue for conditions likely to be experienced in the field. Spacing between trees was sufficient to avoid belowground competition between individuals, as evidenced by the complete lack of overlap between root systems of different individuals at the end of the experiment. Similar or slightly shorter survival times in our study compared to those reported by Adams *et al.* (2009), Anderegg & Anderegg (2013) and Sevanto *et al.* (2014) for similar size pine saplings (or even mature trees in the latter) is probably related to the high temperatures in the greenhouse prior and during the imposed extreme drought (Figure S1 Appendix III). The combination of warmer temperatures with lack of watering has been shown to accelerate the mortality process in several species (Adams et al. 2009, Zhao et al. 2013), including *P. sylvestris* (Matías *et al.*, 2014). Nonetheless, both *Quercus ilex* and *Phillyrea latifolia,* which often coexist with *P. sylvestris,* and were grown under the same treatment conditions, did not show mortality or symptoms of decline during the experimental period of this study.

Survival time since the beginning of the treatment was highly variable among individual trees, ranging more than 100 days. The lack of spatial structure in survival times (Figure S2 Appendix III) indicates that potential artifacts due to microclimatic variability between tree locations were minimized. In addition, resistant and susceptible trees not only differed in Ψ_{pd} (a proxy for soil water availability as perceived by the plant) but resistant trees showed higher g_s at any given Ψ_{pd} (Figure 4.5) or Ψ_{md} (Figure S3 Appendix III) relative to susceptible ones. Therefore, differences in water use across individuals were not only explained by micro-spatial variations of soil water availability inside the greenhouse, but to different stomatal responses. It is important to note that even a small difference in survival time may translate to life or death under field conditions, due to the stochastic nature of rainfall patterns and finite drought durations (see Martínez-Vilalta *et al.* 2002a for a modeling example). In addition, there was substantial variability in responses (see Table 4.1)

suggesting substantial population plasticity which may facilitate acclimation and population recovery to changes in environmental conditions (Lloret *et al.*, 2012; Richter *et al.*, 2012).

Pre-treatment differences between individuals were relevant to explain differences in survival time under drought, unlike results by Sevanto et al. (2014). Trees with better access to soil water, as reflected by less negative Ψ_{pd}, and equipped to assimilate more carbon (higher LA:SA, g_s, A_N under relatively well watered conditions) survived longer under severe drought. Higher carbon uptake capacity exhibited by resistant trees relative to susceptible trees was not clearly associated to higher growth rates prior to the mortality event (Table 4.1). However, higher shoot growth (length) resulted in slightly longer time until death. Despite no clear thresholds in the response of the physiological parameters to Ψ_{pd} (Figure S4 Appendix III), photosynthesis in susceptible trees ceased at Ψ_{pd} ~-3 MPa, a value similar to the water potential inducing 50% embolism in this species (Martínez-Vilalta and Piñol, 2002). Around and below this water potential the photosynthetic machinery started to malfunction, as reflected by low FvFm values (Figure S4 Appendix III), and the carbon balance might become negative.

Carbon uptake is prioritized at the expense of water loss

Many different parameters are involved in plant responses to water shortage, resulting in a variety of plant attributes associated to survival time under extreme drought (Figure 4.6). Variables related to carbon uptake and carbon and water economy were the best predictors of survival time in our study. The strong and positive effect of A.st and gs.st on survival time is contrary to the idea that plants under severe drought must minimize water loss to prevent mortality (Fischer and Turner, 1978; Cowan, 1982; Ehleringer and Cooper, 1988). Importantly, this effect was significant even after accounting for differences in local water availability (Ψ_{pd}) among individuals at the start of the experiment. Prioritizing carbon assimilation may be an advantage for at least two reasons. Firstly, it allows investing more resources belowground to grow a larger root system (even relative to leaf area), with the potential to access more water resources. This is supported by the higher below to aboveground mass

ratio in surviving trees compared to dead individuals in our paired sampling. Secondly, higher assimilation is likely to increase carbon availability, at least in the short term. Carbon is thought to be critical to acquire and retain water and maintain whole plant hydraulic function (Dietze *et al.*, 2014; O'Brien *et al.*, 2014; Sala & Mencuccini, 2014). At the cellular level, both lack of carbon and lack of turgor can be fatal for cellular structure, integrity and metabolism (McDowell *et al.*, 2011), and maintaining both carbon and turgor should be a priority. At the whole plant level, vascular transport should be a priority because if transport fails irreversibly, then whole-plant function fails. These scale-dependent priorities are tightly linked because the maintenance of vascular transport requires turgor in adjacent living cells and turgor requires solutes, including carbon-based solutes (Sevanto *et al.*, 2014). Our results suggest that, at least in *P. sylvestris* and as long as it is sustainable, carbon availability may be as important as stomatal regulation of water loss to maintain hydraulic integrity.

None of the studied trees grew during the spring season in 2012 and hence, the assimilated carbon and NSC reserves were mostly used in maintenance (respiration) and other physiological functions. Carbon supplied by photosynthesis was very low and apparently not enough to meet the carbon demand under drought in both dead and live trees, and consequently NSC in branches declined with respect to the initial concentrations, from ~7 % (Table 4.1) to ~5% (living trees) and ~1.5% (dead trees) (Figure 4.8). The fact that dead trees exhibited much lower NSC values compared with live trees, together with the significant effect of pre-treatment monosaccharides concentration and carbon assimilation on survival time, strongly suggest than NSC depletion is associated to mortality in our study species, consistent with results under field conditions (Galiano *et al.*, 2011) and with the notion that NSC pools can enhance survival under drought (O'Brien *et al.*, 2014). Further, the fact that living trees had all their NSC in soluble fractions suggests that they may all be used in osmoregulation or other hydraulically related functions during an extreme drought (Sala *et al.*, 2012; Dietze *et al.*, 2014).

Large differences in NSC concentration observed between live and dead individuals could be due to NSC consumption after individuals had effectively no chance of surviving. The definition of plant death is inherently difficult and can

range from the point of no return (irreversible collapse of whole-plant function after which tissues locally alive may continue to consume locally available carbon reserves for respiration) to no respiring tissues left (Anderegg *et al.*, 2012; Sevanto *et al.*, 2014). Most likely, our definition of death (brown needles and dry phloem; see Materials and Methods section) was somewhere in between these two points, and was similar to previous studies (Piper *et al.*, 2009; Gaylord *et al.*, 2013; Galvez *et al.*, 2013; Hartmann *et al.*, 2013*a*; Reinhardt *et al.*, 2015). However, regardless of whether NSC differences between live and dead trees reflect thresholds below which trees cannot survive or some NSC consumption prior to declaring a tree dead (i.e. higher NSC thresholds than values measured in dead trees), our results clearly indicate that survival time was related to carbon uptake and availability. Although neutral lipids (not measured in our study) can be an important component of the non-structural mobile carbon pool in pines (Hoch *et al.*, 2002; Hoch and Körner, 2003), Fischer et al. (2015) has recently showed that *P. sylvestris* respiration does not shift from carbohydrates to lipids during drought.

Although for simplicity we refer to susceptible and resistant trees, all trees subjected to drought eventually died after the study period (subsequent to October 2012), even after irrigation. Therefore, if there are specific hydraulic and/or carbon related mortality thresholds, all trees subjected to drought were close to these thresholds or had surpassed them. Interestingly, water potential in trees that survived longer (resistant) recovered fully after irrigation, indicating that they did not experience irreversible hydraulic failure, despite lower hydraulic conductance relative to control trees in mid-July. This suggests that critical hydraulic thresholds were not surpassed in these trees and reinforces the idea that carbon availability was critical for survival.

We conclude that the ability to assimilate carbon is the main factor that explains differences in survival time in *P. sylvestris* trees under extreme drought. Our analysis at the individual level further indicates that the large variation in survival times can be partially explained by predisposing factors (morphological and physiological traits) that determine responses to drought. The prioritization of carbon uptake was somewhat unexpected because *P. sylvestris* is considered a isohydric species and, relative to other coexisting

species at the dry end of its distribution (e.g., *Q. ilex*), it is considered a water-conservative species with strong stomatal regulation of water loss (Aguadé *et al.*, 2015*a*). Our results emphasize the intimate link between carbon metabolism and hydraulic function (McDowell *et al.*, 2011; Sala *et al.*, 2012) and support the view that plants need carbon to move and retain water (Hartmann *et al.*, 2013*a*; Sala and Mencuccini, 2014; Sevanto *et al.*, 2014; Dietze *et al.*, 2014). Accordingly, when plants are close to minimum NSC thresholds that could compromise vascular function, carbon assimilation at the expense of water loss, while risky, may be the only viable strategy in nature, where favorable conditions allowing recovery may occur at any time. Otherwise, respiration would unavoidably continue to deplete carbon. Finally, our study highlights that accounting for variability in functional traits within populations may be useful to understand and predict plant responses to drought in natural settings.

ACKNOWLEDGMENTS

This research was supported by the Spanish government through competitive grants CGL2010-16373 and CGL2013-46808-R. NGF was supported by a FPI scholarship from the Spanish Ministry (MINECO). AS was supported by a sabbatical leave from the University of Montana. We would like to thank Eulalia Serra, Marc Ferrer, Bea Grau and Cristian Morales (IRTA) for their valuable assistance in the fieldwork.

Chapter 5

General discussion

The work done during this thesis includes three experimental approaches to answer multiple questions related with drought responses of plants, with a specific focus on stomatal regulation and carbon and water management in response to drought. Altogether, the three studies advance our current understanding of the mechanisms underlying drought-induced mortality in trees. The thesis gives insights on the critical role of carbon uptake to prolong survival and provides a cautionary note on the dangers of linking the iso/anisohydric behavior of plants with the risks of carbon starvation (CS) or hydraulic failure (HF) under extreme drought.

The non-relationship between iso/anisohydric behavior and hydraulic failure

The idea that plants under severe drought must minimize water loss to prevent mortality (Fischer and Turner, 1978; Cowan, 1982; Ehleringer and Cooper, 1988) was forged at about the same time as stomatal ability to limit transpiration was intensively studied and stressed in the literature (Farquhar and Sharkey 1982). Stomata provide the most obvious mechanism allowing plants to control water transport and reduce water losses under drought (Martínez-Vilalta *et al.*, 2014), and several studies have provided evidence of the tight association between stomatal closure and the occurrence of embolism in the stem xylem (Sparks and Black, 1999; Brodribb *et al.*, 2003; Domec *et al.*, 2006; Choat *et al.*, 2007; Martínez-Vilalta *et al.*, 2014). The continuum between iso and anisohydry (Jones, 1998; Tardieu and Simonneau, 1998) represents an attempt to integrate plants' response to soil water depletion. However, the inability to describe stomatal behavior solely by variations of Ψ_{leaf} (or VPD) (Tardieu *et al.*, 1996; Mcadam and Brodribb, 2014; Brodribb *et al.*, 2014) and the hydraulic disconnection to the soil that some species experience under intense drought (Plaut *et al.*, 2012; Sevanto *et al.*, 2014) complicate the interpretation of stomatal conductance in relation to Ψ_{leaf}. In addition, the iso/anisohydric classification was originally developed in the context of daily variations of predawn and midday water potentials (Jones, 1998; Tardieu and Simonneau, 1998), but it has been frequently applied to seasonal dynamics of water potentials and stomatal regulation. However, the processes regulating the relationship between water potentials and stomatal regulation at short (~diurnal)

and long (~seasonal) timescales are likely to differ, further contributing to the confusion.

In the context of drought-induced mortality, McDowell et al. 2008 assumed that plant's water potential response to declining soil water content was determined entirely by stomatal conductance and hypothesized that the more anisohydric the plant behavior is, the lower the resulting xylem water potentials and, hence, the higher the susceptibility to suffer hydraulic failure. There were also counterexamples, though. For instance, the more anisohydric species in Sparks and Black (1999) exhibited more effective stomatal closure (before reaching the entry water potential, Ψ_e) when comparing the response to drought of dry and wet site species (relatively anisohydric and isohydric, respectively, in their study). Martínez-Vilalta *et al.* (2003) and Plaut *et al.* (2012) showed how anisohydric species frequently are more resistant to xylem embolism than isohydric species, complicating the linkage between lower water potentials and higher hydraulic vulnerability. Rogiers *et al.* (2012) showed how g_s converge to closure in vineyards under severe plant water deficits (including high VPD or not) independently of iso/anisohydric behavior.

We addressed the relationship between stomatal control, water potential dynamics and hydraulic safety margins under drought in chapters 2 and 3. Our results provide no evidence of wider hydraulic safety margins on the relatively isohydric species, exemplified here by *P. edulis* and *Q. ilex.* On the contrary, they suggest that the more isohydric species in both systems seem to be exposed to chronic embolism while the anisohydric species tend to avoid xylem embolism. This finding is important firstly because it warns against establishing a general association between stronger stomatal responses to declines in water potential and wider hydraulic safety margins, and advocates for a more integrative characterization incorporating stomatal and xylem responses to declining water potentials (Klein, 2014; Martínez-Vilalta *et al.*, 2014). In addition, if the higher vulnerability to embolism of isohydric species is found to be general, it should be taken into account in order to improve our understanding of the traits and mechanisms determining survival under drought.

The non-relationship between iso/anisohydric behavior and carbon starvation

Associating a strong regulation of water potential (relatively isohydric behaviour) with carbon starvation assumes that stomatal closure is the basic mechanism explaining different temporal dynamics of water potentials across species, and also fails to account for differences in water use efficiency (assimilation per unit g_s) or carbon economy (sources and sinks other than assimilation) across species. Several studies in the literature mix stomatal responses to water potential with temporal dynamics of stomatal conductance, and use the term “earlier” stomatal closure in both senses, either temporal or in response to Ψ_{leaf}. However, this association is problematic when comparing coexisting species precisely because they may operate at very different water potentials and the fact that one closes stomata at higher Ψ_{leaf} (~isohydric behavior) does not necessarily mean that this species closes stomata earlier in time (at seasonal timescales). It could simply reflect, for instance, differences in rooting depth among species.

In chapters 2 and, mainly 3, we studied how the iso/anisohydric characterization relates to different g_s seasonal dynamics and changes in A_N over time. At these temporal scales, the timing of stomatal closure was similar within the two studied pairs of species: *P. edulis* vs. *J. monosperma*, and *Q. ilex* vs. *P. latifolia*. In the latter case, g_s under extreme drought was even slightly higher in the more isohydric species (*Q. ilex*) relative to *P. latifolia*. These results provide evidence that higher water potentials may not necessarily mean stronger stomatal regulation, as commonly assumed. In addition, the relative anisohydric *J. monosperma* showed slightly higher carbon uptake rates than the isohydric *P. edulis*, but this was not the case in the *Quercus* vs. *Phillyrea* example. *Q. ilex* clearly exhibited a more isohydric behavior but assimilation rates were consistently higher in this species than in *P. latifolia* when drought intensified, again contrary to the classic idea that isohydric behavior constrains assimilation. Although we cannot rule out other differences in the carbon economy of the studied species, as we did not conduct a full carbon balance, our results clearly show that water potential regulation cannot be used as a (sole) proxy for carbon constrains in plants. Recently, Skelton et al. (2015)

suggested a direct measurement of the number of days since water potential in the field exceeded the stomatal closure threshold as a direct measurement of potential carbon limitations that lead to death. However, in the same work, authors re-define the degree of iso/anisohydry as the degree of stomatal regulation of cavitation; in other words, as the difference between the Ψ_w at 12 % of the maximum g_s and the Ψ_w at 50 % loss of hydraulic conductivity, with positive and negative values defined as isohydric and anisohydric, respectively. Although it could be an useful proxy of the degree of stomatal regulation, the proposed re-definition of iso/anisohydry differs from the original concept and may generate more confusion.

The importance of studying coexisting species with contrasted vulnerability to drought

The piñon-juniper system in the SW USA and the holm oak system in NE Spain are very appealing to study drought-induced mortality mechanisms due to the contrasted resistance to drought between species and because of the potential impact that future drought events may have on the dynamics of these widespread communities. Both systems have proven to be very resistant to drought (and/or temperature) and, in both cases, the more isohydric species was more vulnerable to drought-induced mortality. In addition, isohydric species were more vulnerable to xylem embolism and tended to suffer higher loss of hydraulic conductivity during drought. In the *Q. ilex – P. latifolia* example we studied physiological responses over a period of three years, to find that hydraulic constrains together with the lower plasticity to reduce water demand (in terms of leaf-to-sapwood area) in *Q. ilex* relative to *P. latifolia* were the main traits explaining survival differences between species. The high NSC levels and the 'large' increase in NSC concentration in branches exhibited in both species towards the end of the treatment suggests that drought-induced mortality was not triggered by carbon starvation in our study system.

The drought and heat treatments applied to the piñon-juniper system were milder compared to the recurrent extreme droughts (in addition to increased temperature inside the greenhouse) applied to the other experimental system. Still, it is intriguing that there was no piñon mortality after two years of

experiment despite widespread mortality records of this species in SW USA (Shaw *et al.*, 2005; Breshears *et al.*, 2005), particularly considering that experimental conditions were clearly drier than ambient conditions. In 1987, Franklin *et al.* stressed the idea that drought periods predispose plants to die by biotic agents, and this has been confirmed in the case of *P. edulis* trees (Gaylord *et al.*, 2013, 2015). Modelling results show that physiological models that not account for pest dynamics fail to predict mortality in this species (McDowell *et al.*, 2013*a*). By contrast, the situation is different for the holm oak system, where lethal plagues have not been identified (although fungal infections with *Phytophthora cinnamomi* have been described in central and southern Spain, (Sánchez *et al.*, 2002). Accounting for these differences between species or systems is critical to understand mortality mechanisms and long-term vegetation dynamics. Thus, including biotic agents and the mechanisms by which they modify plant physiological process, e.g. carbon allocation, should be a priority to understand the underlying mechanisms triggering drought-induced mortality (Oliva *et al.*, 2014; Anderegg *et al.*, 2015).

Individual level traits as a key to understand mortality mechanisms

When comparing *P. sylvestris* vulnerability to drought against *Q. ilex* (or *P. latifolia*) there is no question about their different vulnerability in the areas where they coexist. The future of *P. sylvestris* at the xeric limits of its distribution is a chronicle of a foretold death, at least in some areas (Hódar *et al.*, 2003; Rigling *et al.*, 2013; Vilà-Cabrera *et al.*, 2013). However, even in these extremely dry populations some individuals die and others survive without showing any sign of decline (Hereş *et al.*, 2012; Poyatos *et al.*, 2013), with strong implications for the short- to mid-term dynamics of these communities. Why is that? Within-species level variability in time to death has important demographic implications, but also provides an opportunity to study the mechanisms leading to drought-induced mortality in a more controlled manner, comparing individuals that share most of their genetic makeup and the overall strategies to face drought.

Our study of the determinants of survival time under extreme drought in *P. sylvestris* (chapter 4) showed that individuals that survived for longer were

those that prioritized carbon acquisition at the expense of higher water loss, showing higher stomatal conductance at a given leaf water potential. These results, together with NSC dynamics, demonstrate that preserving carbon uptake and maintain carbon pools above some critical level is at least as important as saving water to extend survival during drought periods. In this species NSC depletion occurred before mortality, highlighting differences in mortality mechanisms across species. We suggest that improving the integration of carbon and water dynamics during drought in the context of the species-specific strategies to face water shortage should be emphasized in future studies.

Conclusions

1. The tight stomatal control and low levels of embolism experienced by juniper trees in response to drought is contrary to the idea that anisohydric behavior is associated with less strict stomatal control and higher risk of hydraulic failure than isohydric behavior.

2. Similarly, lower water potentials in *P. latifolia* with respect to the more isohydric *Q. ilex* are not necessarily associated with narrower hydraulic safety margins. Thus, we propose a more integrative classification of species drought responses and water potential regulation that integrates both stomatal behavior and embolism resistance.

3. Stronger regulation of leaf water potentials in *Q. ilex* and *P. edulis* compared with *P. latifolia* and *J. monosperma* respectively were not associated with shorter periods of positive gas exchange (assimilation) under drought. Therefore, the iso/anisohydric classification cannot be used as a proxy for the risk of carbon starvation across species.

4. Both, the piñon-juniper study and the *Q. ilex* vs. *P. latifolia* study warn against making direct connections between leaf water potential regulation, stomatal behavior and the mechanisms of drought-induced mortality.

5. Large intraspecific variability in time to death (more than three months) was found when *P. sylvestris* trees were subjected to a lethal drought. This variability may be critical under field conditions due to the stochastic nature of rainfall patterns and, thus, it should be considered when making predictions of drought impacts on vegetation.

6. The best predictors of survival time in *P. sylvestris* were the carbon and carbon/water economy variables measured before and during drought. Sustaining carbon assimilation, even at the expenses of higher water losses, and the maintenance of NSC over some critical threshold were

the main factors explaining survival time of *P. sylvestris* subjected to extreme drought.

7. Higher resistance to xylem embolism and tighter stomatal control (relative to the species-specific water potentials causing generalized xylem embolism) seems to be the most plausible difference between drought-resistant and drought-susceptible species in our paired comparisons. However, when we focus at the intraspecific level, where hydraulic traits should be less variable between individuals, maintaining carbon uptake and carbon stocks above some critical level seems to be critical to prolong survival. We do not know the extent to which this conclusion is species-dependent. In addition, the precise mechanism by which this carbon may contribute to maintain the integrity of the water transport system or other vital processes is still an open question.

References

Ackerly DD, Dudley SA, Sultan SE, *et al.* 2000. The evolution of plant ecophysiological traits: recent advances and future directions? Bioscience **50**, 979–995.

Adams HD, Collins AD, Briggs SP, Vennetier M, Dickman LT, Sevanto S, Garcia-Forner N, Powers HH, McDowell NG. 2015. Experimental drought and heat can delay phenological development and reduce foliar and shoot growth in semiarid trees. Global Change Biology **21**, 42104220.

Adams HD, Germino MJ, Breshears DD, Barron-Gafford G a, Guardiola-Claramonte M, Zou CB, Huxman TE. 2013. Nonstructural leaf carbohydrate dynamics of Pinus edulis during drought-induced tree mortality reveal role for carbon metabolism in mortality mechanism. New phytologist **197**, 1142–1151.

Adams HD, Guardiola-Claramonte M, Barron-Gafford GA, Villegas JC, Breshears DD, Zou CB, Troch PA, Huxman TE. 2009. Temperature sensitivity of drought-induced tree mortality portends increased regional die-off under global-change-type drought. Proceedings of the National Academy of Sciences of the United States of America **106**, 7063–7066.

Aguadé D, Poyatos R, Gómez M, Oliva J, Martínez-Vilalta J. 2015*a*. The role of defoliation and root rot pathogen infection in driving the mode of drought-related physiological decline in Scots pine (Pinus sylvestris L.). Tree Physiology **35**, 229–242.

Aguadé D, Poyatos R, Rosas T, Martínez-vilalta J. 2015*b*. Comparative Drought Responses of Quercus ilex L. and Pinus sylvestris L. in a Montane Forest Undergoing a Vegetation Shift. Forests **6**, 2505–2529.

Allen CD, Breshears DD, McDowell NG. 2015. On underestimation of global vulnerability to tree mortality and forest die-off from hotter drought in the Anthropocene. Ecosphere **6**, 1–55.

Allen CD, Macalady AK, Chenchouni H, *et al.* 2010. A global overview of drought and heat-induced tree mortality reveals emerging climate change risks for forests. Forest Ecology and Management **259**, 660–684.

Anderegg WRL. 2015. Spatial and temporal variation in plant hydraulic traits and their relevance for climate change impacts on vegetation. New Phytologist **205**, 1008–1014.

Anderegg WRL, Anderegg LDL. 2013. Hydraulic and carbohydrate changes in experimental drought-induced mortality of saplings in two conifer species. Tree Physiology **33**, 252–260.

Anderegg WRL, Anderegg LDL, Berry JA, Field CB. 2014. Loss of whole-tree hydraulic conductance during severe drought and multi-year forest die-off. Oecologia **175**, 11–23.

Anderegg WRL, Berry JA, Smith DD, Sperry JS, Anderegg LDL, Field CB.

2012. The roles of hydraulic and carbon stress in a widespread climate-induced forest die-off. Proceedings of the National Academy of Sciences of the United States of America **109**, 233–237.

Anderegg WRL, Hicke JA, Fisher RA, *et al.* 2015. Tree mortality from drought, insects, and their interactions in a changing climate. New Phytologist **208**, 674–683.

Anderegg WRL, Kane JM, Anderegg LDL. 2013*a*. Consequences of widespread tree mortality triggered by drought and temperature stress. Nature Climate Change **3**, 30–36.

Anderegg WRL, Plavcová L, Anderegg LDL, Hacke UG, Berry JA, Field CB. 2013*b*. Drought's legacy: multiyear hydraulic deterioration underlies widespread aspen forest die-off and portends increased future risk. Global change biology **19**, 1188–1196.

Aspinwall MJ, Loik ME, Resco De Dios V, Tjoelker MG, Payton PR, Tissue DT. 2015. Utilizing intraspecific variation in phenotypic plasticity to bolster agricultural and forest productivity under climate change. Plant, Cell & Environment **38**, 1752–1764.

Atkin OK, Macherel D. 2009. The crucial role of plant mitochondria in orchestrating drought tolerance. Annals of botany **103**, 581–97.

Baker NR. 2008. Chlorophyll fluorescence: a probe of photosynthesis in vivo. Annual review of plant biology **59**, 89–113.

Barbeta A, Ogaya R, Peñuelas J. 2013. Dampening effects of long-term experimental drought on growth and mortality rates of a Holm oak forest. Global Change Biology **19**, 3133–3144.

Bombelli A, Gratani L. 2003. Interspecific differences of leaf gas exchange and water relations of three evergreen Mediterranean shrub species. Photosynthetica **41**, 619–625.

Bossel H. 1986. Dynamics of forest dieback: Systems analysis and simulation. Ecological Modelling **34**, 259–288.

Boyer JS. 1982. Plant productivity and environment. Science **218**, 443–448.

Bréda N, Huc R, Granier A, Dreyer E. 2006. Temperate forest trees and stands under severe drought : a review of ecophysiological responses , adaptation processes and long-term consequences. Annals of Forest Science **63**, 625–644.

Breshears DD, Adams HD, Eamus D, McDowell NG, Law DJ, Will RE, Williams AP, Zou CB. 2013. The critical amplifying role of increasing atmospheric moisture demand on tree mortality and associated regional die-off. Frontiers in plant science **4**, 1–4.

Breshears DD, Cobb NS, Rich PM, *et al.* 2005. Regional vegetation die-off in response to global-change-type drought. Proceedings of the National Academy of Sciences of the United States of America **102**, 15144–8.

Breshears DD, Myers OB, Barnes FJ. 2009*a*. Horizontal heterogeneity in the frequency of plant-available water with woodland intercanopy – canopy vegetation patch type rivals that occuring vertically by soil depth. Ecohydrology **519**, 503–519.

Breshears DD, Myers OB, Meyer CW, Barnes FJ, Zou CB, Allen CD, McDowell NG, Pockman WT. 2009*b*. Tree die-off in response to global change-type drought: mortality insights from a decade of plant water potential measurements. Frontiers in Ecology and the Environment **7**, 185–189.

Brodribb TJ, Cochard H. 2009. Hydraulic failure defines the recovery and point of death in water-stressed conifers. Plant physiology **149**, 575–84.

Brodribb TJ, Holbrook NM, Edwards EJ, Gutiérrez M V. 2003. Relations between stomatal closure, leaf turgor and xylem vulnerability in eight tropical dry forest trees.pdf. Plant Cell and Environment **26**, 443–450.

Brodribb TJ, McAdam S a M. 2013. Abscisic acid mediates a divergence in the drought response of two conifers. Plant physiology **162**, 1370–1377.

Brodribb TJ, McAdam S a M, Jordan GJ, Martins SC V. 2014. Conifer species adapt to low-rainfall climates by following one of two divergent pathways. Proceedings of the National Academy of Sciences of the United States of America **111**, 14489–14493.

Bugbee B. 1995. The components of crop productivity: measuring and modeling plant metabolism. American Society for Gravitational and Space Biology **8**, 93–104.

von Caemmerer S. 2000. *Biochemical Models of Leaf Photosynthesis*. Collingwood VIC 3066, Australia: CSIRO PUBLISHING.

Carnicer J, Coll M, Ninyerola M, Pons X, Sánchez G, Peñuelas J. 2011. Widespread crown condition decline, food web disruption, and amplified tree mortality with increased climate change-type drought. Proceedings of the National Academy of Sciences of the United States of America **108**, 1474–1478.

Carnicer J, Coll M, Pons X, Ninyerola M, Vayreda J, Peñuelas J. 2014. Large-scale recruitment limitation in Mediterranean pines: The role of Quercus ilex and forest successional advance as key regional drivers. Global Ecology and Biogeography **23**, 371–384.

Cavender-Bares J, Bazzaz FA. 2000. Changes in drought response strategies with ontogeny in Quercus rubra: implications for scaling from seedlings to mature trees. Oecologia **124**, 8–18.

Chaves MM, Maroco JP, Pereira JS. 2003. Understanding plant responses to drought — from genes to the whole plant. Functional Plant Biology **30**, 239–264.

Choat B, Jansen S, Brodribb TJ, *et al.* 2012. Global convergence in the vulnerability of forests to drought. Nature **491**, 752–755.

Choat B, Sack L, Holbrook NM. 2007. Diversity of hydraulic traits in nine Cordia species growing in tropical forests with contrasting precipitation. New phytologist **175**, 686–698.

Cochard H, Cruiziat P, Tyree MT. 1992. Use of Positive Pressures to Establish Vulnerability Curves. Plant Physiology **100**, 205–209.

Cowan I. 1982. Cowan1982. Regulation of water use in relation to carbon gain in higher plants. Encyclopedia of Plant Physiology. Springer Berlin Heidelberg, 489–613.

DeLucia EH, Maherali H, Carey E V. 2000. Climate-driven changes in biomass allocation in pines. Global change biology **6**, 587–593.

Dickman LT, McDowell NG, Sevanto S, Pangle RE, Pockman WT. 2015. Carbohydrate dynamics and mortality in a piñon-juniper woodland under three future precipitation scenarios. Plant, cell & environment **38**, 729–739.

Dietze MC, Sala A, Carbone MS, Czimczik CI, Mantooth J a, Richardson AD, Vargas R. 2014. Nonstructural Carbon in Woody Plants. Annual review of plant biology **65**, 2.1–2.21.

Dios VR De, Loik ME, Smith R, Aspinwall MJ, Tissue DT. 2015. Genetic variation in circadian regulation of nocturnal stomatal conductance enhances carbon assimilation and growth. Plant, Cell and Environment, 10.1002/pce.12598.

Domec J-C, Gartner BL. 2001. Cavitation and water storage capacity in bole xylem segments of mature and young Douglas-fir trees. Trees **15**, 204–214.

Domec J-C, Johnson DM. 2012. Does Homeostasis or Disturbance of Homeostasis in Minimum Leaf Water Potential Explain the Isohydric Versus Anisohydric Behavior of Vitis Vinifera L. Cultivars? Tree Physiology **32**, 245–248.

Domec J-C, Scholz F., Bucci SJ, Meinzer FC, Goldstein G, Villalobos-Vega R. 2006. Diurnal and seasonal variation in root xylem embolism in neotropical savanna woody species: Impact on stomatal control of plant water status. Plant, Cell and Environment **29**, 26–35.

Duan H, Duursma RA, Huang G, Smith R a, Choat B, O'Grady AP, Tissue DT. 2014. Elevated [CO2] does not ameliorate the negative effects of elevated temperature on drought-induced mortality in Eucalyptus radiata seedlings. Plant, cell & environment **37**, 1598–1613.

Ehleringer JR, Cooper TA. 1988. Correlation between carbon isotope ratio and microhabitat in desert plants. Oecologia **76**, 562–566.

Farquhar GD, von Caemmerer S, Berry J a. 1980. A biochemical model of photosynthetic CO2 assimilation in leaves of C3 species. Planta **149**, 78–90.

Farquhar GD, Sharkey TD. 1982. Stomatal conductance and photosynthesis. Plant Physiology **33**, 317–345.

Fatichi S, Leuzinger S, Körner C. 2014. Moving beyond photosynthesis: From carbon source to sink-driven vegetation modeling. New Phytologist **201**, 1086–1095.

Filella I, Llusià J, Piñol J, Peñuelas J. 1998. Leaf gas exchange and fluorescence of Phillyrea latifolia, Pistacia lentiscus and Quercus ilex saplings in severe drought and high temperature conditions. Environmental and Experimental Botany **39**, 213–220.

Fischer S, Hanf S, Frosch T, Gleixner G, Trumbore S, Hartmann H. 2015. Rapid report Pinus sylvestris switches respiration substrates under shading but not during drought. New Phytologist **207**, 542–550.

Fischer R, Turner NC. 1978. Plant Productivity in the arid and semiarid zones. Ann. Rev.Plant Physiology **29**, 277–317.

Flexas J, Bota J, Galmés J, Medrano H, Ribas-Carbó M. 2006. Keeping a positive carbon balance under adverse conditions: responses of photosynthesis and respiration to water stress. Physiologia Plantarum **127**, 343–352.

Flexas J, Diaz-Espejo A, Gago J, Gallé A, Galmés J, Gulías J, Medrano H. 2014. Photosynthetic limitations in Mediterranean plants: A review. Environmental and Experimental Botany **103**, 12–23.

Franklin JF, Shugart HH, Harmon ME. 1987. Tree Death as an Ecological Process. BioScience **37**, 550–556.

Franks PJ, Drake PL, Froend RH. 2007. Anisohydric but isohydrodynamic: seasonally constant plant water potential gradient explained by a stomatal control mechanism incorporating variable plant hydraulic conductance. Plant, cell & Environment **30**, 19–30.

Galiano L, Martínez-Vilalta J, Lloret F. 2010. Drought-Induced Multifactor Decline of Scots Pine in the Pyrenees and Potential Vegetation Change by the Expansion of Co-occurring Oak Species. Ecosystems **13**, 978–991.

Galiano L, Martínez-Vilalta J, Lloret F. 2011. Carbon reserves and canopy defoliation determine the recovery of Scots pine 4 yr after a drought episode. New phytologist **190**, 750–759.

Galiano L, Martínez-Vilalta J, Sabaté S, Lloret F. 2012. Determinants of drought effects on crown condition and their relationship with depletion of carbon reserves in a Mediterranean holm oak forest. Tree physiology **32**, 478–89.

Galmés J, Conesa MÀ, Ochogavía JM, Perdomo JA, Francis DM, Ribas-Carbó M, Savé R, Flexas J, Medrano H, Cifre J. 2011. Physiological and morphological adaptations in relation to water use efficiency in Mediterranean accessions of Solanum lycopersicum. Plant, cell & environment **34**, 245–60.

Galmés J, Flexas J, Savé R, Medrano H. 2007. Water relations and stomatal characteristics of Mediterranean plants with different growth forms and leaf habits: responses to water stress and recovery. Plant and Soil **290**, 139–155.

Galvez DA, Landhäusser SM, Tyree MT. 2013. Low root reserve accumulation during drought may lead to winter mortality in poplar seedlings. New Phytologist **198**, 139–48.

Garcia-Forner N, Adams HD, Sevanto S, *et al.* 2015. Responses of two semiarid conifer tree species to reduced precipitation and warming reveal new perspectives for stomatal regulation. Plant, Cell & Environment, 10.1111/pce.12588.

Gaylord ML, Kolb TE, Mcdowell NG. 2015. Mechanisms of piñon pine mortality after severe drought : a retrospective study of mature trees. Tree physiology **35**, 806–816.

Gaylord ML, Kolb TE, Pockman WT, Plaut JA, Yepez EA, Macalady AK, Pangle RE, Mcdowell NG. 2013. Drought predisposes piñon-juniper woodlands to insect attacks and mortality. New Phytologist **198**, 567–578.

Grace J. 1988. Temperature as a determinant of plant productivity. Symp Soc Exp Biol **42**, 71–107.

Gratani L, Bombelli A. 1999. Leaf anatomy, inclination, and gas exchange relationships in evergreen sclerophyllous and drought semideciduous shrub species. Photosynthetica **37**, 573–585.

Gratani L, Varone L. 2004. Adaptive photosynthetic strategies of the Mediterranean maquis species according to their origin. Photosynthetica **42**, 551–558.

Gulías J, Flexas J, Abadía A, Madrano H. 2002. Photosynthetic responses to water deficit in six Mediterranean sclerophyll species: possible factors explaining the declining distribution of Rhamnus ludovici-salvatoris, an endemic Balearic species. Tree physiology **22**, 687–697.

Guyot G, Scoffoni C, Sack L. 2012. Combined impacts of irradiance and dehydration on leaf hydraulic conductance: Insights into vulnerability and stomatal control. Plant, Cell and Environment **35**, 857–871.

Hartmann H. 2011. Will a 385 million year-struggle for light become a struggle for water and for carbon? - How trees may cope with more frequent climate change-type drought events. Global Change Biology **17**, 642–655.

Hartmann H, Adams HD, Anderegg WRL, Jansen S, Zeppel MJB. 2015. Research frontiers in drought- induced tree mortality : crossing scales and disciplines. New Phytologist **205**, 965–969.

Hartmann H, Ziegler W, Kolle O, Trumbore S. 2013*a*. Thirst beats hunger - declining hydration during drought prevents carbon starvation in Norway spruce saplings. New Phytologist **200**, 340–349.

Hartmann H, Ziegler W, Trumbore S. 2013*b*. Lethal drought leads to reduction in nonstructural carbohydrates in Norway spruce tree roots but not in the canopy. Functional Ecology **27**, 413–427.

Hereş AM, Martínez-Vilalta J, López BC. 2012. Growth patterns in relation to

drought-induced mortality at two Scots pine (Pinus sylvestris L.) sites in NE Iberian Peninsula. Trees - Structure and Function **26**, 621–630.

Hernández EI, Vilagrosa A, Pausas JG, Bellot J. 2010. Morphological traits and water use strategies in seedlings of Mediterranean coexisting species. Plant Ecology **207**, 233–244.

Herrero A, Castro J, Zamora R, Delgado-Huertas A, Querejeta JI. 2013. Growth and stable isotope signals associated with drought-related mortality in saplings of two coexisting pine species. Oecologia **173**, 1613–1624.

Hoch G, Körner C. 2003. The carbon charging of pines at the climatic treeline: a global comparison. Oecologia **135**, 10–21.

Hoch G, Popp M, Körner C. 2002. Altitudinal increase of mobile carbon pools in Pinus cembra suggests sink limitation of growth at the Swiss treeline. Oikos **98**, 361–374.

Hódar JA, Castro J, Zamora R. 2003. Pine processionary caterpillar Thaumetopoea pityocampa as a new threat for relict Mediterranean Scots pine forests under climatic warming. Biological Conservation **110**, 123–129.

Ilic J, Boland D, McDonald M, Downes G, Blakemore P. 2000. Wood Density Phase 1. National Carbon Accounting System Technical Report no.18. Canberra, Aurstralia: Australian Greenhouse Office, 228.

IPCC. 2013. Intergovernamental Panel on Climate Change. Climate Change 2013: The Physical Science Basis. Contribution of Working Group I to the Fifth Assessment Report of the Intergovernmental Panel on Climate Change.33.

Jones HG. 1990. Physiological Aspects of the Control of Water Status in Horticultural Crops. HortScience **25**, 19–25.

Jones HG. 1998. Stomatal control of photosynthesis and transpiration. Journal of Experimental Botany **49**, 387–398.

Jones HG, Tardieu F. 1998. Modelling water relations of horticultural crops: a review. Scientia Horticulturae **74**, 21–46.

Klein T. 2014. The variability of stomatal sensitivity to leaf water potential across tree species indicates a continuum between isohydric and anisohydric behaviours (S Niu, Ed.). Functional Ecology **28**, 1313–1320.

Körner C. 2015. Paradigm shift in plant growth control. Plant Biology **25**, 107–114.

Kramer PJ, Boyer JS. 1995. Stomata and Gas Exchange. Water relations of plants and soils. Durham, North Carolina: Academic Press, 257–282.

Lajtha K, Barnes FJ. 1991. Carbon gain and water use in pinyon pine-juniper woodlands of northern New Mexico: field versus phytotron chamber measurements. Tree physiology **9**, 59–67.

Larcher W. 1975. *Physiological plant ecology*. Berlin: Springer-Verlag.

Limousin J-M, Bickford CP, Dickman LT, Pangle RE, Hudson PJ, Boutz AL, Gehres N, Osuna JL, Pockman WT, McDowell NG. 2013. Regulation and acclimation of leaf gas exchange in a piñon-juniper woodland exposed to three different precipitation regimes. Plant Cell and Environment **36**, 1812–25.

Limousin J-M, Rambal S, Ourcival J-M, Rodríguez-Calcerrada J, Pérez-Ramos IM, Rodríguez-Cortina R, Misson L, Joffre R. 2012. Morphological and phenological shoot plasticity in a Mediterranean evergreen oak facing long-term increased drought. Oecologia **169**, 565–577.

Linton MJ, Sperry JS, Williams DG. 1998. Limits to water transport in Juniperus osteosperma and Pinus edulis: implications for drought tolerance and regulation of transpiration. Functional Ecology **12**, 906–911.

Lloret F, Escudero A, Iriondo JM, Martínez-Vilalta J, Valladares F. 2012. Extreme climatic events and vegetation: the role of stabilizing processes. Global Change Biology **18**, 797–805.

Lloret F, Peñuelas J, Estiarte M. 2004*a*. Experimental evidence of reduced diversity of seedlings due to climate modification in a Mediterranean-type community. Global Change Biology **10**, 248–258.

Lloret F, Siscart D. 1995. *Los efectos demográficos de la sequía en poblaciones de encina.* Cuadernos de la Sociedad Española de Ciencias Forestales.

Lloret F, Siscart D, Dalmases C. 2004*b*. Canopy recovery after drought dieback in holm-oak Mediterranean forests of Catalonia (NE Spain). Global Change Biology **10**, 2092–2099.

Maherali H, Pockman WT, Jackson RB. 2004. Adaptative variation in the vulnerability of woody plants to xylem cavitation. Ecology **85**, 2184–2199.

Markesteijn L, Poorter L. 2009. Seedling root morphology and biomass allocation of 62 tropical tree species in relation to drought- and shade-tolerance. Journal of Ecology **97**, 311–325.

Martínez-Vilalta J, Cochard H, Mencuccini M, *et al.* 2009. Hydraulic adjustment of Scots pine across Europe. New Phytologist **184**, 353–364.

Martínez-Vilalta J, Mangirón M, Ogaya R, Sauret M, Serrano L, Peñuelas J, Piñol J. 2003. Sap flow of three co-occurring Mediterranean woody species under varying atmospheric and soil water conditions. Tree physiology **23**, 747–758.

Martínez-Vilalta J, Piñol J. 2002. Drought-induced mortality and hydraulic architecture in pine populations of the NE Iberian Peninsula. Forest Ecology and Management **161**, 247–256.

Martínez-Vilalta J, Piñol J, Beven K. 2002*a*. A hydraulic model to predict drought-induced mortality in woody plants: An application to climate change in the Mediterranean. Ecological Modelling **155**, 127–147.

Martínez-Vilalta J, Poyatos R, Aguadé D, Retana J, Mencuccini M. 2014. A

new look at water transport regulation in plants. New phytologist **204**, 105–115.

Martínez-Vilalta J, Prat E, Oliveras I, Piñol J. 2002*b*. Xylem hydraulic properties of roots and stems of nine Mediterranean woody species. Oecologia **133**, 19–29.

Martin-StPaul NK, Longepierre D, Huc R, Delzon S, Burlett R, Joffre R, Rambal S, Cochard H. 2014. How reliable are methods to assess xylem vulnerability to cavitation? The issue of 'open vessel' artifact in oaks. Tree Physiology **34**, 894–905.

Maseda PH, Fernández RJ. 2006. Stay wet or else: three ways in which plants can adjust hydraulically to their environment. Journal of Experimental Botany **57**, 3963–3977.

Matías L, González-Díaz P, Jump AS. 2014. Larger investment in roots in southern range-edge populations of Scots pine is associated with increased growth and seedling resistance to extreme drought in response to simulated climate change. Environmental and Experimental Botany **105**, 32–38.

Matías L, Jump AS. 2014. Impacts of predicted climate change on recruitment at the geographical limits of Scots pine. Journal of Experimental Botany **65**, 299–310.

Mcadam SAM, Brodribb TJ. 2014. Hormonal dynamics contributes to divergence in seasonal stomatal behaviour in a monsoonal plant community. Plant, Cell and Environment, 423–432.

McDowell NG. 2011. Mechanisms linking drought, hydraulics, carbon metabolism, and vegetation mortality. Plant physiology **155**, 1051–9.

McDowell NG, Beerling DJ, Breshears DD, Fisher RA, Raffa KF, Stitt M. 2011. The interdependence of mechanisms underlying climate-driven vegetation mortality. Trends in ecology & evolution **26**, 523–532.

McDowell NG, Fisher RA, Xu C, *et al.* 2013*a*. Evaluating theories of drought-induced vegetation mortality using a multimodel-experiment framework. New Phytologist **200**, 304–321.

McDowell NG, Pockman WT, Allen CD, *et al.* 2008. Mechanisms of plant survival and mortality during drought: why do some plants survive while others succumb to drought? New Phytologist **178**, 719–739.

McDowell NG, Ryan MG, Zeppel MJB, Tissue DT. 2013*b*. Feature: Improving our knowledge of drought-induced forest mortality through experiments, observations, and modeling. New Phytologist **200**, 289–293.

Meinzer FC, Johnson DM, Lachenbruch B, McCulloh KA, Woodruff DR. 2009. Xylem hydraulic safety margins in woody plants: coordination of stomatal control of xylem tension with hydraulic capacitance. Functional Ecology **23**, 922–930.

Meinzer FC, Woodruff DR, Marias DE, McCulloh KA, Sevanto S. 2014. Dynamics of leaf water relations components in co-occurring iso- and

anisohydric conifer species. Plant, cell & environment **37**, 2577–2586.

Meir P, Meir P, Mencuccini M, Dewar RC. 2015. Tansley insight Drought-related tree mortality : addressing the gaps in understanding and prediction. New phytologist **207**, 28–33.

Mencuccini M. 2014. Temporal scales for the coordination of tree carbon and water economies during droughts. Tree Physiology **34**, 439–442.

Mencuccini M, Mambelli S, Comstock J. 2000. Stomatal responsiveness to leaf water status in common bean (Phaseolus vulgaris L.) is a function of time of day. Plant, Cell and Environment **23**, 1109–1118.

Mitchell PJM, O'Grady AP, Tissue DT, White DA, Ottenschlaeger ML, Pinkard EA. 2013. Drought response strategies define the relative contributions of hydraulic dysfunction and carbohydrate depletion during tree mortality. New Phytologist **197**, 862–872.

Mitchell PJM, O'Grady AP, Tissue DT, Worledge D, Pinkard EA. 2014. Co-ordination of growth, gas exchange and hydraulics define the carbon safety margin in tree species with contrasting drought strategies. Tree physiology **34**, 443–458.

Moran E V, Hartig F, Bell DM. 2015. Intraspecific trait variation across scales: implications for understanding global change responses. Global Change Biology.

Moreno-Gutiérrez C, Dawson TE, Nicolás E, Querejeta JI. 2012. Isotopes reveal contrasting water use strategies among coexisting plant species in a mediterranean ecosystem. New Phytologist **196**, 489–496.

Mueller RC, Scudder CM, Porter ME, Talbot Trotter R, Gehring CA, Whitham TG. 2005. Differential tree mortality in response to severe drought: evidence for long-term vegetation shifts. Journal of Ecology **93**, 1085–1093.

Nardini A, Lo Gullo MA, Trifilò P, Salleo S. 2014. The challenge of the Mediterranean climate to plant hydraulics: Responses and adaptations. Environmental and Experimental Botany **103**, 68–79.

Neufeld HS, Grantz DA, Meinzer FC, Goldstein G, Crisosto GM, Crisosto C. 1992. Genotypic variability in vulnerability of leaf xylem to cavitation in water-stressed and well-irrigated sugarcane. Plant physiology **100**, 1020–1028.

Nikinmaa E, Hölttä T, Hari P, Kolari P, Mäkelä A, Sevanto S, Vesala T. 2013. Assimilate transport in phloem sets conditions for leaf gas exchange. Plant Cell and Environment **36**, 655–669.

Nippert JB, Holdo RM. 2015. Challenging the maximum rooting depth paradigm in grasslands and savannas. Functional Ecology, DOI:10.1111/1365–2435.12390.

O'Brien MJ, Leuzinger S, Philipson CD, Tay J, Hector A. 2014. Drought survival of tropical tree seedlings enhanced by non-structural carbohydrate levels. Nature Climate Change **4**, 710–714.

Ogasa M, Miki NH, Murakami Y, Yoshikawa K. 2013. Recovery performance in xylem hydraulic conductivity is correlated with cavitation resistance for temperate deciduous tree species. Tree physiology **33**, 335–344.

Ogaya R, Llusià J, Barbeta A, Asensio D, Liu D, Alessio GA, Peñuelas J. 2014. Foliar CO2 in a holm oak forest subjected to 15 years of climate change simulation. Plant Science **226**, 101–107.

Ogaya R, Peñuelas J. 2003. Comparative field study of Quercus ilex and Phillyrea latifolia: photosynthetic response to experimental drought conditions. Environmental and Experimental Botany **50**, 137–148.

Ogaya R, Peñuelas J. 2006. Contrasting foliar responses to drought in Quercus ilex and Phillyrea latifolia. Biologia Plantarum **50**, 373–382.

Ogaya R, Peñuelas J. 2007. Tree growth, mortality, and above-ground biomass accumulation in a holm oak forest under a five-year experimental field drought. Plant Ecology **189**, 291–299.

Ogaya R, Peñuelas J, Martínez-Vilalta J, Mangirón M. 2003. Effect of drought on diameter increment of Quercus ilex, Phillyrea latifolia, and Arbutus unedo in a holm oak forest of NE Spain. Forest Ecology and Management **180**, 175–184.

Oliva J, Stenlid J, Martínez-Vilalta J. 2014. The effect of fungal pathogens on the water and carbon economy of trees : implications for drought-induced mortality included in theoretical models for drought induced mortality. New Phytologist **203**, 1028–1035.

Oren R, Sperry JS, Katul G, Pataki D, Ewers B, Phillips N, Schäfer K. 1999. Survey and synthesis of intra- and interspecific variation in stomatal sensitivity to vapour pressure deficit. Plant Cell and Environment **22**, 1515–1526.

Palacio S, Hoch G, Sala A, Körner C, Millard P. 2014. Does carbon storage limit tree growth? New Phytologist **201**, 1096–1100.

Parolari AJ, Katul GG, Porporato A. 2014. An ecohydrological perspective on drought-induced forest mortality. Journal of Geophysical Research: Biogeosciences **119**, 965–981.

Peng C, Ma Z, Lei X, Zhu Q, Chen H, Wang W, Liu S, Li W, Fang X, Zhou X. 2011. A drought-induced pervasive increase in tree mortality across Canada's boreal forests. Nature Climate Change **1**, 467–471.

Peñuelas J, Filella I, Lloret F, Piñol J, Siscart D. 2000. Peñuelas BioPlant2000.pdf. Effects of a severe drought on water and nitrogen use by Quercus ilex and Phillyrea latifolia2 **43**, 47–53.

Peñuelas J, Filella I, Llusia J, Siscart D, Pinol J. 1998. Comparative field study of spring and summer leaf gas exchange and photobiology of the mediterranean trees Quercus ilex and Phillyrea latifolia. Journal of Experimental Botany **49**, 229–238.

Pinkard EA, Eyles A, O'Grady AP. 2011. Are gas exchange responses to resource limitation and defoliation linked to source:sink relationships? Plant, cell

& environment **34**, 1652–1665.

Piper FI, Reyes-Díaz M, Corcuera LJ, Lusk CH. 2009. Carbohydrate storage, survival, and growth of two evergreen Nothofagus species in two contrasting light environments. Ecological Research **24**, 1233–1241.

Pivovaroff AL, Pasquini SC, De Guzman ME, Alstad KP, Stemke JS, Santiago LS. 2015. Multiple strategies for drought survival among woody plant species. Functional Ecology, DOI:10.1111/1365–2435.12518.

Plaut JA, Wadsworth WD, Pangle RE, Yepez EA, McDowell NG, Pockman WT. 2013. Reduced transpiration response to precipitation pulses precedes mortality in a piñon-juniper woodland subject to prolonged drought. New Phytologist **200**, 375–387.

Plaut JA, Yepez EA, Hill J, Pangle RE, Sperry JS, Pockman WT, McDowell NG. 2012. Hydraulic limits preceding mortality in a piñon-juniper woodland under experimental drought. Plant Cell and Environment **35**, 1601–1617.

Poyatos R, Aguadé D, Galiano L, Mencuccini M, Martínez-Vilalta J. 2013. Drought-induced defoliation and long periods of near-zero gas exchange play a key role in accentuating metabolic decline of Scots pine. New Phytologist **200**, 388–401.

Poyatos R, Martínez-Vilalta J, Cermák J, *et al.* 2007. Plasticity in hydraulic architecture of Scots pine across Eurasia. Oecologia **153**, 245–259.

Pratt RB, Jacobsen AL, Ramirez AR, Helms AM, Traugh CA, Tobin MF, Heffner MS, Davis SD. 2014. Mortality of resprouting chaparral shrubs after a fire and during a record drought: physiological mechanisms and demographic consequences. Global change biology **20**, 893–907.

Quero JL, Sterck FJ, Martínez-Vilalta J, Villar R. 2011. Water-use strategies of six co-existing Mediterranean woody species during a summer drought. Oecologia **166**, 45–57.

Raschke K. 1975. Stomatal Action. Ann. Rev.Plant Physiology **26**, 309–340.

Regier N, Streb S, Cocozza C, Schaub M, Cherubini P, Zeeman SC, Frey B. 2009. Drought tolerance of two black poplar (Populus nigra L.) clones: Contribution of carbohydrates and oxidative stress defence. Plant, Cell and Environment **32**, 1724–1736.

Reinhardt K, Germino MJ, Kueppers LM, Domec J-C, Mitton J. 2015. Linking carbon and water relations to drought-induced mortality in Pinus flexilis seedlings. Tree Physiology **28**, 1233–1251.

Richter S, Kipfer T, Wohlgemuth T, Calderón Guerrero C, Ghazoul J, Moser B. 2012. Phenotypic plasticity facilitates resistance to climate change in a highly variable environment. Oecologia **169**, 269–279.

Rigling A, Bigler C, Eilmann B, *et al.* 2013. Driving factors of a vegetation shift from Scots pine to pubescent oak in dry Alpine forests. Global Change Biology **19**, 229–240.

Rodà F, Retana J, Gracia CA, Bellot J. 1999. *Ecology of Mediterranean Evergreen Oak Forests* (F Rodà, J Retana, CA Gracia, and J Bellot, Eds.). Springer-Verlag Berlin Heldeiberg.

Rogiers SY, Greer DH, Hatfield JM, Hutton RJ, Clarke SJ, Hutchinson P a., Somers A. 2012*a*. Stomatal response of an anisohydric grapevine cultivar to evaporative demand, available soil moisture and abscisic acid. Tree Physiology **32**, 249–261.

Rogiers SY, Greer DH, Hatfield JM, Hutton RJ, Clarke SJ, Hutchinson P a, Somers A. 2012*b*. Stomatal response of an anisohydric grapevine cultivar to evaporative demand, available soil moisture and abscisic acid. Tree physiology **32**, 249–261.

Rosas T, Galiano L, Ogaya R, Peñuelas J, Martínez-Vilalta J. 2013. Dynamics of non-structural carbohydrates in three Mediterranean woody species following long-term experimental drought. Frontiers in plant science **4**, 1–16.

Rowland L, Lobo-do-Vale RL, Christoffersen BO, *et al.* 2015. After more than a decade of soil moisture deficit, tropical rainforest trees maintain photosynthetic capacity, despite increased leaf respiration. Global Change Biology, n/a–n/a.

Sala A, Hoch G. 2009. Height-related growth declines in ponderosa pine are not due to carbon limitation. Plant, cell & environment **32**, 22–30.

Sala A, Mencuccini M. 2014. Ecosystem science: Plump trees win under drought. Nature Climate Change **4**, 666–667.

Sala A, Piper F, Hoch G. 2010. Physiological mechanisms of drought-induced tree mortality are far from being resolved. New Phytologist **186**, 274–264.

Sala A, Woodruff DR, Meinzer FC. 2012. Carbon dynamics in trees: feast or famine? Tree physiology **32**, 764–775.

Salleo S, Trifilò P, Esposito S, Nardini A, Gullo MA Lo. 2009. Starch-to-sugar conversion in wood parenchyma of field growing Laurus nobilis plants: a component of the signal pathway for embolism repair? Functional Plant Biology **36**, 815–825.

Sánchez ME, Caetano P, Ferraz J, Trapero A. 2002. *Phytophtora* disease of *Quercus ilex* in south-western Spain. Forest Pathology **32**, 5–18.

Saura-Mas S, Bonas A, Lloret F. 2015. Plant community response to drought-induced canopy defoliation in a Mediterranean Quercus ilex forest. European Journal of Forest Research **134**, 261–272.

Schneider SH, Semenov S, Patwardhan A, *et al.* 2007. Assessing key vulnerabilities and the risk from climate change. Impacts, Adaptation and Vulnerability. Contribution of Working Group II to the Fourth Assessment Report of the Intergovernmental Panel on Climate Change. UK: Cambridge University Press, 779–810.

Secchi F, Zwieniecki MA. 2011. Sensing embolism in xylem vessels: The role of sucrose as a trigger for refilling. Plant, cell & Environment **34**, 514–524.

Serrano L, Peñuelas J, Ogaya R, Savé R. 2005. Tissue-water relations of two co-occurring evergreen Mediterranean species in response to seasonal and experimental drought conditions. Journal of plant research **118**, 263–269.

Sevanto S, Hölttä T, Holbrook NM. 2011. Effects of the hydraulic coupling between xylem and phloem on diurnal phloem diameter variation. Plant, Cell and Environment **34**, 690–703.

Sevanto S, McDowell NG, Dickman LT, Pangle RE, Pockman WT. 2014. How do trees die? A test of the hydraulic failure and carbon starvation hypotheses. Plant Cell and Environment **37**, 153–161.

Shaw JD, Steed BE, DeBlander LT. 2005. Forest inventory and analysis (FIA) annual inventory answers the question: What is happening to pinyon-juniper woodlands? Journal of Forestry **103**, 280–285.

Sparks JP, Black RA. 1999. Regulation of water loss in populations of Populus trichocarpa: the role of stomatal control in preventing xylem cavitation. Tree Physiology **19**, 453–459.

Sperlich D, Chang CT, Peñuelas J, Gracia C, Sabaté S. 2015. Seasonal variability of foliar photosynthetic and morphological traits and drought impacts in a Mediterranean mixed forest. Tree Physiology, DOI:10.1093/treephys/tpv017.

Sperry JS. 2000. Hydraulic constraints on plant gas exchange. Agricultural and Forest Meteorology **104**, 13–23.

Sperry JS, Adler FR, Campbell GS, Comstock JP. 1998. Limitation of plant water use by rhizosphere and xylem conductance: results from a model. Plant, Cell & Environment **21**, 347–359.

Sperry JS, Hacke UG, Oren R, Comstock JP. 2002. Water deficits and hydraulic limits to leaf water supply. Plant, cell & Environment **25**, 251–263.

Stocker O. 1956. Die Abhängigkeit des transpiration von den umweltfaktoren. In: Ruhland W, ed. Encyclopedia of Plant Physiology. Berlin: Springer, 436–488.

Taeger S, Sparks T., Menzel A. 2014. Effects of temperature and drought manipulations on seedlings of Scots pine provenances. Plant Biology **17**, 361–372.

Tang A-C, Boyer JS. 2002. Growth-induced water potentials and the growth of maize leaves. Journal of experimental botany **53**, 489–503.

Tardieu F, Lafarge T, Simonnfau T. 1996. Stomatal control by fed or endogenous xylem ABA in sunflower : interpretation of correlations between leaf water potential and stomatal conductance in anisohydric species. Plant Cell and Environment **19**, 75–84.

Tardieu F, Simonneau T. 1998. Variability among species of stomatal control under fluctuating soil water status and evaporative demand : modelling isohydric and anisohydric behaviours Franc. Journal of Experimental Botany **49**, 419–432.

Trifilò P, Barbera PM, Raimondo F, Nardini A, Gullo M a Lo, Meinzer FC. 2014. Coping with drought-induced xylem cavitation: Coordination of embolism repair and ionic effects in three Mediterranean evergreens. Tree Physiology **34**, 109–122.

Tyree MT, Zimmermann MH. 2002. *Xylem structure and the ascent of sap* (T Timell, Ed.). Syracuse: Springer-Verlag.

Urli M, Porté AJ, Cochard H, Guengant Y, Burlett R, Delzon S. 2013. Xylem embolism threshold for catastrophic hydraulic failure in angiosperm trees. Tree physiology **33**, 672–683.

Vilà-Cabrera A, Martínez-Vilalta J, Galiano L, Retana J. 2013. Patterns of Forest Decline and Regeneration Across Scots Pine Populations. Ecosystems **16**, 323–335.

Vilagrosa A, Hernández EI, Luis VC, Cochard H, Pausas JG. 2014. Physiological differences explain the co-existence of different regeneration strategies in Mediterranean ecosystems. New Phytologist **201**, 1277–1288.

West AG, Hultine K, Jackson T, Ehleringer JR. 2007. Differential summer water use by Pinus edulis and Juniperus osteosperma reflects contrasting hydraulic characteristics. Tree physiology **27**, 1711–1720.

Wheeler JK, Huggett BA, Tofte AN, Rockwell FE, Holbrook NM. 2013. Cutting xylem under tension or supersaturated with gas can generate PLC and the appearance of rapid recovery from embolism. Plant, cell & environment **36**, 1938–1949.

Will RE, Wilson SM, Zou CB, Hennessey TC. 2013. Increased vapor pressure deficit due to higher temperature leads to greater transpiration and faster mortality during drought for tree seedlings common to the forest-grassland ecotone. New phytologist **200**, 366–74.

Williams AP, Allen CD, Macalady AK, *et al.* 2013. Temperature as a potent driver of regional forest drought stress and tree mortality. Nature Climate Change **3**, 292–297.

Willson CJ, Manos PS, Jackson RB. 2008. Hydraulic traits are influenced by phylogenetic history in the drought-resistant, invasive genus Juniperus (Cupressaceae). American journal of botany **95**, 299–314.

Wilson CC. 1948. The effect of some environmental factors on the moevements of guard cells. Plant physiology **23**, 5–37.

Woodruff DR. 2014. The impacts of water stress on phloem transport in Douglas-fir trees. Tree Physiology **34**, 5–14.

Zeppel MJB, Harrison SP, Adams HD, *et al.* 2015. Drought and resprouting

plants. New Phytologist **206**, 583–587.

Zhang Y, Oren R, Kang S. 2011. Spatiotemporal variation of crown-scale stomatal conductance in an arid Vitis vinifera L. cv. Merlot vineyard: direct effects of hydraulic properties and indirect effects of canopy leaf area. Tree physiology **32**, 262–279.

Zhao J, Hartmann H, Trumbore S, Ziegler W, Zhang Y. 2013. High temperature causes negative whole-plant carbon balance under mild drought. New phytologist **200**, 330–339.

Zwieniecki MA, Holbrook NM. 2009. Confronting Maxwell's demon: biophysics of xylem embolism repair. Trends in Plant Science **14**, 530–534.

Appendix I

Tables

Table S1. Summary of the linear mixed models of ψ_{pd} over time for both species. The response variable was the log of $|\psi_{pd}|$.

Species	Fixed Effects	numDF	denDF	F-value	p-value
J. mono.	Intercept	1	353	1.46459	0.2270
	Date	13	353	162.33675	<.0001
	Heating	1	9	0.00348	0.9542
	Drought	1	19	0.98511	0.3334
	Date:heating	13	353	3.89529	<.0001
	Date:drought	13	353	8.31225	<.0001
	Heating:drought	1	9	0.05862	0.8141
	Date:heating:drought	13	353	2.11037	0.0131
P. edulis	Intercept	1	351	0.88431	0.3477
	Date	13	351	74.79700	<.0001
	Heating	1	12	0.23055	0.6398
	Drought	1	14	0.37138	0.5520
	Date:heating	13	351	3.26616	0.0001
	Date:drought	13	351	5.86383	<.0001
	Heating:drought	1	12	4.76966	0.0495
	Date:heating:drought	-	-	-	-

Note: Full model: lme(log(abs(ψ_{pd})) ~ date*heating*drought, random=~1|chamber/tree, na.action=na.omit, method="ML")

Table S2. Summary of the linear mixed models of ψ_{sf} over time for both species. The response variable was ψ_{sf}.

Species	Fixed Effects	numDF	denDF	F-value	p-value
J. mono.	Intercept	1	368	1977.0741	<.0001
	Date	13	368	105.4403	<.0001
	Heating	1	10	0.0269	0.8731
	Drought	1	19	0.1682	0.6863
	Date:heating	13	368	2.6542	0.0014
	Date:drought	13	368	4.7575	<.0001
	Heating:drought	-	-	-	-
	Date:heating:drought	-	-	-	-
P. edulis	Intercept	1	350	65.27089	<.0001
	Date	13	350	13.55676	<.0001
	Heating	1	13	0.08783	0.7716
	Drought	1	14	0.09656	0.7606
	Date:heating	13	350	1.67341	0.0648
	Date:drought	13	350	2.67611	0.0013
	Heating:drought	-	-	-	-
	Date:heating:drought	-	-	-	-

Note: Full model: lme(ψ_{sf} ~ date*heating*drought, random=~1|chamber/tree, na.action=na.omit, method="ML")

Table S3. Summary of the linear mixed models of PLC over time for both species. The response variables were the log of PLC or the sqrt of PLC for *J. monosperma* and *P. edulis*, respectively.

Species	Fixed Effects	numDF	denDF	F-value	p-value
J. mono.	Intercept	1	368	682.0664	<.0001
	Date	13	367	143.2692	<.0001
	Heating	1	10	0.0881	0.7727
	Drought	1	19	0.4568	0.5073
	Date:heating	13	368	2.4711	0.0031
	Date:drought	13	368	5.3880	<.0001
	Heating:drought	-	-	-	-
	Date:heating:drought	-	-	-	-
P. edulis	Intercept	1	350	421.0890	<.0001
	Date	13	350	12.0993	<.0001
	Heating	1	13	0.1008	0.7559
	Drought	1	14	0.1030	0.7530
	Date:heating	13	350	1.6102	0.0802
	Date:drought	13	350	2.8866	0.0006
	Heating:drought	-	-	-	-
	Date:heating:drought	-	-	-	-

Note: Full model: lme(log or sqrt(PLC) ~ date*heating*drought, random=~1|chamber/tree, na.action=na.omit, method="ML")

Table S4. Summary of the linear mixed models of A_N over time for both species. The response variable was the sqrt of A_N.

Species	Fixed Effects	numDF	denDF	F-value	p-value
J. monosperma	Intercept	1	356	829.6153	<.0001
	Date	13	356	65.7613	<.0001
	Heating	1	9	0.3929	0.5464
	Drought	1	19	0.0001	0.9916
	Date:heating	13	356	3.7593	0.0001
	Date:drought	13	356	4.1367	0.0001
	Heating:drought	1	9	0.0102	0.9217
	Date:heating:drought	13	356	1.8336	0.0368
P. edulis	Intercept	1	356	706.0698	<.0001
	Date	13	356	66.4499	<.0001
	Heating	1	12	2.7330	0.1242
	Drought	1	15	1.0984	0.3112
	Date:heating	13	356	2.6384	0.0016
	Date:drought	13	356	3.0209	0.0003
	Heating:drought	1	12	10.7268	0.0066
	Date:heating:drought	-	-	-	-

Note: Full model: lme(sqrt(A_N) ~ date*heating*drought, random=~1|chamber/tree, na.action=na.omit, method="ML")

Table S5. Summary of the linear mixed models of g_s over time for both species. The response variable was the sqrt of g_s.

Species	Fixed Effects	numDF	denDF	F-value	p-value
J. mono.	Intercept	1	356	586.2840	<.0001
	Date	13	356	77.5507	<.0001
	Heating	1	9	1.4353	0.2615
	Drought	1	19	0.0009	0.9765
	Date:heating	13	356	4.3530	<.0001
	Date:drought	13	356	5.5101	<.0001
	Heating:drought	1	9	0.0620	0.8090
	Date:heating:drought	13	356	2.1376	0.0118
P. edulis	Intercept	1	355	445.1740	<.0001
	Date	13	355	72.2485	<.0001
	Heating	1	12	0.1248	0.7301
	Drought	1	15	3.2669	0.0908
	Date:heating	13	355	2.8292	0.0007
	Date:drought	13	355	3.0909	0.0002
	Heating:drought	1	12	8.6828	0.0122
	Date:heating:drought	-	-	-	-

Note: Full model: lme(sqrt(g_s) ~ date*heating*drought, random=~1|chamber/tree, na.action=na.omit, method="ML")

Table S6. Summary of the linear mixed models of the relationship between ψ_{pd} and SWC (average from 0 to 40 cm depth) for both species. The response variable was the log of $|\psi_{pd}|$.

Species	Fixed Effects	numDF	denDF	F-value	p-value
J. mono.	Intercept	1	272	79.68936	<.0001
	Log(swc)	1	272	164.77779	<.0001
	Heating	-	-	-	-
	Drought	-	-	-	-
	Log (swc):heating	-	-	-	-
	Log (swc):drought	-	-	-	-
	Heating:drought	-	-	-	-
	Log(swc):heating:drought	-	-	-	-
P. edulis	Intercept	1	237	55.39814	<.0001
	Log (swc)	1	237	104.50441	<.0001
	Heating	1	7	11.07428	0.0126
	Drought	1	13	0.23607	0.6351
	Log (swc):heating	1	237	13.46695	0.0003
	Log (swc):drought	1	237	0.72907	0.3940
	Heating:drought	1	7	2.41565	0.1641
	Log(swc):heating:drought	1	237	2.85393	0.0925

Note: Full model: lme(log(abs(ψ_{pd})) ~ log(swc)*heating*drought, random=~1|chamber/tree, na.action=na.omit, method="ML")

Table S7. Summary of the linear mixed models of the relationship between ψ_{sf} and SWC (average from 0 to 40 cm depth) for both species. Non transformed ψ_{sf} was used as the response variable in the model.

Species	Fixed Effects	numDF	denDF	F-value	p-value
J. mono.	Intercept	1	273	451.5937	<.0001
	Log(swc)	1	273	163.3432	<.0001

	Heating	-	-	-	-
	Drought	-	-	-	-
	Log(swc):heating	-	-	-	-
	Log(swc):drought	-	-	-	-
	Heating:drought	-	-	-	-
	Log(swc):heating:drought	-	-	-	-
P. edulis	Intercept	1	238	0.120667	0.7286
	Log(swc)	1	238	13.311933	0.0003
	Heating	1	8	3.135220	0.1146
	Drought	1	13	2.181454	0.1635
	Log(swc):heating	1	238	3.740975	0.0543
	Log(swc):drought	1	238	2.970122	0.0861
	Heating:drought	-	-	-	-
	Log(swc):heating:drought	-	-	-	-

Note: Full model: lme(ψ_{sf} ~ log(swc)*heating*drought, random=~1|chamber/tree, na.action=na.omit, method="ML")

Table S8. Summary of the linear mixed models of the relationship between PLC and SWC (average from 0 to 40 cm depth) for both species. The response variables were the log of PLC or the sqrt of PLC for *J. monosperma* and *P. edulis*, respectively.

Species	Fixed Effects	numDF	denDF	F-value	p-value
J. monosperma	Intercept	1	273	307.8331	<.0001
	Log(swc)	1	273	230.2635	<.0001
	Heating	1	-	-	-
	Drought	-	-	-	-
	Log(swc):heating	1	-	-	-
	Log(swc):drought	-	-	-	-
	Heating:drought	-	-	-	-
	Log(swc):heating:drought	-	-	-	-
P. edulis	Intercept	1	239	22.1020509	<.0001
	Log(swc)	1	239	19.424345	<.0001
	Heating	1	8	2.250007	0.1720
	Drought	1	13	1.577912	0.2312
	Log(swc):heating	1	239	2.713893	0.1008
	Log(swc):drought	1	-	-	-
	Heating:drought	-	-	-	-
	Log(swc):heating:drought	-	-	-	-

Note: Full model: lme(log or sqrt (PLC) ~ log(swc)*heating*drought, random=~1|chamber/tree, na.action=na.omit, method="ML")

Table S9. Summary of the linear mixed models of the relationship between A_N and SWC (average from 0 to 40 cm depth) for both species. The response variable was the A_N.

Species	Fixed Effects	numDF	denDF	F-value	p-value
J. mono.	Intercept	1	273	161.39836	<.0001

	Log(swc)	1	273	113.01770	<.0001
	Heating	1	9	1.92003	0.1992
	Drought	-	-	-	-
	Log(swc):heating	1	273	3.94073	0.0481
	Log(swc):drought	-	-	-	-
	Heating:drought	-	-	-	-
	Log(swc):heating:drought	-	-	-	-
P. edulis	Intercept	1	239	172.65921	<.0001
	Log(swc)	1	239	109.59460	<.0001
	Heating	1	8	5.19799	0.0521
	Drought	-	-	-	-
	Log(swc):heating	1	239	5.84481	0.0164
	Log(swc):drought	-	-	-	-
	Heating:drought	-	-	-	-
	Log(swc):heating:drought	-	-	-	-

Note: Full model: lme(A_N ~ log(swc)*heating*drought, random=~1|chamber/tree, na.action=na.omit, method="ML")

Table S10. Summary of the linear mixed models of the relationship between g_s and SWC (average from 0 to 40 cm depth) for both species. The response variable was the g_s.

Species	Fixed Effects	numDF	denDF	F-value	p-value
J. mono.	Intercept	1	272	193.59916	<.0001
	Log(swc)	1	272	182.2739	<.0001
	Heating	1	9	7.94834	0.0201
	Drought	1	16	0.08854	0.7699
	Log(swc):heating	1	272	13.03811	0.0004
	Log(swc):drought	-	-	-	-
	Heating:drought	-	-	-	-
	Log(swc):heating:drought	-	-	-	-
P. edulis	Intercept	1	235	196.07939	<.0001
	Log(swc)	1	235	141.76349	<.0001
	Heating	1	8	12.27870	0.0080
	Drought	1	13	3.16680	0.0985
	Log(swc):heating	1	235	13.38750	0.0003
	Log(swc):drought	1	235	3.42296	0.0656
	Heating:drought	-	-	-	-
	Log(swc):heating:drought	1	235	0.05622	0.8128

Note: Full model: lme(g_s ~ log(swc)*heating*drought, random=~1|chamber/tree, na.action=na.omit, method="ML")

Table S11. Summary of the linear mixed models of the relationship between $\Delta\psi$ and ψ_{pd} for both species. Non transformed $\Delta\psi$ and log of $|\psi_{pd}|$ were used as response and explanatory variables in the model, respectively.

Species	Fixed Effects	numDF	denDF	F-value	p-value
J. mono.	Intercept	1	402	761.6926	<.0001
	Log($\|\psi_{pd}\|$)	1	402	207.8590	<.0001

	Heating	-	-	-	-
	Drought	1	19	2.9963	0.0997
	Log($\|\psi_{pd}\|$)heating	-	-	-	-
	Log($\|\psi_{pd}\|$):drought	-	-	-	-
	Heating:drought	-	-	-	-
	Log($\|\psi_{pd}\|$)heating:drough t	-	-	-	-
P. edulis	Intercept	1	388	1925.6429	<.0001
	Log($\|\psi_{pd}\|$)	1	388	765.1678	<.0001
	Heating	-	-	-	-
	Drought	-	-	-	-
	Log($\|\psi_{pd}\|$):heating	-	-	-	-
	Log($\|\psi_{pd}\|$) :drought	-	-	-	-
	Heating:drought	-	-	-	-
	Log($\|\psi_{pd}\|$):heating:droug ht	-	-	-	-

Note: Full model: lme($\Delta\psi$~ log(abs(ψ_{pd})) *heating*drought, random=~1|chamber/tree, na.action=na.omit, method="ML")

Table S12. Summary of the linear mixed models of the relationship between g_s and ψ_{sf} for both species. Sqrt of g_s and non transformed ψ_{sf} were used as response and explanatory variables in the model, respectively.

Species	Fixed Effects	numDF	denDF	F-value	p-value
J. mono.	Intercept	1	245	9.45556	0.0023
	ψ_{sf}	1	245	286.28375	<.0001
	Heating	1	9	0.09344	0.7668
	Drought	1	19	0.38791	0.5408
	ψ_{sf}:heating	1	245	0.30199	0.5831
	ψ_{sf} :drought	1	245	0.98972	0.0851
	Heating:drought	1	9	1.44457	0.2601
	ψ_{sf}:heating:drought	1	-	-	-
P. edulis	Intercept	1	238	332.9162	<.0001
	ψ_{sf}	1	238	14.5400	0.0002
	Heating	-	-	-	-
	Drought	1	14	8.6822	0.0106
	ψ_{sf}:heating	-	-	-	-
	ψ_{sf}:drought	-	-	-	-
	Heating:drought	-	-	-	-
	ψ_{sf}:heating:drought	-	-	-	-

Note: Full model: lme((Sqrt(g_s)) ~ ψ_{sf} *heating*drought, random=~1|chamber/tree, na.action=na.omit, method="ML")

Table S13. Summary of the linear mixed models of the relationship between g_s and PLC for both species. Log of PLC and sqrt of PLC were used as explanatory variables in the model for *J. monosperma* and *P. edulis* respectively, and sqrt of g_s was used as response variable.

Species	Fixed Effects	numDF	denDF	F-value	p-value
J. mono.	Intercept	1	246	326.2233	<.0001
	PLC	1	246	541.2242	<.0001
	Heating	1	10	0.0324	0.8608
	Drought	1	19	1.9436	0.1794

	PLC:heating	1	246	3.3349	0.0690
	PLC :drought	-	-	-	-
	Heating:drought	1	-	-	-
	PLC:heating:drought	-	-	-	-
P. edulis	Intercept	1	238	103.89731	<.0001
	PLC	1	238	14.5763	0.0002
	Heating	-	-	-	-
	Drought	1	13	8.52856	0.0119
	PLC:heating	-	-	-	-
	PLC :drought	-	-	-	-
	Heating:drought	-	-	-	-
	PLC:heating:drought	-	-	-	-

Note: Full model: lme((sqrt (g_s) ~ log or sqrt (PLC) *heating*drought, random=~1|chamber/tree, na.action=na.omit, method="ML")

Figures

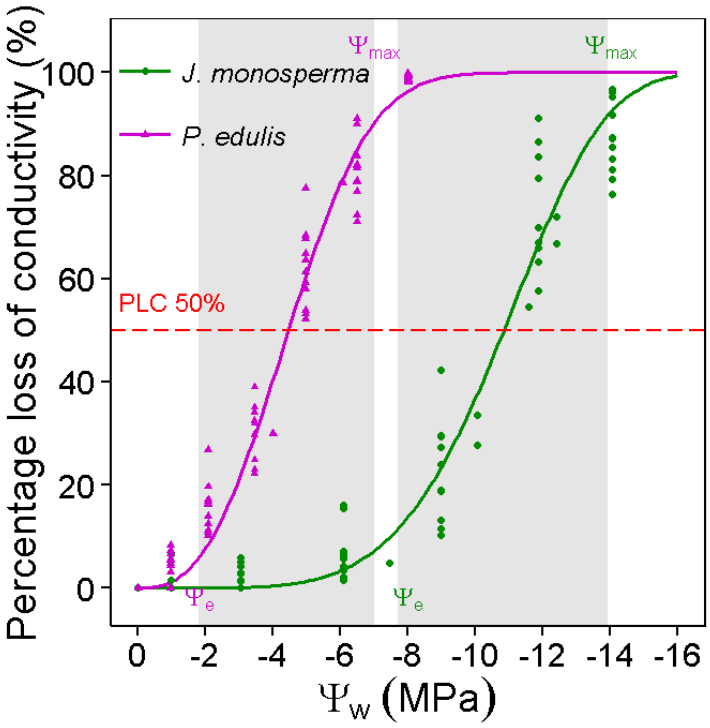

Figure S1. Vulnerability curves to cavitation for *P. edulis* and *J. monosperma* at the Los Alamos Survival/Mortality Experiment. Data points represent individual branches and lines are the adjusted curves for 12 trees per species. Shadowed regions indicate PLC variation between the species air-entry point (ψ_e) and the non-conductive point (ψ_{max}).

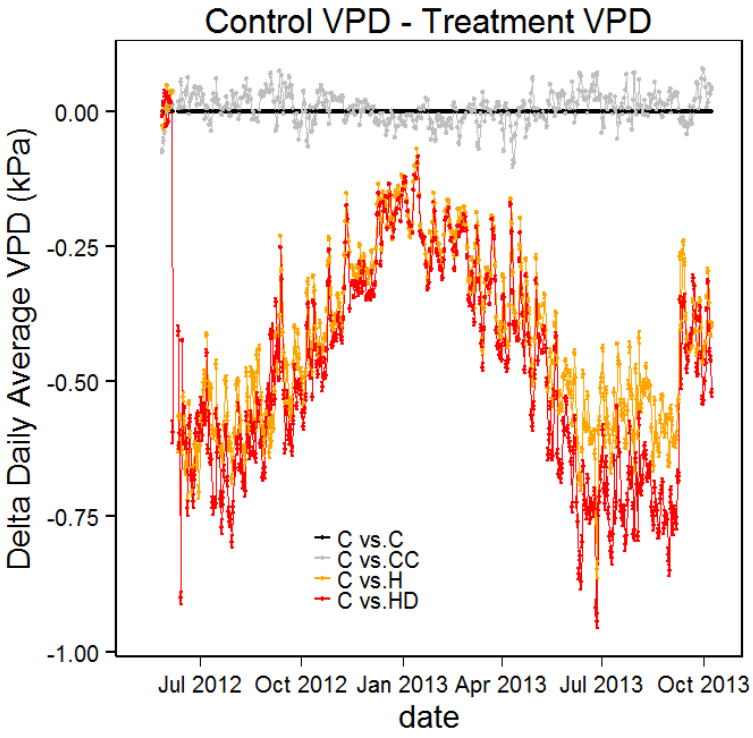

Figure S2.
Difference (delta) in daily average VPD between Control (C) and all other treatments: Control Chamber (CC), drought (D), heat (H) and heat and drought (HD).

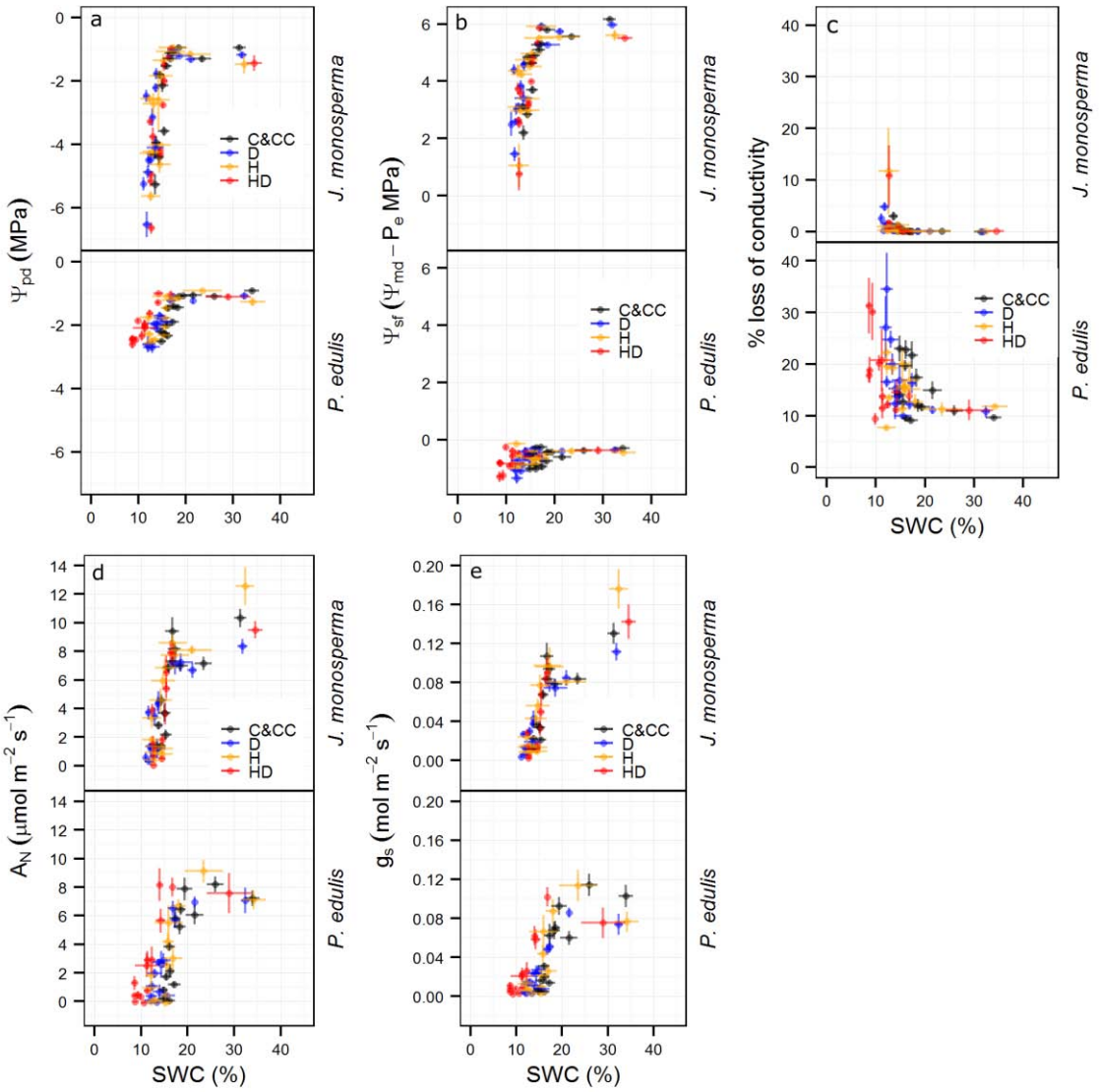

Figure S3.
Relationship between pre-dawn water potential (ψ_{pd}, a), hydraulic safety margin (ψ_{sf}, b), percentage loss of hydraulic conductivity (PLC, c), net assimilation rate (A_N, d), and stomatal conductance (g_s, e) with soil water content (SWC) in *P. edulis* and *J. monosperma* (different panels in each plot). Different colors indicate different treatments. Data correspond to average values by date, species and treatment carried out through the experiment (N=303 and 265 for *J. monosperma* and *P. edulis*, respectively). Treatment effects are summarized in Tables S6-S10 in this Appendix.

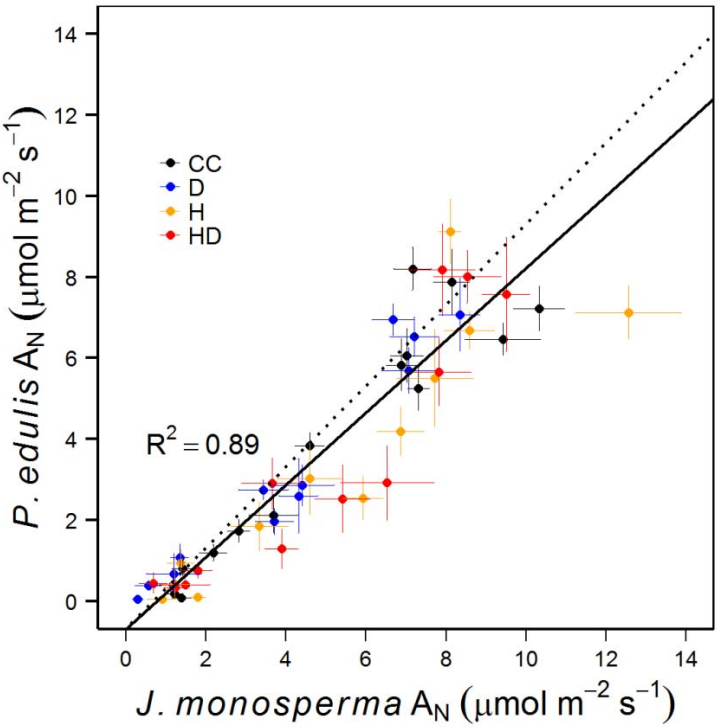

Figure S4.
Relationship between net assimilation rate (A_N) in leaves of *J. monosperma* and *P. edulis* through the experimental period. Means and standard errors for different combinations of campaign and treatment are shown. N varies from five to 13 depending on treatment and species. The dotted line shows the 1:1 relationship, and the solid line shows the regression between the A_N of both species.

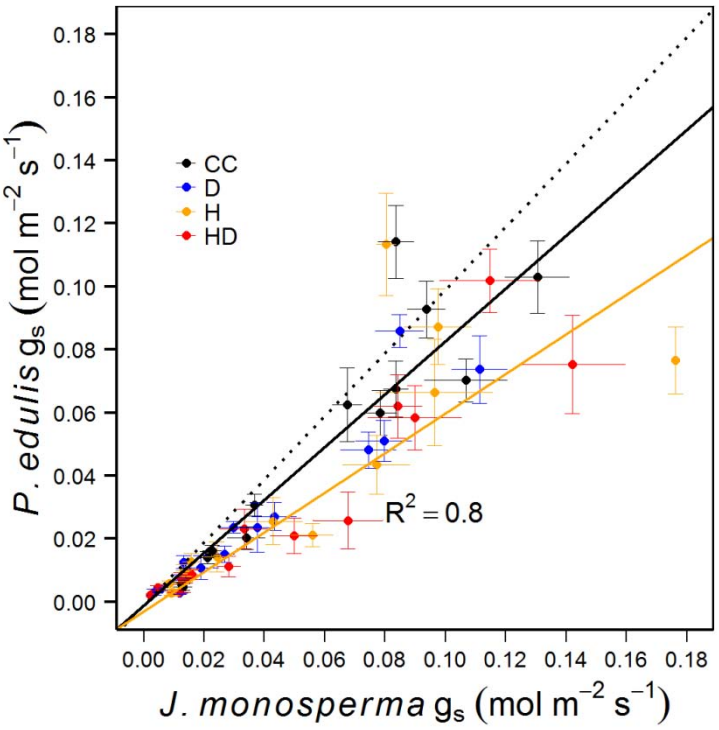

Figure S5.
Relationship between stomatal conductance (g_s) in leaves of *J. monosperma* and *P. edulis* through the experimental period. Means and standard errors for different combinations of campaign and treatment are shown. N varies from five to 13 depending on treatment and species. The dotted line shows the 1:1 relationship, and the solid line shows the regression between the g_s of both species.

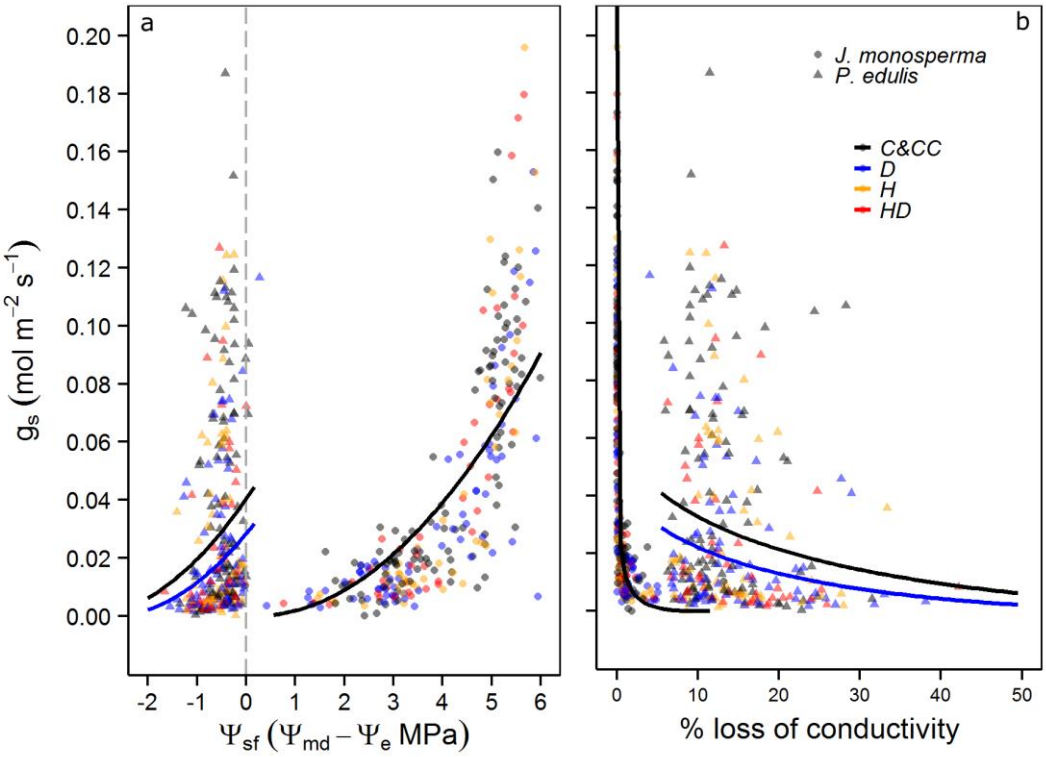

Figure S6.
Relationship between stomatal conductance (g_s) and hydraulic safety margin (ψ_{sf}; a) and between g_s and percentage loss of hydraulic conductivity (PLC; b) in *P. edulis* and *J. monosperma* (solid triangles and circles respectively). Different colors indicate different treatments. In Fig. S6a, the red dashed line indicates the point at which the Ψ_{md} reaches the air-entry point, Ψ_e. Data correspond to values measured in all trees during the different campaigns carried out through the experiment (N=280 and 269 for *J. monosperma* and *P. edulis*, respectively).

Appendix II

Tables

Table S1. Model of ψ_{pd} over time for both species. Response variable was the sqrt of $|\psi_{pd}|$. Full model: lme(sqrt(abs(ψ_{pd})) ~ date*sp*treatment, random=~1|tree, na.action=na.omit, method="ML")

Fixed Effects	numDF	denDF	F-value	p-value
Intercept	1	701	53.48286	<.0001
Date	13	701	23.54486	<.0001
Species	1	80	2.88972	0.0930
treatment	1	80	0.12428	0.7254
Date:sp	13	701	2.63345	0.0013
Date:treatment	13	701	15.97324	<.0001
Sp:treatment	1	80	0.86240	0.3559
Date:sp:treatment	13	701	1.97294	0.0205
			Model AIC = -189.6102	

Table S2. Model of ψ_{md} over time for both species. Response variable was ψ_{md}. Full model: lme(ψ_{md} ~ date*sp*treatment, random=~1|tree, na.action=na.omit, method="ML")

Fixed Effects	numDF	denDF	F-value	p-value
Intercept	1	715	15.407785	<.0001
Date	13	715	24.148815	<.0001
Species	1	80	4.713988	0.0329
treatment	1	80	4.448591	0.0381
Date:sp	13	715	9.434207	<.0001
Date:treatment	13	715	9.323201	<.0001
Sp:treatment	1	80	4.229087	0.0430
Date:sp:treatment	-	-	-	-
			Model AIC = 1625.761	

Table S3. Model of A_N over time for both species. Response variable was A_N. Full model: lme(A_N ~ date*sp*treatment, random=~1|tree, na.action=na.omit, method="ML")

Fixed Effects	numDF	denDF	F-value	p-value
Intercept	1	694	85.12213	<.0001
Date	13	694	15.82206	<.0001
Species	1	80	0.08035	0.7776
treatment	1	80	0.00025	0.9875
Date:sp	13	694	5.61061	<.0001
Date:treatment	13	694	4.89141	<.0001
Sp:treatment	1	80	0.91070	0.3428
Date:sp:treatment	-	-	-	-
			Model AIC = 3828.548	

Table S4. Model of g_s over time for both species. Response variable was sqrt of g_s. Full model: lme(sqrt(g_s) ~ date*sp*treatment, random=~1|tree, na.action=na.omit, method="ML")

Fixed Effects	numDF	denDF	F-value	p-value

Intercept	1	694	154.59823	<.0001
Date	13	694	16.14292	<.0001
Species	1	80	1.23951	0.2689
treatment	1	80	0.72462	0.3972
Date:sp	13	694	3.92137	<.0001
Date:treatment	13	694	5.97617	<.0001
Sp:treatment	1	80	0.36511	0.5474
Date:sp:treatment	-	-	-	-
			Model AIC = -2370.197	

Table S5. Model of R_d over time for both species. Response variable was sqrt of $|R_d|$. Full model: lme(sqrt($|R_d|$) ~ date*sp*treatment, random=~1|tree, na.action=na.omit, method="ML")

Fixed Effects	**numDF**	**denDF**	**F-value**	**p-value**
Intercept	1	287	328.6619	<.0001
Date	5	287	12.5588	<.0001
Species	1	57	7.8850	0.0068
treatment	1	57	11.9341	0.0010
Date:sp	5	287	3.7169	0.0028
Date:treatment	-	-	-	-
Sp:treatment	-	-	-	-
Date:sp:treatment	-	-	-	-
			Model AIC = -32.57648	

Table S6. Model of F_vF_m over time for both species. Response variable was F_vF_m. Full model: lme(F_vF_m ~ date*sp*treatment, random=~1|tree, na.action=na.omit, method="ML")

Fixed Effects	**numDF**	**denDF**	**F-value**	**p-value**
Intercept	1	695	2393.5641	<.0001
Date	13	695	2.9564	0.0003
Species	1	80	3.6520	0.0596
treatment	1	80	0.0027	0.9588
Date:sp	13	695	1.3084	0.2022
Date:treatment	13	695	4.4246	<.0001
Sp:treatment	1	80	0.2701	0.6047
Date:sp:treatment	13	695	2.2046	0.0082
			Model AIC = -3255.389	

Table S7. Summary of the linear mixed models of the relationship between g_s and Ψ_{pd}. The response variable was the log of g_s. Full model: lme(log(g_s)~ ~|Ψ_{pd}|*sp*treatment, random=~1|tree, na.action=na.omit, method="ML").

Fixed Effects	**numDF**	**denDF**	**F-value**	**p-value**
Intercept	1	730	2149.8051	<.0001
$\|\Psi_{pd}\|$	1	730	315.0744	<.0001
sp	1	82	16.2300	<.0001
Treatment	-	-	-	-
$\|\Psi_{pd}\|$:sp	1	730	16.0310	<.0001
$\|\Psi_{pd}\|$:Treatment	-	-	-	-
sp:treatment	-	-	-	-
$\|\Psi_{pd}\|$:sp:treatment	-	-	-	-
			Model AIC = 1166.873	

Table S8. Summary of the linear mixed models of the relationship between A_N and Ψ_{pd}. The response variable was the log of g_s. Full model: lme(log(A_N)~ ~|Ψ_{pd}|*sp*treatment, random=~1|tree, na.action=na.omit, method="ML").

Fixed Effects	numDF	denDF	F-value	p-value
Intercept	1	727	1850.0050	<.0001
$\|\Psi_{pd}\|$	1	727	349.2183	<.0001
sp	1	82	0.6676	0.4163
Treatment	-	-	-	-
$\|\Psi_{pd}\|$:sp	1	727	8.7878	0.0031
$\|\Psi_{pd}\|$:Treatment	-	-	-	-
sp:treatment	-	-	-	-
$\|\Psi_{pd}\|$:sp:treatment	-	-	-	-
			Model AIC = 1172.218	

Table S9. Summary of the model II simple linear regression of average g_s values by campaign between species, *P. latifolia* and *Q. ilex*. The method used was maximum axis (MA). Full model: lmodel2($g_{s[Q.\ ilex]}$ ~ $g_{s[P.\ latifolia]}$, range.y = "relative", range.x = "relative", nperm = 99).

N=28	r=0.8954	r-sqd.=0.8017	P-values(2-tailed) = $1.26e^{-10}$	P-values(1-tailed) = $6.30e^{-10}$

Regression results

Method	Intercept	Slope	Angle (º)	P-perm (1-tailed)
MA	0.02384	0.8803	41.3576	0.01

Confidence intervals

Method	2.5%-Intercept	97.5%-Intercept	2.5%-Slope	97.5%-Slope
MA	0.01149	0.0342	0.7173	1.0748

Table S10. Summary of the model II simple linear regression of average A_N values by campaign between species, *P. latifolia* and *Q. ilex*. The method used was maximum axis (MA). Full model: lmodel2($A_{N[Q.\ ilex]}$ ~ $A_{N[P.\ latifolia]}$, range.y = "relative", range.x = "relative", nperm = 99).

N=28	r=0.8596	r-squared=0.7387	P-values(2-tailed)=$4.67e^{-9}$	P-values(1-tailed)=$2.33e^{-9}$

Regression results

Method	Intercept	Slope	Angle (º)	P-perm (1-tailed)
MA	2.8480	0.6019	31.0451	0.01

Confidence intervals

Method	2.5%-Intercept	97.5%-Intercept	2.5%-Slope	97.5%-Slope
MA	1.8465	3.7289	0.4656	0.7569

Table S11. Summary of the linear mixed models of the relationship between g_s and A_N using the Ball-Berry model (Eq. 1). Full model:

lme(sqrt(gs)~VarZ*sp*treatment, random=~1|tree,na.action=na.omit,method="ML"). VarZ= $\frac{A_N * RH}{C_a}$.

Fixed Effects	numDF	denDF	F-value	p-value
Intercept	1	730	166.1607	<.0001
VarZ	1	730	541.8764	<.0001
Sp	1	80	11.8723	0.0009
Treatment	1	80	0.3887	0.5348
VarZ:sp	1	730	0.8888	0.3461
VarZ:treatment	1	730	0.1289	0.7197
Sp:treatment	1	80	0.0211	0.8848
VarZ:sp:treatment	-	-	-	-
			Model AIC = -3027.666	

Table S12. Model of basal area increment (BAI) over time for both species. Response variable was sqrt(BAI+2). Full model: lme(sqrt(BAI+2) ~ date*sp*treatment, random=~1|tree, na.action=na.omit, method="ML")

Fixed Effects	numDF	denDF	F-value	p-value
Intercept	1	112	388.7419	<.0001
Date	2	112	9.4954	0.0002
Species	1	96	4.5813	0.0349
treatment	1	96	16.0984	0.0001
Date:sp	2	114	1.7250	0.1829
Date:treatment	2	112	20.7675	<.0001
Sp:treatment	1	112	1.7995	0.1829
Date:sp:treatment	2	112	3.54062	0.0333
			Model AIC = 178.0404	

Table S13. Model of branches growth in diameter (RGR.D) over time for both species. Response variable was RGR.D. Full model: lme(RGR.D ~ date*sp*treatment, random= ~1|tree, na.action=na.omit, method="ML")

Fixed Effects	numDF	denDF	F-value	p-value
Intercept	1	112	191.29987	<.0001
Date	2	112	39.33703	<.0001
Species	1	96	0.04811	0.8268
treatment	1	96	9.19617	0.0031
Date:sp	2	112	1.17755	0.3118
Date:treatment	2	112	1.34702	0.2642
Sp:treatment	1	96	1.10910	0.2949
Date:sp:treatment	2	112	2.19593	0.1160
			Model AIC = -267.1841	

Table S14. Model of branches growth in lenght (RGR.L) over time for both species. Response variable was RGR.L. Full model: lme(RGR.D ~ date*sp*treatment, random= ~1|tree, na.action=na.omit, method="ML")

Fixed Effects	numDF	denDF	F-value	p-value
Intercept	1	112	139.80060	<.0001
Date	2	112	28.58536	<.0001
Species	1	96	13.19533	0.0005

treatment	1	96	1.71775	0.1931
Date:sp	2	112	5.25247	0.0066
Date:treatment	2	112	0.02845	0.9720
Sp:treatment	1	96	5.34854	0.0229
Date:sp:treatment	2	112	3.50817	0.0333
			Model AIC = -125.5237	

Table S15. Model of leaf shedding in branches over time for both species. Response variable was sqrt(A_L:$A_{S.br}$). Full model: lme(sqrt(A_L:$A_{S.br}$) ~ date*sp*treatment, random= ~1|tree, na.action=na.omit, method="ML")

Fixed Effects	**numDF**	**denDF**	**F-value**	**p-value**
Intercept	1	114	208.70525	<.0001
Date	2	114	17.15256	<.0001
Species	1	55	13.85243	0.0007
treatment	1	55	3.33229	0.0734
Date:sp	2	114	3.86230	0.0238
Date:treatment	-	-	-	-
Sp:treatment	1	55	3.26369	0.0763
Date:sp:treatment	-	-	-	-
			Model AIC = -268.8693	

Figures

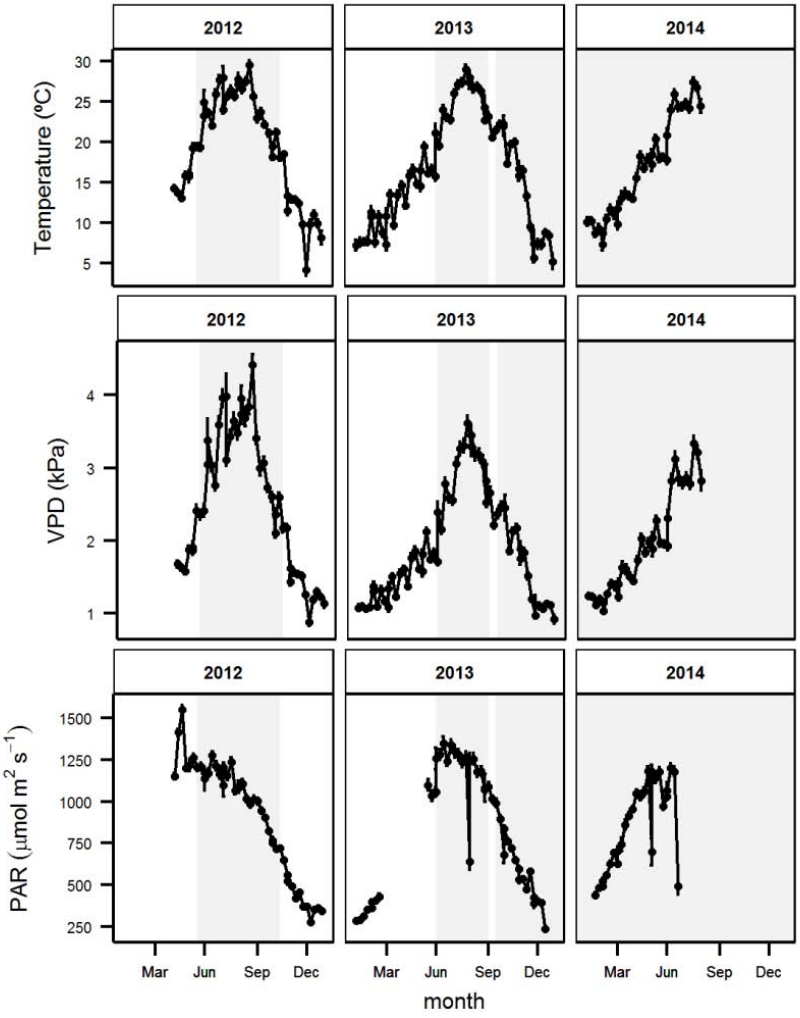

Figure S1.
Meteorological conditions inside the greenhouse during the course of the experiment from April 2011 to September 2014. Dots and lines indicate the weekly average of Temperature (a) and VPD (b), and the average of the maximum weekly PAR (c). Bars indicate the standard error.

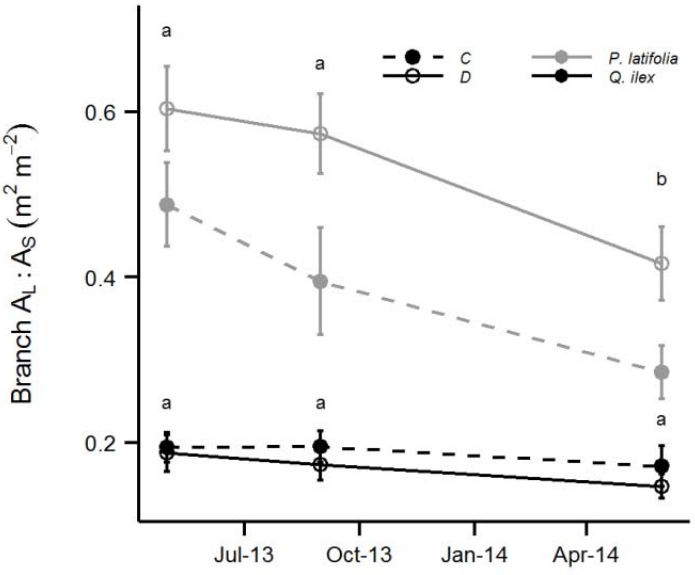

Figure S2.
Leaf shedding measured in branches during 2013 and 2014. N is 23 for D trees in both species and 8 and 6 trees, respectively, for *Q. ilex* and *P. latifolia*. Means and standard error are shown. Letters indicate temporal differences within species.

Appendix III

Tables

Table S1. Summary of the linear mixed models of the relationship between g_s and Ψ_{pd}. The response variable was the sqrt of g_s. The interaction between Ψ_{pd} and survival was not significant and was not included in the best model.

Fixed Effects	numDF	denDF	F-value	p-value
Intercept	1	57	316.5397	<.0001
Ψ_{pd}	1	57	16.7650	0.0001
survival(susceptible)	1	23	8.1284	0.009
Ψ_{pd}:survival(susceptible)	-	-	-	-

Note: Full model: lme(sqrt(g_s)~Ψ_{pd}, random=~1|tree, na.action=na.omit, method="ML")

Table S2. Summary of the linear mixed models of the relationship between g_s and Ψ_{md}. The response variable was the sqrt of g_s. The interaction between Ψ_{md} and survival was not significant and was not included in the best model.

Fixed Effects	numDF	denDF	F-value	p-value
Intercept	1	57	132.79948	<.0001
Ψ_{pd}	1	57	4.61382	0.0360
survival(susceptible)	1	23	13.45086	0.0013
Ψ_{pd}:survival(susceptible)	-	-	-	-

Note: Full model: lme(sqrt(g_s)~Ψ_{md}, random=~1|tree, na.action=na.omit, method="ML")

Figures

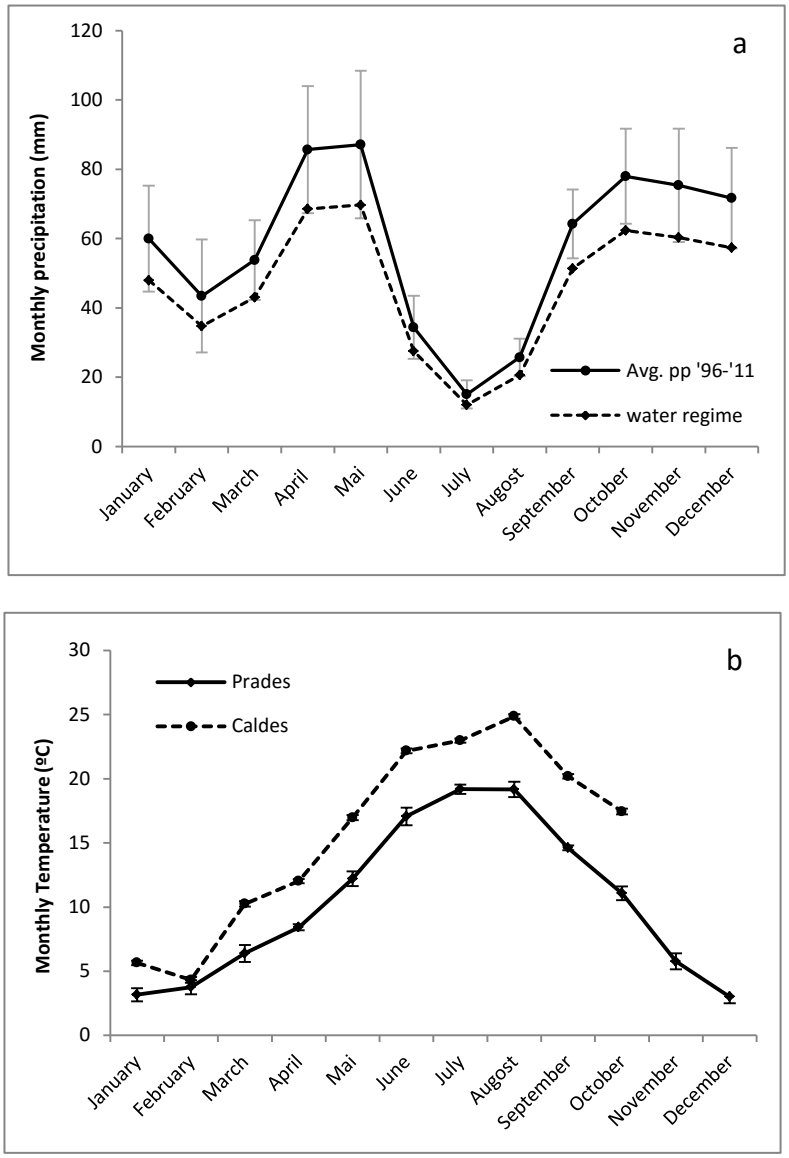

Figure S1.
Comparison of seasonal precipitation and temperature patterns between our greenhouse and the Prades site (close to the southern limit of Scots pine distribution). (a) Mean monthly precipitation in Prades (16 year mean 1996 – 2011; solid line) and applied water regime in the tunnel greenhouse (80% of the monthly average; dashed line). (b) Mean monthly temperature in Prades (7 year mean 2001 – 2010; solid line) and ambient temperature outside the tunnel greenhouse during the experimental year (Caldes de Montbui meteorological station). Error bars indicate standard error.

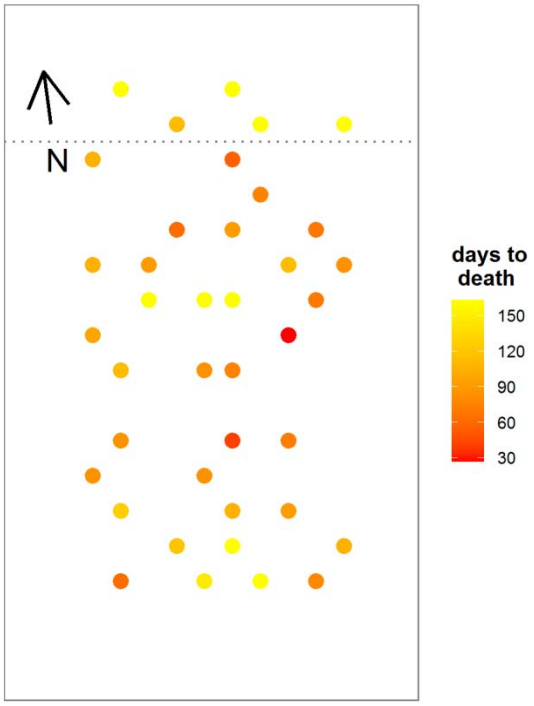

Figure S2.
Map of the greenhouse showing the location of all *Pinus sylvestris* trees in the tunnel greenhouse. Dotted line indicates the separation between controls and droughted trees. Scale color gradient shows time until death for each tree. Yellow trees remained alive at the end of the study period. Censored trees are not shown (see Material and Methods section).

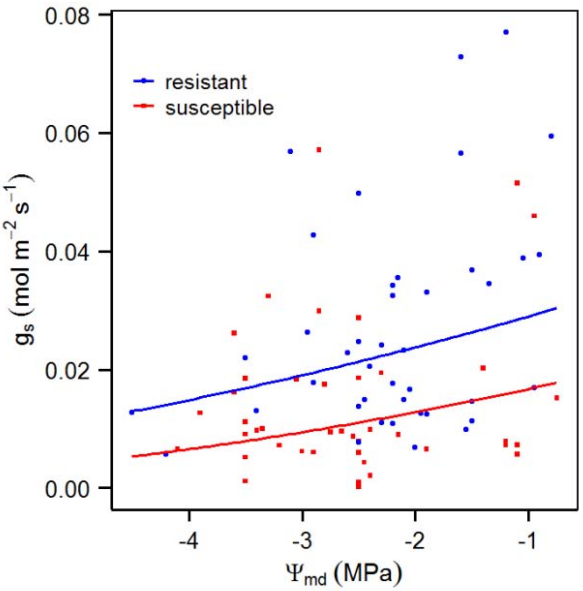

Figure S3.
Relationship between stomatal conductance (g_s) and midday water potential (Ψ_{pd}). Data correspond to values measured in the droughted trees during the study period. Blue squares and red circles indicate resistant and susceptible trees, respectively, and solid lines depict the fitted models (Table S1 in this Appendix)

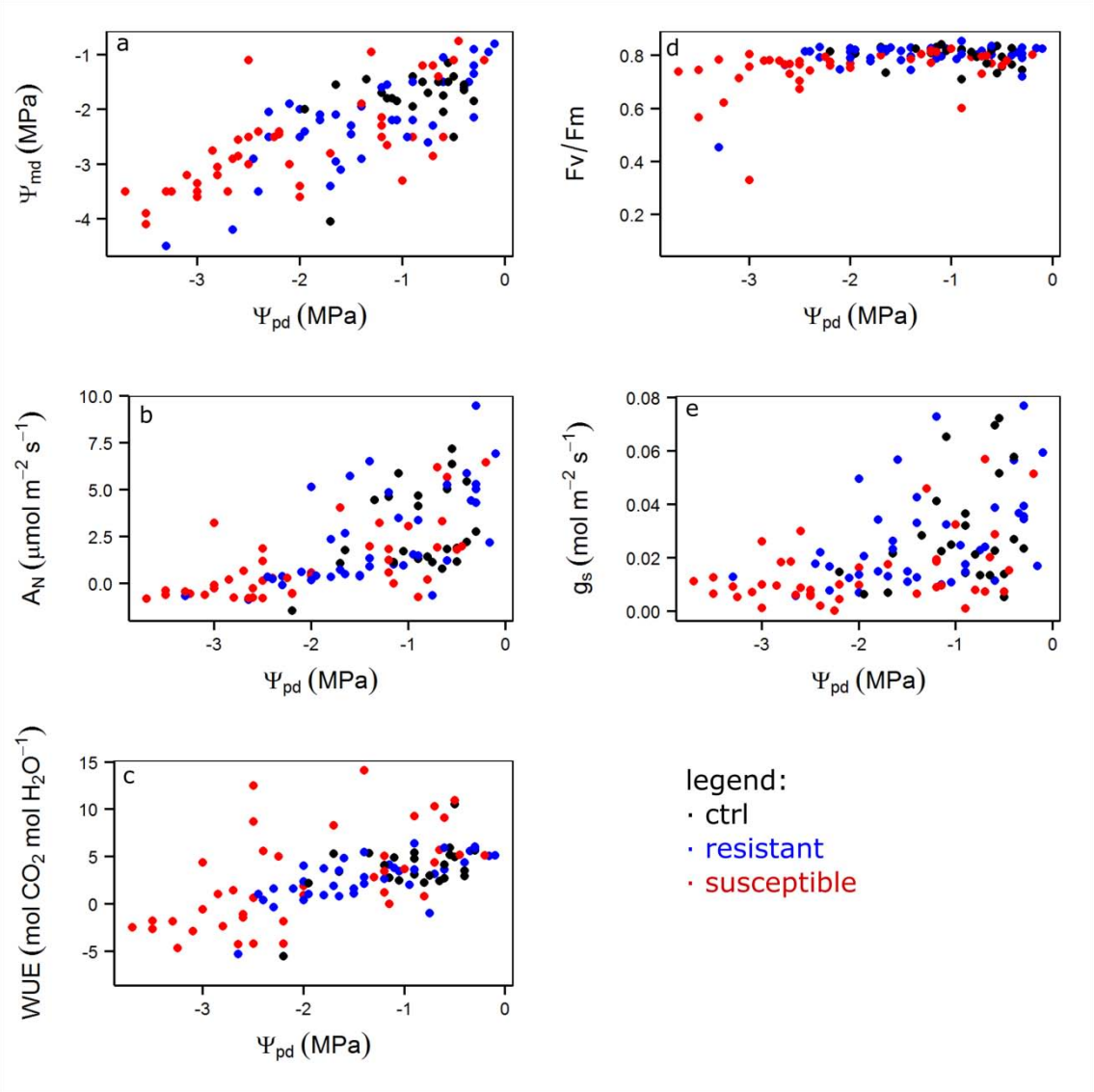

Figure S4.
Relationship between predawn water potential and midday water potential (Ψ_{md}, panel a), net assimilation rate (A_N, b), water use efficiency (WUE, c), maximum quantum yield (FvFm, d) and stomatal conductance (g_s, e). Data corresponds to individual measurements on *P. sylvestris* trees during the study period.

Publications

Published papers

Garcia-Forner N, Adams HD, Sevanto S, Collins AD, Dickman LT, Hudson PJ, Zepper M JB, Jenkins MW, Powers H, Martínez-Vilalta J, McDowell NG 2015. Responses of two semiarid conifer tree species to reduced precipitation and warming reveal new perspectives for stomatal regulation. Plant, Cell & Environment, DOI:10.1111/pce.12588

Adams HD, Collins AD, Briggs SP, Vennetier ML, Dickman LT, Sevanto S, Garcia-Forner N, Powers HH, McDowell NG 2015. Experimental drought and heat can delay phenological development and reduced foliar and shoot growth in semiarid trees. Global Change Biology **21**,4210-4220

Papers under peer-review or in preparation

Garcia-Forner N, Sala A, Biel C, Savé R, Martínez-Vilalta J (submitted) Individual traits as determinants of time to death under extreme drought in *Pinus sylvestris*.

Garcia-Forner N, Biel C, Savé R, Martínez-Vilalta J (in preparation) Isohydric species do not necessarily show lower assimilation during drought.

Adam DC, Ryan MG, Adams HD, Dickman LT, Garcia-Forner N, Grossiord C, Power HH, Sevanto S, McDowell NG (in preparation) Foliar respiration and carbon dynamics of mature piñon and juniper trees in response to experimental drought and heat.

Resum

Les plantes estan exposades a diversos estressos ambientals incloent la sequera i temperatures extremes els quals poden limitar el seu creixement i supervivència. La disponibilitat d'aigua es considera el principal factor limitant per a la productivitat vegetal. Les plantes presenten una sèrie d'estratègies per fer front a la sequera i mantenir un balanç hídric adequat entre les quals s'inclouen modificacions de l'àrea foliar, control estomàtic, canvis en l'assignació de biomassa, modificacions del balanç de carboni font/embornal, i la resistència a l'embolisme del xilema. Tot i així, la mortalitat forestal induïda per sequera és un fenomen generalitzat, amb grans implicacions a nivell d'ecosistema, i s'espera que incrementi degut a l'augment dels episodis de sequera com a resultat de les condicions de canvi climàtic actuals. Entendre com la complexa xarxa de trets que presenten les plantes implicats en la resistència a la sequera determina la seva supervivència tant a nivell d'espècie com d'individu és fonamental per avaluar la vulnerabilitat de la vegetació actual als canvis del clima, i l'impacte potencial en el serveis ecosistèmics.

Al 2008, McDowell *et al.* varen sintetitzar els mecanismes de mortalitat induïda per sequera en un marc hidràulic coherent i senzill. La seva hipòtesi incloïa dos mecanismes fisiològics, no excloents, com a principals causants de la mortalitat d'arbres induïda per sequera: la fallida hidràulica i l'exhauriment de carboni. La fallida hidràulica és el punt en que el transport d'aigua de tota la planta queda bloquejat per cavitació com a resultat de tensions crítiques al xilema. L'exhauriment de carboni és la situació en que el subministrament de carboni provinent de la fotosíntesi, d'estocs de carboni o d'autofàgia no satisfà les necessitats metabòliques mínimes. En aquest marc, la preponderància d'un o altre mecanisme depèn de la intensitat i duració de la sequera, així com de la capacitat de les plantes per regular el seu potencial hídric (Ψ_w). Les especies isohídriques serien més vulnerables a l'exhauriment de carboni degut a un tancament estomàtic més ràpid per tal de mantenir el Ψ_w relativament constant (i evitar l'embolisme), mentre que les especies anisohídriques serien més susceptibles a la fallida hidràulica a mesura que el sòl s'asseca ja que operen

amb marges de seguretat hidràulica més estrets degut als seus Ψ_w més negatius.

El marc previ es centra en el comportament estomàtic sense tenir en compte la plètora de trets que també intervenen en resposta a la sequera. A més a més, els estomes responen a altres factors a banda del Ψ_w, i és per això que assumir que la regulació iso/anisohídrica del Ψ_w és capaç d'explicar completament el comportament estomàtic pot ser enganyós. Per aquest motiu, els principals objectius d'aquesta tesi foren: (2) determinar si les diferències en la regulació estomàtica entre especies estan relacionades amb comportaments iso/anisohídrics i com s'associen aquests als distints mecanismes de mortalitat en condicions de sequera, escalfament o ambdós factors; (2) testar les assumpcions que relacionen comportaments anisohídrics amb majors conductàncies estomàtiques i marges de seguretat hidràulica més amplis; i (3) comprendre com i en quina mesura expliquen els trets morfològics i fisiològics, així com la seva plasticitat, el temps fins la mort en resposta a la sequera dins d'espècie.

Per abordar els objectius (1) i (2) vàrem estudiar dos sistemes models amb contrastada vulnerabilitat a l'embolisme entre espècies: la formació boscosa piñon-juniper i l'alzinar Mediterrani. En ambdós casos vàrem comparar les respostes a la sequera entre espècies isohídriques (*Pinus edulis* i *Quercus ilex*) i espècies anisohídriques (*Juniperus monosperma* i *Phillyrea latifolia*), fent èmfasi en la regulació estomàtica i l'economia de l'aigua i el carboni. En aquestes especies, observem que un comportament més anisohídric no es tradueix necessàriament amb menor sensitivitat estomàtica al Ψ_w i, per tant, amb major taxa d'embolisme. De la mateixa manera, una major regulació del Ψ_w (comportament isohídric) no s'associa amb un tancament estomàtic més ràpid en condicions de sequera ni tampoc amb majors limitacions de carboni. Ambdós estudis desafien les idees previes i adverteixen de la confusió que pot generar l'associació directa de la iso/anisohidria amb un comportament estomàtic contrastat i els mecanismes de mortalitat. A nivell d'individu en *Pinus sylvestris* (3), mantenir activa l'adquisició de carboni i els estocs de carboni per sobre d'un nivell crític fou clau per perllongar la supervivència front a una sequera extrema, fins i tot a costa de majors pèrdues d'aigua. Una completa

integració de l'economia del carboni i l'aigua és el repte per poder avançar en el coneixement de les respostes de les plantes a la sequera i els mecanismes de mortalitat.

Acknowledgements /Agraïments

Arribat aquest moment ja no tinc més excuses i m'he de posar amb la part més important de la tesi, donar-vos les gràcies. Se que alguns penseu que seria capaç de començar i acabar amb aquesta frase però crec que l'ocasió mereix molt més. Començarem pel principi i això vol dir agrair a Jordi, Rafa i Javi per confiar amb mi per fer aquesta tesi aquí i amb vosaltres.

En segon lloc i sense dubte, mil gràcies a tu Jordi. He de confessar que abans de venir em feia un poc de por començar una tesi sense conèixer-te però al primer instant se'm va passar i ara només faig balanç positiu. Creu-me si et dic que l'única cosa negativa d'aventurar-me en això de la tesi al teu costat és lo exageradament positiu que ets, com pots riure quan s'inunda l'hivernacle després de dos anys de sequera?, t'haguera matat! De veres, gràcies per deixar-me aprendre, per guiar-me, per tenir sempre la porta oberta i per mil coses més, però sobretot per ser com ets i haver-ho fet tan fàcil.

Si em paro a pensar segurament un dels primers records que tinc del CREAF ets tu Rafa, i no sols perquè em vas 'liar' la segona setmana per passar un pont treballant a Prades!, sinó perquè al principi sempre costa arrencar i tu vares estar de copilot una bona estona, m'haguera agradat molt tenir-te com a codirector.

Ara sens dubte he de botar a Torre Marimon. Quan encara no tenia molt més que un ordinador al CREAF ja m'havien fet un espai la gent de l'IRTA. El Robert i la Carme sobretot, però també el Xavi i la Feli han segut un gran suport en cada pas que he donat en aquell hivernacle. He pogut comptar amb la vostra experiència, ajuda i energia (sobretot la teva Robert!) durant els quatre anys i això no te preu. Però no només vosaltres, si no haguera segut pel Marc, l'Eulàlia, Cristian, Bea i molts altres que m'han ajudat, encara estaria allí traient herbes, obrint rases, disfressant els arbres de caputxins i contant 2+2++5+4+5+6++3++6+7+3+3... Sense treure-li mèrit a la radio, la companya més fidel per fer mesures a l'alba, la vostra ajuda i sobretot la vostra conversa han fet dels tres anys de mesures un plaer i un èxit, gràcies!.

Llavors va tocar tornar al CREAF i començar amb els malsons: R! R! R! Sort dels caferets amb Stefania i companyia, i de les escapades al SAF amb tots aquells a qui he aconseguit enganyar. Per cert, si encara no us heu adonat, lo de la beca FPI és mentida, queda clar que sóc relacions publiques del SAF, oi?. Els 'creafitos' van i venen però l'ambient que sempre hi ha al centre fa que un moment com el dinar sigui més que això, gràcies a tots.

And then, I went to Los Alamos. Thanks for giving me the opportunity to go there, participate in your lab routines and experiments, but also, in less scientific activities including my first soup party! I was there only for three months and I tried to learn and collaborate with you as much as I could, however, I've definitely received much more. I really appreciate your generosity. Thank you so much.

Segona estada pero no menys important: Sala lab! Raúl, Gerard, Sean, Beth and Sharon. Short but intense, this is how I define my stay in Missoula. Now I love Montana and this is partly your fault, for sharing with me really good times in the lab, pubs or in the mountain. I sobretot a tu, Anna, no se si n'ets del tot conscient de la passió que transmets. Vaig viatjar a Missoula en un d'eixos moments en que comences a no saber que estàs fent, i vaig tornar d'allà amb l'energia del principi i agradant-me més si cap l'ecofisiologia vegetal. Escoltar-te i poder discutir amb tu sobre ciència és un privilegi que espero gaudir per molt temps.

Tere, moltes gràcies tant a tu com al Josep (però lo de pa sec no t'ho perdono eh!) per haver-vos deixat molestar tant durant aquests últims temps. Per les discussions científiques, les pseudo-científiques i la resta, totes ens ajuden a créixer.

Si arribat a aquest punt voleu saber alguna cosa més d'aquesta tesi no cal que seguiu llegint, pregunteu-li a Conso. Has estat al meu costat de principi a fi en aquesta aventura de 'matar pins' i sempre m'has escoltat, has sabut quan empènyer-me o quan pegar-me una colzada per parar. Gràcies per ser-hi!

I perquè el camí cap a aquesta tesi va començar fa molt temps quan llegir dos renglons ens costava tota la tarda, gràcies als meus pares.